UNIVERSITY OF NOVA GORICA
GRADUATE SCHOOL

# QUANTIFICATION OF BIOCOMPONENTS IN FUELS BY $^{14}C$

DISSERTATION

**Romana Krištof**

Mentors: Dr. Jasmina Kožar Logar
Dr. Cristina Otero Hernandez

Nova Gorica, 2015

UNIVERZA V NOVI GORICI
FAKULTETA ZA PODIPLOMSKI ŠTUDIJ

# DOLOČEVANJE VSEBNOSTI BIOKOMPONENT V GORIVIH Z UPORABO $^{14}C$

DISERTACIJA

**Romana Krištof**

Mentorici: Dr. Jasmina Kožar Logar
Dr. Cristina Otero Hernandez

Nova Gorica, 2015

# *Acknowledgements*

I would like to thank my supervisors, Dr. Jasmina Kožar Logar and Dr. Cristina Otero Hernandez, for all their help and guidance. My measurements would not have been possible without Customs Administration of Slovenia, Camelina Company España and Biodiesel Chiapas Mexico who generously donated the samples. I am thankful to the Petrol d.d. and the National Institute for Cryogenic and Isotope Technologies, Râmnicu Valcea, Romania for conducted measurements. My gratitude goes to the AMES d.o.o. and the Josef Stefan Institute, who enabled my research, and my family for all of their support. My gratitude also goes to colleagues at the Jožef Stefan Institute and the Institute of Catalysis and Petrochemistry who in any way helped me with my research.

Operation part financed by the European Union, European Social Fund.

## *Abstract*

Biofuels are added to conventional fuels in an attempt to decrease the impact of transport on the environment. Varieties of bio-components with different characteristics are already known and several of them are still in the research phase. Many specific analytical methods for the quantification of biofuels have also been developed. The challenge to obtain a fast and accurate general method for the quantification of biofuels in fuel mixtures has been addressed. The liquid scintillation technique seems to be a good candidate, and this thesis is devoted to a method with easy sample preparation. The advantages of developing this general method are robustness, considering that no chemical preparation of the sample is required, which reduces errors and saves time. Furthermore, the decomposition of bio-components and their chemical composition does not affect the measurement with the newly developed method. Drawbacks in the form of chemical and color quenching were tackled through an analytical approach and a newly developed system of calibration curves.

A new protocol was developed and applied to nine different biodiesels, which were produced and characterized within the scope of this thesis. Oils of camelina, corn, jatropha, rapeseed, soya, sunflower and waste cooking oil were used as the corresponding feedstock. The chosen feedstock oils covered the majority of existing oils in the EU market and some are promising, non-edible, second-generation oils. We showed that different feedstock oils could be trans-esterified with the same synthesis protocol.

Two different types of analytical protocols were applied, depending on the quenching properties of the analyzed samples. Changes in the counting efficiency had to be taken into account in both protocols. Bio-ethanol and Hydrotreated Vegetable Oil (HVO) were measured with a pre-designed $^{14}C$ protocol in the range from 0 to 100 % of biofuel. The analyses of severely quenched biodiesel samples were tackled with changes in the counting protocol, specifically a coincidence bias setup.

A new approach was also taken in the determination of the counting efficiency. The base of the quench curve determination was taken in biodiesel samples themselves and their blends. The samples showed great variety of quench. The dynamic quench balanced counting window took into account the relationship between the observed quench and the position of the $^{14}C$ peak. This successful approach improved the method, especially with respect to its measurement range and detection limit.

The applied protocols were validated in accordance with standard ISO 17025, where the detection limits, linearity, repeatability, reproducibility, sensitivity and trueness were evaluated. A comparison with another independent LSC method and a survey of Slovenian fuel market were also conducted.

***Keywords:*** *LSC, direct method, biofuels, fossil fuels, biodiesel, color quenching, SQP(E), protocol, balanced counting window*

# *Povzetek*

Biogoriva se dodajajo gorivom v želji po zmanjšanju vpliva prometa na okolje. Poznamo več vrst biogoriv z različnimi lastnostmi, mnogo goriv pa je še v razvojni fazi. Vsebnost biogoriv v gorivih se določa z mnogimi specifičnimi metodami. V doktorski raziskavi sem si zastavila za izziv razvoj hitre in natančne splošne metode, ki bo uporabna za analizo vsebnosti biogoriv. Izbrana metoda je bila tekočinskoscintilacijska spektrometrija s preprosto pripravo merjencev. Prednosti razvite metode so: robustnost, hitrost ter odsotnost kemijske pred-priprave merjencev. Dodatna prednost pred uveljavljenimi metodami je tudi neobčutljivost na razgradljivost biogoriva ter njihovo kemijsko sestavo. Kemijsko in barvno dušenje sta večji pomanjkljivosti uporabljene metode, vendar sem jih z novim analitičnim pristopom kalibracije in interpretacije rešila.

Nov analitični pristop sem razvila in testirala na devetih različnih biodizlih, ki smo jih v okviru raziskave tudi proizvedli. Za proizvodnjo biodizlov sem uporabila olja jatrofe, koruze, navadnega rička, oljčne repice, soje, sončnice ter odpadno kuhinjsko olje. Olja so bila izbrana na način, da pokrivajo večino trenutnega evropskega trga z dodatkom nekaj obetavnih ne-jedilnih olj. Biodizle smo proizvedli z nespremenjenimi sinteznimi pogoji ne glede na uporabljeno olje.

Pri meritvah biogoriv sem zaradi opaženega dušenja v nekaterih vzorcih uporabila dva različna protokola meritev in interpretacije. V obeh primerih sem upoštevala spremembe izkoristka štetja. S prednastavljenim merskim protokolom sem uspešno analizirala vzorce bioetanola in z vodikom obdelanega rastlinskega olja (HVO) v količinah do 100 % biogoriva. Za analize močno dušenih vzorcev biodizla sem spremenila koincidenčne nastavitve merskega protokola.

Nov pristop se uporabila tudi pri določevanju izkoristka štetja. Za osnovo krivulje dušenja so bili izbrani kar vzorci biodizlov, saj se je dušenje merjencev močno spreminjalo v odvisnosti od vsebnosti biogoriva. Pri interpretaciji rezultatov meritev sem uspešno vpeljala dinamična števna okna. Le-ta upoštevajo spremembe v legi, višini in širini izmerjenega spektra. S tem pristopom sem izboljšala metodo,

predvsem njeno uporabnost za meritve vsebnosti do 100 % deleža biodizla ter znižala njene meje detekcije.

Uporabljene merske protokole sem preverila v skladu z določili standarda ISO 17025. Tako sem analizirala meje detekcije, linearnost, ponovljivost, občutljivost in pravilnost metode. Opravila sem še primerjavo z drugo, že uveljavljeno in neodvisno metodo ter preverila uporabnost metode na realnih gorivih na Slovenskem trgu.

***Ključne besede:*** *LSC, direktna metoda, biogoriva, fosilna goriva, biodizel, barvno dušenje, SQP(E), štev ni protokol, premikajoča štev na okna*

## *Table of Contents*

# *List of tables*

# *List of figures*

## *Abbreviations*

| | |
|---|---|
| ASTM | American Society for Testing and Materials |
| DL | Detection limit |
| EN | European Standard |
| FAME/FAEE | Fatty Acid Methyl / Ethyl Esters |
| FM | Figure of Merit |
| HVO | Hydrotreated Vegetable Oil |
| ISO | International Standardization Organization |
| LSC | Liquid Scintillation Counting |
| MCA | Multi Channel Analyzer |
| PAC | Pulse Amplitude Comparator |
| PMT | Photo-Multiplier Tube |
| PSA | Pulse Shape Analyzer |
| SQP(E) | Standard Quench Parameter of External standard |
| TA | Tran-esterified acids |

# 1 Introduction

Fossil-fuel resources are the driving force for the world's economy and lifestyle because they are used for the production of energy and many chemical compounds. Environmental changes caused by the emission of greenhouse gases are being observed [1, 2], and due to the continuous increase in the exploitation of fossil-fuel resources, a concern has been made for their cost, natural reserves and sustainability [3, 4]. The countries of the European Union have decided to promote the use of sustainable and renewable resources [5]. Since a large part of the greenhouse emissions are produced by the transportation of goods, an emphasis on replacing fossil fuels by biofuels has been made [6].

The prices for a metric ton of the crude fossil oil and sustainable crops resources are comparable, or even in favor of the renewable source. The refinement of fossil fuels has already been improved but the exploitation of bio-resources is still in its early phase, and so the so-called biofuels are more expensive and often with limitations for their use [2]. Therefore, the use of such fuels is stimulated by a reduction of taxes [5, 7]. The consequence of such a political decision is the need for fast and reliable methods that can determine the content of bio-components in fuel samples [8–28]. The liquid scintillation technique (LSC) is one of the techniques that can be used for this purpose [8–11, 16, 27, 29].

The characterization of biofuels by liquid scintillation spectrometry is based on a determination of the $^{14}C$ activity in the sample [8–12, 16, 29]. Radiocarbon is a cosmogenic radionuclide; it is produced in the atmosphere from $^{14}N$ by neutron capture. The production of $^{14}C$ in the air is relatively constant. At the same time $^{14}C$ undergoes a radioactive decay to nitrogen, with a half-life of roughly 5700 years. These processes in the atmosphere are in equilibrium. The ratio $^{14}C/^{12}C$ is well monitored and relatively constant. All living organisms uptake $^{14}C$ via photosynthesis, ingestion or inhalation; therefore, in living tissue, the ratio of $^{14}C$ to $^{12}C$ closely follows that of the environment. After death or harvest, the uptake stops, which leads to a reduction of their $^{14}C$ isotopic proportion due to the radioactive decay [30, 31]. All of the $^{14}C$ in fossil fuel has decayed while bio-components still have all the activity from the growth, and thus a differentiation can be made, simply

by measuring the sample's $^{14}C$ activity. Liquid scintillation spectrometry is suitable and common technique for determination of $^{14}C$ in liquid samples.

Several procedures for the preparation of LSC samples are in place. The most commonly used is a chemical pre-treatment, which for the $^{14}C$ determination consists of the preparation of $CO_2$ or benzene. Both procedures will be discussed further in the text. But there is also the so-called direct LSC method, where a pre-treatment is not necessary. So far several authors have tried to apply a simple direct LSC method for the determination of biofuels. Edler [9] and Dijs *et al.* [8] reported that this can be done without any pre-treatment in the case of ethanol and gasoline/bioethanol blends in amounts up to 100 % of biofuel. Yunoki and Saito [29] reported the application of a two-step water extraction for a determination of the bioethanol content in gasoline. The application was tested for up to 10 % of a bio-ethanol/gasoline blend. A heavy quench is observed in the determination of commonly used biodiesel, which limits the quantitative determination of the bio-component in such fuel [11, 16, 26, 27, 32]. A direct LSC method for up to 20 % of different feedstock biodiesels and new, renewable diesel was reported by Norton *et al.* [12, 16]. Takahashi *et al.* [26] reported direct LSC measurements of 1 g of biodiesel or oil. This approach is suitable for fuels with a large amount of bio-component, although it suffers because of the high detection limits. From the literature, it can be understood that quenching has a major role in the measurement of biofuels. Similar situations were observed in measurements of wine and various biological samples, e.g., urine and blood. This problem can be resolved on two different ways: the addition of a sample pre-treatment step, prior to the LSC measurement, or a careful study of the quench, which would lead to a new measurement, calculation and interpretation approach. Reports of dry oxidation, chemical solubilization and decolorization with $H_2O_2$ as well as the use of pre-treatment resins and dilution in a scintillation cocktail can be found in the literature [26, 32–35]. This thesis focuses on the second option, where the relation between the detected released energy and the quench was studied and a new analytical approach and a system of calibration curves were developed, and proposed as a suitable method.

The thesis deals with the development and implementation of a simple, accurate and fast method for a determination of biological samples using liquid scintillation counting. A successful determination of ethanol and renewable diesel (in the form of

hydrotreated vegetable oil) reported by some authors had been repeated and calibrations were made in the range up to 100 % of the bio-component. Biodiesel samples from known feedstocks and their characteristics are not easily available. However, biodiesel from camelina (2x), corn, jatropha, rapeseed, sunflower (2x) and waste cooking oils were produced and characterized for use in this thesis. Sunflower oils were chosen for a comparison of the pre-treatment (refination), while the camelina oils had different geographical origins. We managed to produce all the biodiesels with more than 90 % of ester yield using the same procedure for all the feedstock oils. The quench interferences were further studied on these nine different biodiesel samples. The focus of the quench-interferences research was related to the observed quench and the position of the sample spectra, and thus the detected energy of the $^{14}C$ decay. The correlation between those two parameters led to a new calculation and interpretation protocol that enabled the determination of highly quenched biological samples represented with the biodiesel. In addition to the new protocol, the thesis addresses the problems of the preparation of the quench calibration samples and its effect on the measurement. The difference between chemical quenched LSC samples and LSC samples with chemical and color quench is addressed. It has been determined that the combination of chemical and color quench in the LSC samples decreases the released energy to such extent that it is lower than the pre-designed protocol's threshold. Although this dissertation is based on a determination of the $^{14}C$, similar interferences and problems can be observed in a determination of samples such as blood or urine, especially in the case of low-energy radionuclides. The method has also been validated and compared with other methods, while the usability of the protocol for other biological samples and radionuclides was discussed.

Biofuels were used for development of a protocol that will allow a determination of organic samples; their short description is provided later in the text. A description of the spectrometer is provided with an emphasis on possible solutions for improvements to the LSC sample measurements. These are limited due to the sample color and various chemical compositions, thus affecting the measurements through the quench.

## *1.1 Biofuels*

According to Soetaert and Vandamme [4] the name biofuels or bio-components refers to any fuel component in the gaseous, liquid or solid state that is made out of renewable material. In the framework of this dissertation, the meaning of the terms biofuel and bio-component is a liquid fuel made from biomass that is used for vehicle movement. Vehicles have different types of internal combustion engines. The most widely used in Europe are diesel powered vehicles; therefore, such fuel is the most attractive for the development and introduction of renewables to the market. Together with gasoline and ethanol in some countries, all fuels for internal combustion engines are included [1, 2, 4, 36].

Improvements and the development of ecologically acceptable engines led to improved fuels. Vehicles in Europe are mostly diesel or gasoline powered, so two standards have been adopted to make sure that all vehicles are propelled with fuels of the same quality. The standard EN 590 (Automotive fuels-Diesel-Requirements and test methods) contains requirements like cetane number, sulfur content, flash point, carbon residue, ash content, viscosity, etc. [37]. The requirements for gasoline are written in the EN 228 standard (Automotive fuels-Unleaded petrol-Requirements and test methods) and involve the octane number, vapor pressure, boiling point, volatility, oxygenates, sulfur, and lead content [38]. Biofuels are usually added to fossil fuels in small amounts as a part of fuels' composition.

The so-called first-generation biofuels, consisted of Fatty Acid Methyl Esters (FAME), Ethyl Tertiary Butyl Ether (ETBE) and bio-ethanol are the most popular and common forms of the biofuels on the global market at the moment [5]. FAME can have various chemical compositions and therefore different characteristics, so the quality is prescribed by the standard EN 14214 (Automotive fuels-Fatty acid methyl esters (FAME) for diesel engines-Requirements and test methods) [39]. FAME is used as an addition to fossil diesel; thus some requirements are the same as for the standard EN 590. However, the bio-component characteristics, like ester content, oxidation stability, acid value, iodine value, glycerol content, etc., have to be measured separately in order to meet the criteria when they are used as a fuel or an additive [39]. The production of biofuels, like Hydrotreated Vegetable Oil (HVO) and Fischer-Tropsch products (BTL), is being improved and used on pilot tests in

recent years [36, 40, 41]. The above-mentioned standards EN 590, EN 228 and EN 14214 cover only the first generation of biofuels. Due to the fact that the second and the third generations of biofuels are still in development and research, such fuels are not yet applicable for massive production [4, 36, 41, 42]. Some of the properties of the bio-components and their production are discussed in the following subchapters.

### *1.1.1 Fatty Acid Methyl/Ethyl Esters (FAME/FAEE)*

FAME/FAEEs are the most used diesel bio-components and are often referred to as biodiesel. They are characterized by their yellow color and high viscosity. FAME/FAEEs are produced via a trans-esterification, which refers to the catalyzed chemical reaction of vegetable oil and an alcohol to yield the fatty acid alkyl esters and glycerol [1, 3, 4, 43, 44]. Processes differ regarding the type of applied catalyst. KOH and $H_2SO_4$ are the most widely used catalysts; in recent experimental studies enzymatic catalysts are used [3, 4, 43–50]. In general, the triglycerides, the main components of vegetable oil, react with alcohol and their three fatty acid chains are released from the glycerol skeleton. The released fatty acids combine with alcohol to yield fatty acid alkyl esters. If methanol is used, fatty acid methyl ester or FAME is produced [44]. Fatty acid ethyl ester (FAEE) is produced when the ethanol is used for a production. The difference between those two could be observed in reaction speed, but the final product should be of the same quality. Due to the reversibility of the reaction, excess alcohol is used to shift the equilibrium towards the product's side [4].

First-generation bio-components made from vegetable oils have had an impact on food stocks and their prices. Thus, new processes were developed using non-edible oils [42, 44, 45, 51]. The type of oil used differs in terms of the composition of fatty acids. Rapeseed oil is the most commonly used vegetable oil for the production of biodiesel; oils from soybean, sunflower, corn, peanut, coconut, etc. are also used [47]. Biodiesels are biodegradable and unstable from the oxidation point of view. The aim of the oxidative stability control is to satisfy the quality demands during the storage of fuel [37, 39]. Samples of biodiesel with known data for the quality and production feedstock are difficult to obtain. Thus, some biodiesels were produced and characterized in the frame of this work.

### *1.1.2 Ethyl Tertiary Butyl Ether (ETBE)*

ETBE is a clear, colorless liquid organic compound with a distinctive ether-like odor. It is produced from ethanol (47 %v/v) and isobutylene (53 %v/v). Ethanol can be produced from any renewable source, while the isobutylene is derived from a crude oil or natural gas. Like the methyl tertiary butyl ether (MTBE) and ethanol, ETBE is one of the oxygenates of gasoline used as octane boosters to replace the toxic compounds such as lead. A high octane number, low boiling point and low vapor pressure are characteristics of the ETBE [4, 52]. It can be added to fuels in levels up to 15 % [3].

### *1.1.3 Bio-ethanol*

Bio-ethanol is a colorless liquid produced from a biomass. In blends up to 5 % (in EU) or 10 % (in US) it is used as a fuel additive, in some countries it is used as a fuel. According to Mielenz [53], ethanol can be obtained from any kind of biomass by two procedures. Both of them begin with milling and blending. Concentrated sulfuric acid is used to hydrolyze the biomass prior to the fermentation in one of the procedures. In the other procedure ethanol is simultaneously saccharificated and co-fermented. Enzymes convert the cellulose and hemicellulose to sugars that are fermented to ethanol in both processes [41, 53]. The ethanol is mainly produced from corn and sugarcane. Fewer process stages and lower energy requirements are some of the advantages of ethanol production using sugarcane. However, the excessive water requirements, temperature and the length of the growing season are the disadvantages, thus crops such as sorghum have been tested for the production of the ethanol [54]. The progress of producing ethanol from lignocellulosic biomass such as forest, agriculture or industrial wastes and energy crops has been made in recent years. The process of converting that biomass to fuel consists of the delignification, depolymerization and fermentation to ethanol [55].

### *1.1.4 Hydrotreated Vegetable Oil (HVO)*

HVO is a clear and colorless liquid obtained from animal fat or vegetable oil. Hydrotreated vegetable oils (HVO) can be used as a bio-component addition to diesel or its subsidy [36]. In some cases HVO can be added to gasoline (see Section 8.2.1 on page 97). The production process consists of treating the fats or oils and the isomerization with hydrogen. Such fuel is only present on some fuel markets around

the European Union because of the higher costs and the challenging procedures. The oxygen from the triglycerides is removed and the triglyceride is split in multiple chains during the production [21, 36, 40, 56, 57]. The fuel obtained is chemically similar to diesel fuel; it consists of simple chained paraffin. Furthermore, the characteristics of the obtained fuel are fully in line with the standard EN 590 for diesel fuels. The storage problems of biodiesel, such as water intake, oxidation and degradability, are not a concern for HVO [36, 40].

### *1.1.5 New generations of biofuels*

New generations of biofuels are produced from various ranges of non-edible biomass or its residues by gasification and/or pyrolysis. A synthesis gas (syngas) is produced first in both methods, containing carbon monoxide and hydrogen. The so-called Biomass to Liquid (BtL) or Fischer-Tropsch products (FT), bio-methanol and bio-hydrogen, can be obtained from the syngas with the use of a catalysts, high temperatures and pressure [41, 55, 58, 59]. Pyrolysis oil can also be produced from the biomass by undergoing fast pyrolysis with the absence of oxygen. The characteristics of the pyrolysis oil are a liquid of a dark-red brown to black color, a density up to 1200 kg/m$^3$, large water content and a varying viscosity [3]. Additional treatment steps are necessary to make them useful in vehicles.

## *1.2 Determination of biofuel content*

The determination and certification of the bio-component content is carried out in different ways. Several analytical techniques are used; some of the methods are standardized. Methods for the determination of the biodiesel quantity are widely explored since biodiesel is the most used biofuel. Its identification is standardized with the standard EN 14078 [60], where near-infrared spectrometry with transreflectance-fiber optics (FTNIR) is used. The ethanol and ETBE quantity can be determined as oxygenates using procedures detailed in the standard EN 1601 [61] (oxygenate flame ionization detector) or EN 13132 [62] (gas chromatography using column switching). Neither method can differentiate between the biofuel and the fossil fuel. The certification of biofuels can only be made by a determination of the $^{14}$C content with AMS (Accelerator Mass Spectrometry) or any of the LSC methods. The standard ASTM D6866 (Standard Test Methods for Determining the Biobased Content of Solid, Liquid, and Gaseous Samples Using Radiocarbon Analysis)

describes the AMS and LSC methods with benzene synthesis [13]. The quantity of HVO can also be determined only by a measurement of the $^{14}C$ activity, due to the similarity of the diesel and HVO compositions.

### *1.2.1 Accelerator Mass Spectrometry (AMS)*

Accelerator Mass Spectrometry is a technique for precise measurements of atomic mass. A method for the determination of the biofuel content in fuels is described in the standard ASTM D6866. The sample is prepared by converting organic carbon to $CO_2$, which is further catalytically reduced to graphite. The individual isotopes of carbon are separated and quantified in an accelerator that is coupled with a mass detection spectrometer [17, 19, 28, 63–66]. Three carbon isotopes, $^{14}C$, $^{13}C$ and $^{12}C$, have to be determined with great accuracy. The ratio $^{14}C/^{12}C$ is needed for the determination of the biomass content, while the ratio $^{13}C/^{12}C$ is used for the correction of the isotopic fractionation [17, 67]. The method can be used for a quantitative determination of all the bio-components, but extensive sample treatment and expensive equipment is demanded. The method can also be used for archaeological purposes, because only small amounts of the samples are needed. On the other hand, the drawback of the small quantity samples is, due to high surface to volume ratio, the risk for the contamination during the sample preparation. Due to the precision of the method, all the measurements have to be corrected for isotopic fractionation. In biofuels the fractionation occurs in the plant-growing period due to the different isotope intake [17, 19, 28, 63–67].

### *1.2.2 Liquid scintillation counting*

Liquid scintillation counting (LSC) is a spectroscopic technique where the quantity of biofuels is determined by comparing the count rate for samples of fossil and modern origin [17]. Three methods for the determination of the bio-component in fuels are based on LSC [13, 28, 63]. Two methods need a sample pre-treatment, similar to the AMS method. The conversion of organic carbon to $CO_2$ is a crucial step for both LSC methods. In the first method (LSC-A), $CO_2$ is absorbed on an absorbent, for example, Carbosorb E or directly into scintillation cocktail [68]. In the second (LSC-B) method, $CO_2$ is carbonized at 600 °C and benzene is synthesized [28, 63, 64]. Both methods are mainly applicable for measurements of environmental samples, such as the exhaust of a nuclear power plant, samples for age determination

and the activity of $^{14}C$ in water [69–72]. The LSC-A and LSC-B methods need additional caution when used for a determination of the biofuels content due to a potential self-ignition [73].

The third method is the so-called direct method and it is explored in detail in this thesis. The method does not need any sample pre-treatment; the samples are prepared by mixing a suitable scintillation cocktail with fuel. From the literature, this method can easily be used to determine the bio-content in various blends with bioethanol in fossil ethanol or gasoline [8–11, 17, 28, 29, 63]. Analyses of the biodiesel were also reported, but to a limited extent due to the extensive quench induced by the yellow color of the sample. Namely, the generated light in liquid scintillation cocktail is predominately blue, what is the complementary color of the yellow sample. Hence, the absorption of induced photons is very effective and so do quench [9, 10, 16, 26, 27]. The highest per-cent of successfully determined biodiesel (20 %) was reported by Norton and co-workers [16]. The color of the sample is intense and persistent, disturbs the light transfer between the scintillation cocktail and the photo-multiplier tube. Attempts to degrade and limit the color were also reported [35, 74]. In addition, the biodiesel's oxidative stability limits the usability of the bio-component and disrupts the calibration [74]. However, with changes in the measurement protocol and the calculations described in this thesis, a successful determination of the pure biodiesel was achieved.

### *1.2.3 Transreflectance-fiber optics near infrared spectrometry (FTNIR)*

Transreflectance-fiber-optics near-infrared spectroscopy (FTNIR) is proposed in the American standard ASTM D7371 [75] and the European standard EN 14078 [60]. The determination of the biodiesel blend is executed in the infrared region around 1745 $cm^{-1}$ by a comparison of the absorption in fossil fuel and biodiesel [24, 57]. The absorption in this region occurs due to the ester carbonyl bond present in the biodiesel [75]. The method has difficulty determining biodiesel percentages larger than 20. Oliveira and co-workers [20] reported an improved method that can be used for blends up to 100 % of biodiesel by combining FTNIR with partial least-squares regression (PLS) and an artificial neural network (ANN). Several calibration models have been made due to different fatty acids' compositions [20]. Since the method is

based on fossil and biodiesel measurements in a precise absorption region it is not applicable for a variety of different bio-components.

### *1.2.4 Gas chromatography (GC)*

Gas-chromatography (GC) can resolve different fatty acids types and can also be used to determinate fatty acid composition. The EN 14103 standard [76] describes a method for a determination of the total biodiesel and linolenic acid methyl ester. During the analysis, a detailed separation of the biodiesel occurs. The volumetric percentages of the biodiesel in the blends are calculated by comparing the signals of fatty esters to external standards [49]. Many versions of the method were reported by Monteiro and co-workers [18]. They reported a change of the sample pre-treatment protocol and the use of additional internal standards [18].

### *1.2.5 Other methods*

Some additional methods to determine the biodiesel content were described in the literature. Knothe [15] reported that blend levels of biodiesel can be determined by $^{1}$H Nuclear Magnetic Resonance Spectroscopy (NMR). The author compared the new method to the near-infrared (NIR) technique on methyl soyate in blends up to 100 %. It was concluded that the results are in excellent agreement and are often in the experimental error range of the sample preparation [15].

HPLC methods for the identification of fatty methyl esters, mono-, di-, and triacylglycerol in different kinds of biodiesel were described. An UV detector is normally used and its response is proportional to the number of double bonds. If an evaporative light scattering detector (ELSD) is used, the response is related to the mass of injected solute. The sensitivity of the ELSD decreases with increasing amounts of double bonds. Such a detector is nevertheless more suitable for biodiesel measurements than a UV detector [18].

Ventura and co-workers [22, 23] reported the use of thermal lens spectroscopy for measuring biodiesel blends. The determination is based on thermal and mass diffusion effects in measurements of different biodiesel blends and impurities. The use for a quality determination of the biodiesel was also reported.

# 2 Liquid Scintillation Spectrometry

## 2.1 Detection principle

Liquid scintillation spectrometry is used for measurements of radioactivity. It is especially suitable to detect β emitting isotopes. A β emitting isotope $^{14}C$ is involved in the determination of the biofuel quantification. This isotope is naturally produced in the atmosphere by neutron capture (see equation 1). When β decay occurs, an electron/positron and an antineutrino/neutrino are released (see equation 2). The energy of the decay is distributed among the particles produced. Therefore, the β particle produces a continuous spectra corresponding to a continuum of energies from $E_0$ to $E_{max}$ [31, 77]. Commonly measured isotopes are $^{3}H$ and $^{14}C$, but also $^{32}P$, $^{90}Sr$, $^{210}Pb$, $^{210}Po$, $^{228}Ra$ and $^{239}Pu$ and others [31, 78].

$$^{14}N \xrightarrow{neutron\ capture} {}^{14}C \quad [1]$$

$$^{14}C \xrightarrow{decay} {}^{14}N + \beta^- + \bar{\nu} \quad [2]$$

where: $\bar{\nu}$ is antinevtrino

The radioactive material is mixed with a scintillation cocktail that is a mixture of 3 types of chemicals: solvent, emulsifier and fluorescence material (scintillator). The energy from the β decay is absorbed in the emulsifier at the beginning of the scintillation process. That energy is then transferred to the fluorescent material through the solvent present in the scintillation cocktail. The fluorescence material or scintillator then emits the energy in the form of light. The scintillations are detected by the photomultiplier tube (PMT), which converts the detected light to an electrical pulse. The PMTs are usually paired and a coincidence circuit is applied. If no interferences occur during the measurement, the measured count rate is directly proportional to the amount of activity contained in the sample. In cases like measurements of biofuels, the counting efficiency must be considered through the proper transformation of counts to activity [31, 77–81] because of substantial effects of quenching and luminescence. The attenuation of detected counts in direct measurement will be further discussed in the following subchapters.

### *2.1.1 Quenching*

The energy transfer between the radioactive isotope and the scintillation cocktail can be disturbed, which results in reduced photon production. The outcome is a spectrum shifted towards lower energies and a reduced number of counts [77]. The two most known quenching processes described in the literature can have an effect on the biofuel measurement: chemical and color quench.

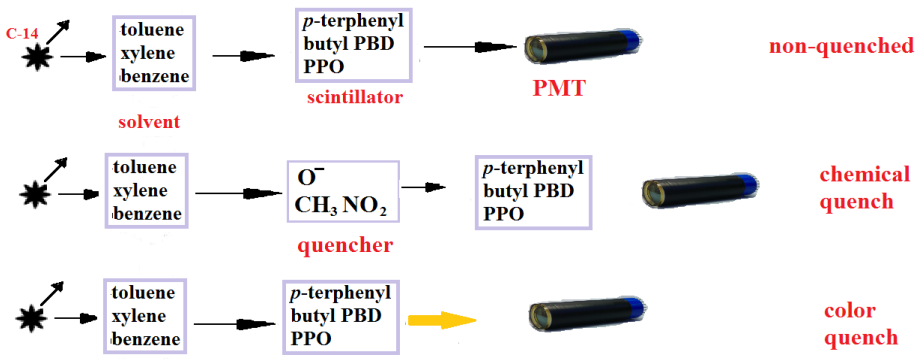


**Figure 1: Forms of quenching.** Top scheme presents ideal scintillation process. The second scheme presents energy transfer, where chemical quench is observed. The disturbed energy transfer due to color quench is depicted in the bottom scheme.

#### *2.1.1.1 Chemical quench*

Chemical quench is a process where the transmission of energy between the solvent and the scintillator is disturbed. Thus, it reduces the number of photons produced in the scintillation cocktail and detected by PMT [78, 81]. The liquid scintillation system's energy transfer is described as a donor-acceptor system, and thus each non-fluorescent molecule could interfere with the transfer of the excitation energy from the solvent to the fluor (scintillator). When chemical quenching occurs, non-fluorescent molecules convert the excitation energy into heat via vibrational relaxation [82]. According to Neary and Budd [83] chemical quenching can be approximated with an exponential function of the quencher concentration. The most common causes for such quenching are the presence of oxygen, halogenated hydrocarbons, nitro-methane, etc. [83].

#### *2.1.1.2 Color quench*

Unlike the chemical, color quench impedes the last step in the mechanism. The light produced in the scintillator is attenuated by the quenching molecule, which exhibits absorption within the emission of the fluor [83]. A higher color quench can

be observed with orange-colored samples due to the complementarity with the scintillation light, being predominantly blue [84]. The shifted spectra of the color-quenched sample appears as depressed and spread out because the path length between the scintillation event and the PMT alters the pulse-height distribution. Compared to the chemical quench, which behaves differently, this could cause an experimental error and a misinterpretation of the results (see Figure 2) [81, 83, 84]. According to Neary and Budd [83] in spectra of higher energy β like $^{14}C$, the difference is more pronounced.

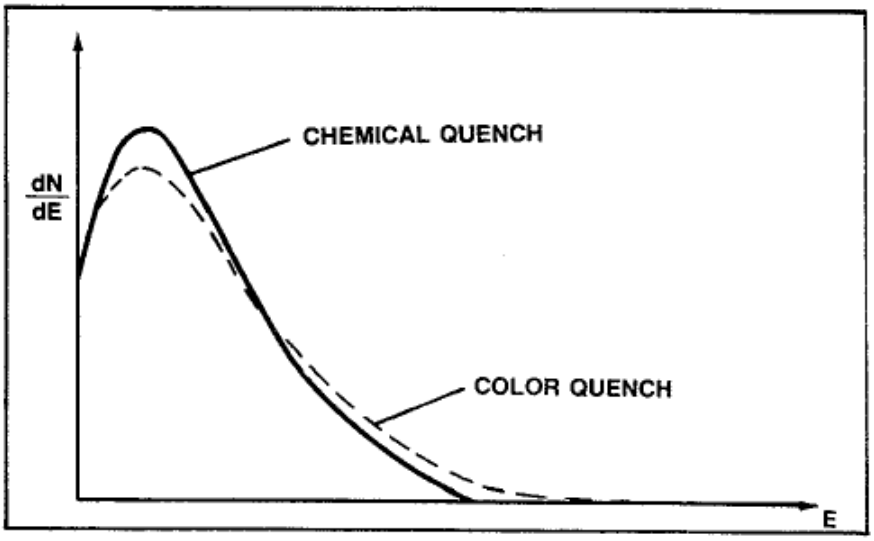


**Figure 2: Spectral difference between color and chemical quench** [81]**.**

### *2.1.2 Chemo-luminescence / Photo-luminescence*

The light produced in the scintillation cocktail is observed as flashes of luminescence. When light is formed and released from the LSC sample, an additional disturbance can arise. Samples containing peroxides or having an alkaline pH are subjected to chemo-luminescence [81]. The mechanism of a chemically produced light differs from the scintillation, which is a consequence of the radioactive decay. Radioactive decay produces multiple photons, while chemo-luminescence produces a single photon. The use of the two opposing PMTs and the electronic coincidence gate eliminate such an event. If two chemo-luminescence events occur in the time span of the coincidence gate, the pulses are accepted as a radioactive decay [31, 78]. Photo-luminescence occurs when the fluor in a scintillation cocktail is excited by UV light in the sample-preparation period. The photo-luminescence decays in a matter of

minutes. We were able to sufficiently eliminate photo-luminescence with applied time for the adaption of samples to the counter's temperature [81].

### *2.1.3 Counting efficiency*

For a determination of the activity, it is necessary to take into account the counting efficiency. Part of the decreased counting efficiency is due to the PMT characteristics, but the majority is related to the observed quenching [81]. For a description of the level of quenching, quench-indicating parameters are used. Different manufacturers of LSC counters use different names and protocols to describe and calculate them. The literature often divides the quench-indicating parameters into three groups according to the spectra used, namely: the external standard spectrum, a sample spectrum and internal standardization [31, 81, 85]. The external standard spectrum and the internal standardization were used in this research, and thus a short description is provided later in the text. Quench-indicating parameters calculated from the sample spectra describe the relation of the spectra gravity and the counting efficiency. Two of the most common representatives are the Spectral Quench Parameter of the Internal standard (SQP(I)) and the Spectral Index of the Sample (SIS).

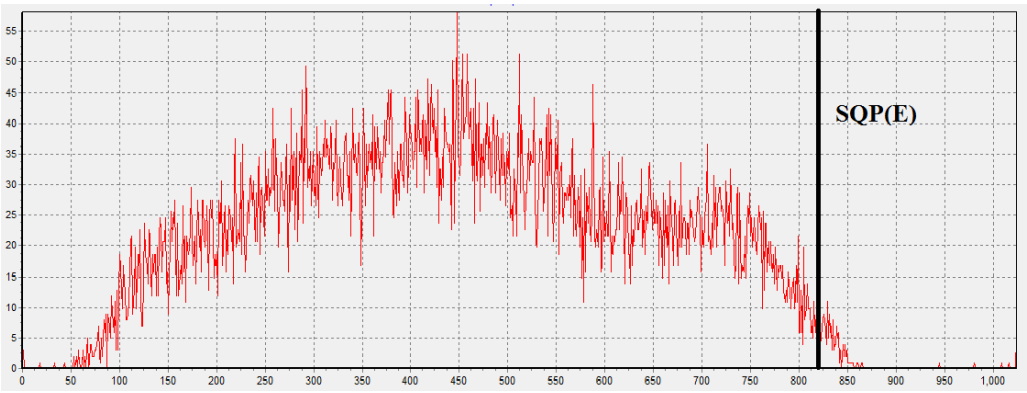


**Figure 3: External standard spectra.** SQP(E) value of measured sample was 817 that was obtained from the 99 percentile of the spectral area.

In the Quantulus 1220 (PerkinElmer, Wallac Oy), the Spectral Quench Parameter of the External standard method SQP(E) is used to determine the degree of quench in the sample. It is calculated from the position of the 99 percentile of the area under the $^{152}$Eu spectrum (see Figure 3). A measurement of the standard usually takes one additional minute. Some of advantages for use of this parameter for a fast quench

evaluation are: the method is a non-destructive and its high precision is independent of the activity of the sample [78].

Internal standardization is one of the procedures where the counting efficiency is determined by the addition of a known activity of a radionuclide in a vial. The determined efficiency is correct when the addition of the internal standard does not change the sample-quenching level. The procedure consists of four steps: the sample's count rate determination, the addition of a known amount of standard, the standard's count-rate determination and an efficiency calculation [81].

## *2.2 Spectrometer Quantulus 1220*

All our measurements were performed on an ultra-low-level liquid scintillation spectrometer Quantulus 1220 (Wallac Oy, PerkinElmer) purchased in 2006 (serial number 386). All such LSC spectrometers consist of 2 dual programmable multichannel analyzers (MCA) and enable simultaneous measurements of 4 spectra with a 1024 channel resolution (see Figure 4 and Table 1). The channel is a logarithmic conversion from the analogue to the digital signal. Due to the logarithmic scale, the optimization of the measuring conditions can be made with an improved energy resolution and signal-to-noise ratio [86]. The conversion of the channels to the corresponding energy can be made with equation 3. The parameters of the conversion were empirically determined for the specific Quantulus.

$$E = e^{a \cdot \frac{ch}{b}} \qquad [3]$$

where: $a$ is a constant (6.91)
$b$ is the total number of channels (1024)
$ch$ is the channel number.

The background count rate in the measurements of environmental samples is very important. The background in the Quantulus is reduced with both passive and active shielding. The passive shield consists of asymmetrically positioned lead coupled with a layer of copper around the measurement chamber, which reduces the counts from cosmic radiation and radiation resulting from the interactions of cosmic radiation and the shielding material. Active shielding is positioned in the guard and consists of a

mineral oil scintillator above the measurement chamber and two PMTs (see Figure 4). The PMTs in the guard detect the scintillations caused by the external radiation. In pre-designed protocols such signals can be observed in the second MCA. Since thermal noise in PMT's can have a great influence on the efficiency and stability of the counter the Quantulus, is equipped with a Peltier cooling unit to stabilize the temperature in the measurement chamber or change it by up to 12°C from the counter's surroundings [78, 86].

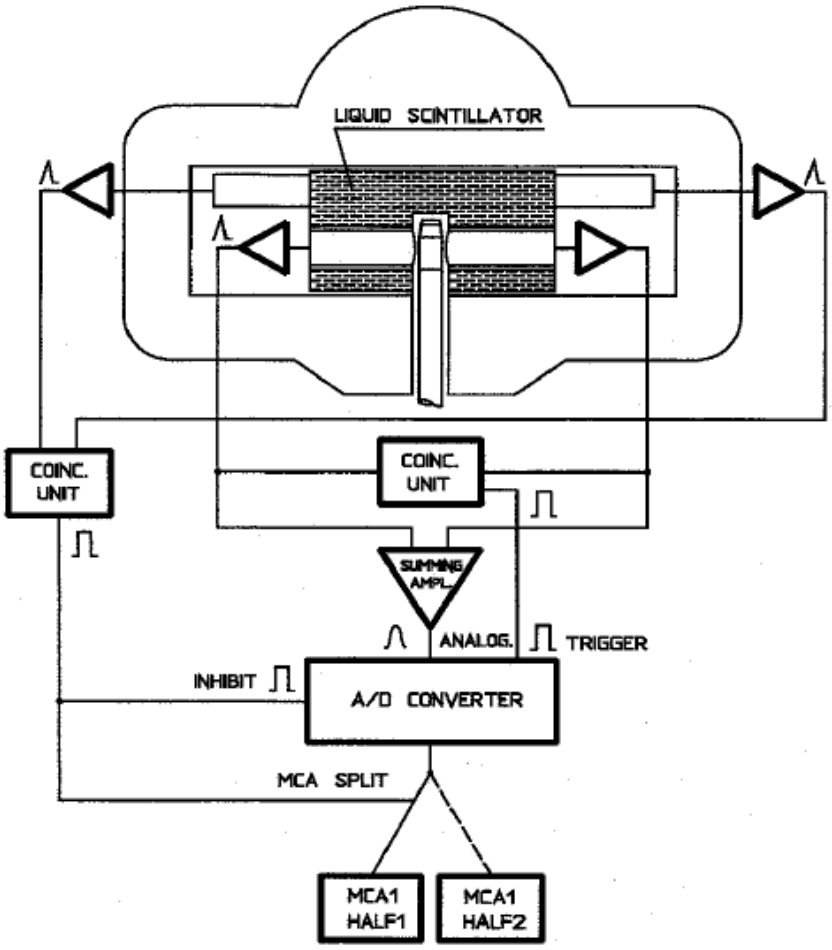


**Figure 4: Wallac Quantulus 1220 circuit scheme** [86]**.** Quantulus consists from 4 PMTs, two coincidence units and two multichannel analyzers. The coincidental events recorded in the sample PMTs are amplified, converted to a digital signal and directed to a pre-determined multichannel analyzer.

### *2.2.1 Pre-designed counting protocol for $^{14}C$ measurements*

The Quantulus has two fully programmable MCAs, which can be split into two halves. In Table 1 a pre-designed setup for the $^{14}C$ measurements is presented. The protocol is set up in a manner such that one MCA covers the guard (MCA2) and the

other analyses the sample count rate. The events in the sample spectrum (MCA1 half 1) have to be coincidental in the PMT's of the measurement chamber. This is used as a trigger for the analog-to-digital conversion (ADC Trigger). If the converted events are not coincidental with the guard pulse or rejected by the pulse amplitude comparator (PAC) they are directed in the first half of MCA1, otherwise they are directed to the second half of MCA1 [86, 87].

**Table 1: $^{14}$C pre-designed protocol configuration.** Event is shown in the sample spectrum (MCA1 half 1) if it is coincidental in both PMTs and it is not rejected by the PAC setting.

| | MCA1 | MCA2 |
|---|---|---|
| **ADC Input** | LRSUM | GSUM |
| **ADC Trigger** | L*R | G |
| **Inhibit** | N | N |
| **Memory Split** | PAC+G | L*R |

Several parameters can be changed in such a protocol: observed spectra, PAC (Pulse Amplitude Comparator) value, coincidence bias, etc. Furthermore, a special setup programmable according to the user's demands can be made, all four functions of the circuit can be changed and functions such as Delayed Coincidence (DCOS), PAC and Pulse Shape analysis (PSA) can be applied [87]. Due to the optimization experiments some changes of the protocol have been made, and in addition the subsequent text explains the meaning of PAC and PSA.

### *2.2.2 Pulse Amplitude Comparator (PAC)*

External radiation and/or trace amounts of radioactive nuclei in the glass envelope of the PMT can cause Cerenkov or fluorescence events. If such an event occurs, the affected PMT pulse will have a large amplitude with the ability to cause a small amplitude pulse in the opposing PMT. Such signals are often referred to as optical crosstalk (see Figure 5). Events in the sample create signals with much smaller differences. Since the PMTs are independent of each other, a comparison of the signal amplitudes can be made. The PAC refines the coincidence of the two facing PMTs by gating on the ratio of the smaller to larger pulse. It is user-adjustable

in scale from 1, where amplitudes can be highly different (no PAC), to 256, where the amplitude ratio is about 0.8 [78, 86]. The amplitudes of all events are compared and sorted into the MCA halves when the PAC is used as a trigger.

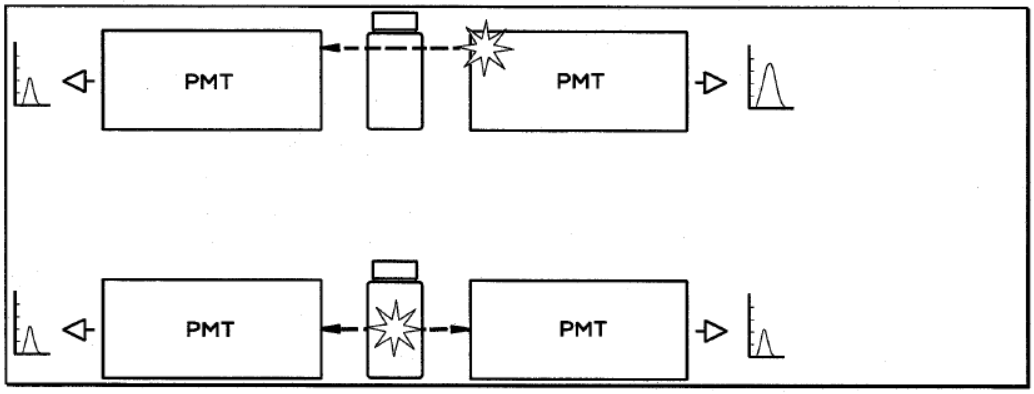


**Figure 5: PAC scheme** [86]**.** In PAC the amplitude of the event recorded by PMT is compared. If the ratio of both PMTs is equal or above the prescribed ratio the event is accepted and shown in the sample spectrum.

### *2.2.3 Pulse Shape Analysis (PSA)*

The Pulse Shape Analysis circuit differs between the alpha and beta pulses by measuring the pulse decay time or length. Alpha-like particles contain a slow florescence component and therefore give a longer pulse, while the beta-like radiation consists of the fast florescence component and gives a shorter pulse (see Figure 6). Some slow florescence events can be observed in the glass-vial background measurements due to the radioactivity of the vial material [78]. The background can be decreased if a correctly set PSA value is applied, where all the beta-like signals will be directed to one spectrum and alpha-like to the other. As in the PAC circuit, the PSA value can also be changed from level 1 to 256. The value 1 means that all the events are alpha-like and the value of 256 for all events are beta-like [86]. The settings of the PSA value are specific for the spectrometer, and thus the measurements should be repeated for each counter applied. Some effects of the sample quench on the PSA value were reported in the literature [86, 88–92]. The counter electronics could be misled because the increased quench shortens the pulse length [86, 89]. Pates *et al.* [92] and Villa *et al.* [88] explained the shifting PSA with the dependence of the value on the radionuclide decay energy.

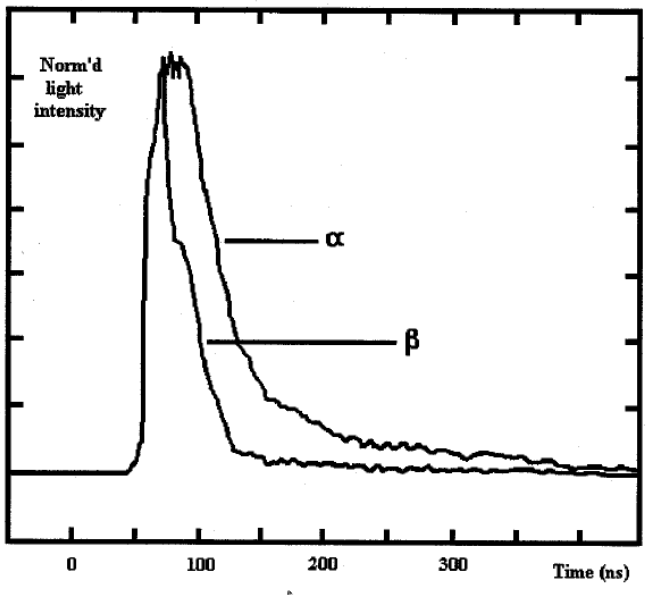


**Figure 6: Differentiation of event origin** [86]**.** Alpha-like events are represented with slow fluorescence and thus give a longer pulse. On the other hand, beta-like events consist of fast fluorescence, and thus their pulse is shorter.

# 3 Synthesis of biodiesels and their characteristics

## 3.1 Introduction to biodiesel synthesis

Biodiesel is produced via the trans-esterification of the fatty acids of vegetable oils and animal fats. Several potential biodiesel resources from different feedstocks are reported and discussed in the literature [42, 47, 51, 58, 93, 94]. Refined vegetable oils are the raw material of the first generation. But there is a lot of controversy regarding the competition with foods and the high transformation costs. For that reason non-edible seeds, algae and waste cooking oil (WCO) have been studied recently [47]. However, such oils can have high contents of free fatty acids (FFA), phospholipids (PL), odorants, etc., while refined oils usually have a low content of impurities. Impurities, especially FFA, greatly affect the trans-esterification with alkali catalysts by causing saponification [1, 4, 44]. Based on the characteristics of the raw material researchers chose between alkaline, acidic, enzymatic or heterogeneous catalysts. According to Ma and Hanna [47] alkaline catalysts are more effective and give faster reaction speeds than acid catalysts, but they require low FFA contents (< 0.5 % w/w). The reduction of the FFA content and the avoidance of saponification can be achieved by pre-esterification. Helwani *et al.* [95] reported that even a reaction catalyzed by alkali (NaOH or KOH) at 60–70 °C, atmospheric pressure and with excess alcohol can take several hours to complete. The use of an acid catalyst eliminates the problem of saponification. The most often applied acid catalysts are sulfuric, phosphoric, hydrochloric and organic sulfonic acids. Meher *et al.* [96] reported the superior catalytic activity of sulfuric acid compared to the hydrochloric acid in the conversion of WCO. In the literature researches are focused on methanolysis, but since ethanol is less toxic and it is mainly derived from a renewable biomass, ethanol was used in the production processes of this thesis.

The production of biofuels was conducted in the laboratory of Group of Biocatalysis and Bioenergy at the Institute of Catalysis and Petrochemistry in Madrid, Spain. In this study, the acid-catalyzed reactions of several oils reported in the literature were compared. The reaction conditions were optimized and applied on WCO, where the effect of the type of substrates agitation, catalyst loading, temperature and molar ratio were determined. The optimal conditions obtained by

WCO were applied in the scale-up production of biodiesel from an additional 8 feedstock oils. Refined and non-refined oils of first and second generation were used.

## *3.2 Materials and methods*

### *3.2.1 Materials*

Refined oils of corn (*Zea mays*), rapeseed (*Brassica napus*) and soya (*Glycine max*) were purchased from the Slovenian market. Non-refined oils of camelina (*Camelina sativa*) and sunflower (*Helianthus annuus*) were also obtained from the Slovenian market. Refined sunflower oil was obtained from the Spanish market. Other samples of non-refined camelina oil were a generous gift from the Camelina Company España. Non-refined jatropha oil (*Jatropha curcas*) was kindly provided by Biodiesel Chiapas (Tuxtla Gutiérrez, Chiapas, Mexico). The waste cooking oil, also used for obtaining the biodiesel production conditions, was collected from restaurants on the Campus of the Autonomous University of Madrid, Spain. The sulfuric acid ($H_2SO_4$, 96 %) was used as a catalyst and purchased from Panreac (Barcelona, Spain). The internal standard, hexadecane and 0.5M sodium methoxide in methanol were obtained from SIGMA-ALDRICH (Madrid, Spain). From Supelco (Bellefonte, PA) 37 FAME Mix GC standard was bought. Other employed solvents were GC-grade from Scharlab (Barcelona, Spain).

### *3.2.2 Methods*

The waste cooking oil was filtered for the removal of any suspended matter. Furthermore, molecular sieves were added to the resultant filtered oil and left through the night at 60 °C.

Monitoring of the esterification stages and the final product were conducted by GC analysis with the method described in Hernandez and Otero [49]. At different reaction times, 400 μL aliquots of samples were taken. Water (0.2 mL) and hexane (2 mL) were added to all the aliquots, which were vigorously mixed with a vortex for 5 min. The ethyl esters in the hexane layer were extracted and dried with sodium sulfate. One μL of the extract was analyzed on Agilent 6890N GC fitted with a flame ionization detector (FID). The Supelco 37 FAME Mix was used for the identification of various fatty acids.

## *3.3 Optimal production conditions*

Most non-edible vegetable and low cost oils contain high FFA and water levels. Thus the selection of the catalyst was under consideration. A strong acid catalyst ($H_2SO_4$) was chosen. Once the optimal reaction conditions determined for the waste cooking oil conversion were tested, a wide variety of feedstock oils was pursued. In this process, the type of agitation, the loading of the catalyst, the effect of temperature and the ethanol:oil molar ratio were evaluated.

### *3.3.1 Type of agitation*

The reaction mixtures had to be agitated in order to facilitate the mass transfer of the two non-miscible reactants (alcohol and oil). Orbital and magnetic agitations were compared in terms of the homogeneity of the mixture and the complete interactions between the reactants. Two sets of reactions were performed using orbital or magnetic agitation at 200 rpm, 60 $^oC$, and 6:1 molar ratio of EtOH: to oil, 10 % w/w $H_2SO_4$ and 24 h reaction. According to the obtained results magnetic agitation was more effective, obtaining 98 % trans-esterified acids (TA) after 7 h. Meanwhile, 91 % TA was obtained with orbital agitation. These results suggested that when a magnetic type of agitation was used an efficient mixing of the reactants and the proper catalyst-substrate interaction were obtained. Therefore, magnetic agitation was used for further trials.

Different agitation speeds were not evaluated in our research, but the effectiveness of the tested speed (200 rpm) was already noted by Stamenković *et al.* [97], who reported that the esterification of vegetable oil could be performed with speeds in the range from 200 to 600 rpm. At lower temperatures (25-60 $^oC$), Helwani *et al.* [95] reported the use of slightly higher agitation speeds (300-700 rpm) when sunflower oil was trans-esterified.

### *3.3.2 Loading of catalyst*

Trials for the determination of the optimal catalyst loading were conducted using magnetic agitation at 200 rpm, a molar ratio of 6:1 (EtOH:oil) at 100 $^oC$ for 24 h. The tested loadings were 2, 5 and 10 % of $H_2SO_4$ with respect to the weight of the substrate's mixture. The effect of catalyst loading on biodiesel production is depicted in Figure 7. The results show that the use of 5 % w/w $H_2SO_4$ ensures 98 % TA after

7 h. This assures the presence of a sufficient percent of catalyst to convert all the fatty acid residues into TA. This was considered as the optimal catalyst loading for further tests. The results obtained with 2 % of catalyst were similar to those with 5 %, and after 7 h of reaction 95 % TA was converted. The increase of catalyst loading did not increased the production of TA or permitted to reduce the reaction time. In fact, the reactions with 10 % of the $H_2SO_4$ were the slowest ones.

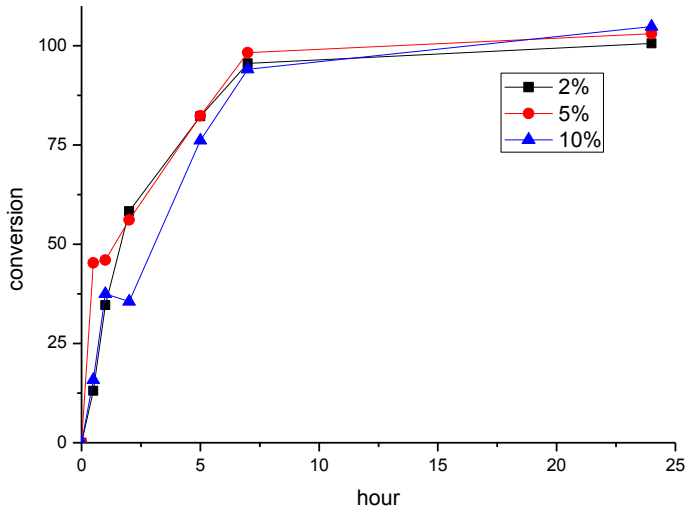


**Figure 7: Catalyst loading and the production of biodiesel.** The reactions were conducted at 100 °C, 200 rpm magnetic agitation and 6:1 (EtOH:oil) molar ratio. Reaction with 5 % of catalyst was shown as the best. Total ester yield is shown as larger than 100 % due to measurement's uncertainty.

### *3.3.3 Effect of temperature*

The reaction rate and ester yield are influenced by the reaction temperature where an increased temperature facilitates the mass transfer and increases the reaction speed [98]. However, the process economy demands a temperature below the alcohol's boiling point. A set of samples in reactors with magnetic agitation at 200 rpm, 6:1 molar ratio (EtOH:oil) and 5 % w/w $H_2SO_4$ were prepared for these experiments. Temperatures of 60, 80 and 100 $^oC$ were evaluated.

Already after a relatively short reaction time (< 7 h), high conversion rates were observed. The reaction at 60 $^oC$ reached 92 % TA, which was also the maximal conversion of fatty acids for this temperature. At the same reaction time, reactions at 80 $^oC$ and 100 $^oC$ obtained 95 and 98 % conversion to TA, respectively. Both

reactions were completed when tested after 24 h. Nevertheless, the reaction at 100 $^{o}$C was faster and gave sufficient yield. Thus this temperature was chosen for further experiments. Miao *et al.* [46] reported the fastest reaction and the highest ester yield (98 %) at the highest explored temperature (120 $^{o}$C). According to Ma and Hanna [47], the reaction temperatures in alkali-catalyzed reactions are lower than in acid-catalyzed processes. In our acid-catalyzed reactions the tests were conducted with waste cooking oil where, due to free fatty acids content, saponification and reducing ester yield is a real problem using alkali-catalysts.

### *3.3.4 Molar ratio evaluation*

Trans-esterification is a reversible reaction. Thus the ethanol:oil molar ratio significantly influences the fatty acids conversion. Nevertheless, a higher molar ratio also increases the miscibility of final products: biodiesel and glycerol. Studies with different substrate molar ratios are reported in the literature. Vyas *et al.* [44] reported a reaction with ratios from 6:1 to 30:1 (MeOH:oil) with $H_2SO_4$ as a catalyst. Wang *et al.* [99] reported a high TA yield after 10 h of reaction with a 20:1 (MeOH:oil) ratio and 4 % of $H_2SO_4$. Keeping in mind the easy separation of the final products, the ratios 3:1, 6:1 and 9:1 (EtOH:oil) were explored in this thesis. The effect of the reagents' molar ratio was evaluated at 24 h, 100 °C, 5 % w/w $H_2SO_4$ and 200 rpm magnetic agitation. The TA yield for the 3:1 ratio was the highest after the first hour of reaction, but the final yield was only around 80 %. A fast reaction was also obtained with the 9:1 ratio, but after 7 h the 6:1 ratio had the same TA yield (around 100 %). Because the content of TA after 7 h of reaction time was comparable for both 6:1 and 9:1 ratios, the 6:1 was considered as a sufficient ratio for the optimal acid-catalyzed trans-esterification reaction.

## *3.4 Scale-up production from various feedstock oils*

Different vegetable oils were used for biodiesel production on a larger scale. With the intention to cover both the existing and possible future feedstock, the choice was made between first- and second-generation vegetable oils. Refined oils of corn, soybean, rapeseed and sunflower as well as non-refined sunflower oil were chosen as representatives of the first generation. Jatropha and two *Camelina sativa* oils were taken as second-generation representatives. The scale-up production of the vegetable oils was conducted using the previously optimized conditions for WCO on a small

scale, namely: with 200 rpm magnetic agitation, 5 % w/w $H_2SO_4$ and 6:1 EtOH:oil ratio. The reactor size was increased from 20 mL to 1 L. The reaction speed and ester yield were similar at 80 and 100 °C. Thus it has been decided to use the lower temperature in a further experiment. The esterification process in each reactor was stopped when at least 90 % TA was obtained. From the results reported in Figure 8 the maximal conversion obtained under these conditions could be higher than those obtained at 7 h. The separation of final products was conducted by decantation overnight.

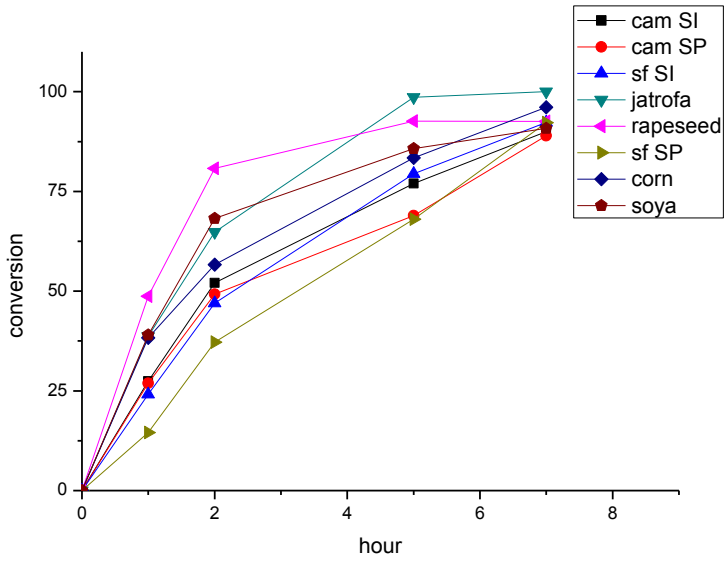


**Figure 8: Scale-up reaction monitoring.** Scale-up was made on oils of corn, jatropha, soya, rapeseed, sunflower (Slovenia, Spain) and camelina (Slovenia, Spain). The highest yield in 7 h was obtained by jatropha oil, while all other oils had yields between 90 and 95 % TA.

During the first two hours of the reaction the highest reaction rate was observed for rapeseed oil, while Spanish sunflower was the lowest with 40 % converted TA. After 5 h of the reaction the highest yield (98 %) was obtained with jatropha oil. Rapeseed, soybean and corn oils also gave yields above 80 % for 5 h of reaction. After 7 h of reaction the jatropha oil gave 100 % of ester yield. Other oils gave yields between 90 and 95 % of TA.

According to the literature, pre-treatment affects the speed of esterification and catalyst performance in the industrial production of biodiesel [46, 47]. In this thesis biodiesels from both refined and non-refined oils were prepared. Thus a comparative analysis could be made. Oils of corn, rapeseed and soya from the Slovenian market

and sunflower from the Spanish market were refined, while all the other oils were non-refined. The average TA yield of the refined oils was 92.9 ± 2.2 %, while the average of the non-refined oils was 92.8 ± 5.0 % TA. In the tested oils and for the used catalyst it has been shown that pre-treatment does not play a significant role. Furthermore, the use of an acid catalyst ($H_2SO_4$) is supported with economical and technical (no production of soaps) reasons [4, 47].

## *3.5 Characterization of produced biodiesels*

The chemical composition and/or physic-chemical properties of biodiesels can have a severe effect on LSC measurement, due to the quench explained in Section 2.1.1 (see page 12). For the same reason the direct LSC method is not commonly used for the measurements of biodiesel. In other LSC methods (see Section 1.2.2 on page 8) the chemical characteristics of the sample do not affect the measurement because they change during sample preparation. In LSC measurements of the reported literature, the studies of various biodiesels are only focused on their different overall carbon percentage. The differences among bio-based materials were noted by Norton and Devlin [17] and Culp *et al.* [64] when bio-based carbon was determined in accordance with the ASTM D-6866 standard. But Norton *et al.* [16] discussed that these differences in various biodiesel materials should be insignificant because their average carbon chain lengths are in the range C16-C20. These authors also stated that the difference in the activity of the sample (about 7 %) could be related to the petrochemically produced alcohol used in the trans-esterification process [16].

In order to investigate the effect of biodiesel characteristics on a direct LSC measurement, the characterization of the produced fuels was necessary. Biodiesels given to the market had to be tested in accordance with the EN 14214 standard [39]. But those data are almost impossible to obtain. In order to define the properties of the biofuels produced in the laboratory, some measurements were performed under the EN 14214 standard. Three parameters that could be important for further LSC measurements were determined immediately after production at the biocatalysts and bioenergy laboratory of the Institute of Catalysis and Petrochemistry. These parameters were the fatty acid composition, oxidative stability and acid number. Regarding the fatty acid composition, the standard EN 14214 is limited to the

contents of linolenic acid and the total ester content. Instead of that the complete fatty acid composition was evaluated. The oxidative stability was evaluated in relation to biodiesel's ageing process, while the acid number could give an insight into the chemical quench present at LSC measurement. In accordance with EN 14214 the cold filter plugging point, density, water content, sulfur and phosphorus content, iodine number, content of glycerol and glycerides, total ester content and content of linoleic ester were determined at the laboratory for fuel measurements at Petrol d.d. The fatty acid composition was also measured one year after production by Petrol d.d. for the evaluation of the chemical change by ageing.

### *3.5.1 Fatty acids composition*

**Table 2: Fatty acid composition of produced biodiesels**

| | FA | C16:0 | C18:0 | C18:1 | C18:2 | C18:3 |
|---|---|---|---|---|---|---|
| Non-refined oils [%m] | Camelina SI | 7.33 | 0.81 | 23.33 | 31.17 | 37.36 |
| | Camelina SP | 12.25 | 6.34 | 34.16 | 47.25 | 5.8 |
| | Sunflower SI | 1.54 | 2.15 | 83.79 | 12.52 | |
| | Jatropha | 13.31 | | 31.76 | 53.8 | |
| | Waste cooking oil | 13.02 | 0.27 | 36.24 | 50.47 | |
| Refined oils [%m] | Rapeseed | 7.19 | | 39.61 | 51.95 | 1.24 |
| | Sunflower SP | 7.33 | 3.63 | 23.33 | 61.71 | |
| | Corn | 10.67 | | 19.64 | 68.75 | |
| | Soya | 14.51 | | 28.99 | 54.87 | 1.62 |

The fatty acids composition was determined in order to obtain the total number of C atoms. The GC analysis in accordance with the Hernandez-Martin and Otero [49] procedure (see Section 3.2.2 on page 21) was used for a determination of the fatty acid composition. The compositions of the produced biodiesels are presented in Table 2. Palmitic (C16:0), oleic (C18:1) and linoleic (C18:2) acids esters were measured in all the produced biodiesels. From the evaluation of the differences encountered among the non-refined and refined biodiesels, we concluded that

biodiesels produced from refined oils obtained a higher percentage of polyunsaturated (linoleic) acid than those made from non-refined oils. In the literature, similar fatty acids levels were reported for the same feedstock biodiesels, despite their different production substrates and synthesis methods, either using alkali or acid-catalyzed trans-esterification with methanol or ethanol [100–102].

### *3.5.2 Oxidative stability and acidity value*

The parameter of oxidative stability is a direct indicator of the biodiesel's lifetime, with each hour of induction time equivalent to one month of usability as a fuel [39]. The test method for the determination of the oxidative stability is described by EN 14112 and called the Rancimat method [103]. In this thesis a 743 Metrohm Rancimat apparatus (Herisau) operating at a temperature of 110 °C was employed. The analysis consists of weighting 2.5 g of biodiesel into a glass vessel and adding 50 mL of deionized water to the conductiometric cells connected with a heated sample. The obtained induction time is used as an indicator of the oxidative stability. The acidity value of the oils determines the quantity of KOH (in mg) needed for neutralizing the biodiesel (1 g) and it is an indicator of free fatty acidscontent. The procedure is specified in the EN 14104 standard [104]. The importance of biodiesel's acidity value in LSC measurements was evaluated with the idea of using this parameter as an indicator of the chemical quench. The levels of these two parameters are prescribed in the EN 14214 standard. For the oxidative stability, the limit is 6 h while for the acidity value a maximum of 0.5 mg KOH/g [39] is prescribed. The obtained results are divided in accordance with the oil pre-treatment and are presented in Table 3.

The acidity value is lower in the case of biodiesels from refined oils than in those from non-refined ones. However, only three biodiesels would comply the prescribed values in standard EN 14214 for the acidity value (< 0.5). These are the biodiesels from soya, rapeseed and jatropha. Although the acidity value for biodiesel from waste cooking oil was expected to be higher (AV above 1), the highest observed level was that of the biodiesel produced from the sunflower oil of the Slovenian market. This high value could be explained by the large amount of unreacted FFA, since this was one of the oils with a lower conversion level (see Figure 8 on page 25). As will be shown further in the text (see Section 7.4 on page 69), LSC

measurements of this fuel obtained the highest counting efficiencies. Consequently, the acidity value could not be used as an indicator for a chemical quench. Furthermore biodiesels with low acidity values obtained a large variety of observed quench values. From the literature, Ramos *et al.* [105] reported acidity values for rapeseed, soya, sunflower and corn biodiesel of 0.16, 0.14, 0.15 and 0.15, respectively. These values are not in agreement with our measurements. Our higher values could be a consequence of the higher water content that produces hydrolysis of the glycerol.

**Table 3: Oxidative stability (OS) and acidity value (AV) measurements**

| | Non-refined [$\%_m$] | | | | | Refined [$\%_m$] | | | |
|---|---|---|---|---|---|---|---|---|---|
| **Parameter** | Cam. SI | Cam. SP | SF SI | Jat. | WCO | Rape | SF SP | Corn | Soya |
| **AV [mg KOH/g]** | 1.27 | 0.97 | 2.64 | 0.5 | 1.28 | 0.38 | 0.76 | 0.75 | 0.38 |
| **OS [h]** | 2.58 | 2.18 | 23.32 | 5.48 | 0.9 | 2.8 | 24.47 | 5.52 | 20.8 |

Oxidative stability is a characteristic of each individual oil/biodiesel, since it is related to FA composition and the antioxidant content of the feedstock. This can be demonstrated with the biodiesel produced from sunflower and camelina oils whose oxidative stability values were similar. Waste cooking oil has been reheated several times during its use, thus it has a low oxidative stability, as expected. In order to comply with the standard EN 14214 oxidative stability requirement, all biodiesels with less than 6 h of stability need more additives to increase their oxidative stability. Compared to the values reported in the literature (0.15 and 2 h [105]), the values obtained for sunflowers were above this range, while others were comparable within 1 h.

### *3.5.3 EN 14214 measurements*

Some measurements demanded in the EN 14214 standard were conducted for an evaluation of the physical and chemical characteristics of the produced biodiesels, and to compare them with some industrial biodiesels from the literature. The results

of those measurements are presented in Table 4 and discussed in individual subchapters.

**Table 4: Physical characterization in accordance to EN 14214.** Order of biodiesels from left to right: camelina Slovenia, camelina Spain, sunflower Slovenia, jatropha, waste cooking oil, rapeseed, sunflower Spain, corn and soya.

| | Non-refined [%m] | | | | | Refined [%m] | | | |
|---|---|---|---|---|---|---|---|---|---|
| **Parameter** | Cam. SI | Cam. SP | SF SI | Jat. | WCO | Rape | SF SP | Corn | Soya |
| **Cold filter plugging point [°C]** | -9 | -8 | -4 | -6 | -7 | -10 | -6 | -11 | -7 |
| **Density [kg/m$^3$]** | 880.4 | 882.9 | 872.4 | 873 | 884.6 | 879.2 | 881.6 | 870.5 | 873 |
| **Water [mg/kg]** | > 1000 | > 1000 | 660 | > 1000 | > 1000 | > 1000 | > 1000 | > 1000 | > 1000 |
| **Sulphur [mg/kg]** | > 60 | > 60 | > 60 | > 60 | > 60 | > 60 | > 60 | > 60 | > 60 |
| **Phosphorus [mg/kg]** | < 3 | < 3 | < 3 | < 3 | < 3 | < 3 | < 3 | < 3 | < 3 |
| **Iodine number [g I/100g]** | 202.9 | 198.6 | 165.5 | 142.9 | 139.6 | 169.3 | 148.7 | 148.2 | 154.2 |
| **Ester [%m]** | 43.8 | 44 | 84.6 | 41.0 | 36.1 | 53.6 | 26.5 | 27.1 | 30 |
| **Linolenic [%m]** | 22.6 | 21.1 | 0.2 | 0.2 | 0.2 | 5.3 | 0.1 | 0.7 | 4.2 |

#### *3.5.3.1 Cold filter plugging point*

The cold filter plugging point (CFPP) is a characteristic which determines the temperature sensitivity of biodiesel, specifically at which temperature glycerol from the biodiesel would plug the filter [105]. The average environmental temperatures differ across Europe. Thus this characteristic is based on the temperature of the climatic zone and determined individually for each country. The CFPP parameter

should be at least -20 °C for Central and Western Europe diesel in the winter period [106, 107]. From observation of the data obtained for the biodiesels, manufactured on our own for the purpose of the thesis, the additives to improve their CFPP values would be nedded. However, in the summer period, these measures would not be necessary. According to the largest distributor of fuels in Slovenia [108], such additives are used in all fuels sold in the winter season. The lowest temperature sensitivity was obtained for rapeseed and corn biofuels, which could be one of the reasons for the popularity of these feedstocks on the fuel market [47]. From the literature, Ramos *et al.* [105] reported CFPP temperatures for rapeseed, soya and corn biodiesels within the range of our measurement uncertainty (2 °C).

#### *3.5.3.2 Density*

According to the standard procedure, the density is determined at 15 °C [109, 110]. The EN 14214 standard limits the density to 860-900 kg/m$^3$. Thus all our biodiesels comply with this requirement [39]. As can be observed from Table 4, all the biodiesels had a density around 880 kg/m$^3$. This was not expected, since a great variety of values have been described in the literature. Srivastava [111] reported biodiesels of sunflower, soya and rapeseed oils with densities of 916, 913 and 911 kg/m$^3$, respectively. While Demibras [112] reported a densities of waste cooking oil and its biodiesel of between 897 and 924 kg/m$^3$.

#### *3.5.3.3 Water content*

Biodiesel is hydrophilic, and the water content depends on the storage conditions [4]. Our biodiesels were stored in plastic bottles at room temperatures in a locker. The effect of unsuitable storage conditions and a long period between production and measurement is clearly shown in the water content. Measurements show that none of the biodiesel produced would comply with the EN 14214 standard limit for water content, which is 500 mg/kg [39]. The closest to the limit is the biodiesel from Slovenian sunflower, which could be dehydrated with molecular sieves. This desiccant was used to treat waste cooking oil before biodiesel production. Although water content is rarely mentioned in the literature, Demirbas [112] reported a water content of 460 mg/kg for biodiesel produced from waste cooking oil.

#### *3.5.3.4 Sulfur content*

Fossil diesel often contains large amounts of sulfur. It has been widely demonstrated that sulfur represents one of the greatest environmental risks, due to the formation of acid rain. One of the major advantages of biodiesel is its low sulfur content. However, organic compounds containing sulfur produce a protective layer on the metal surfaces of engines, therefore increasing their lifetime [2, 4]. The EN 14214 standard limits the sulfur content in fuels to 10 mg/kg. Environmentally undesirable components in fuels are reduced in refineries worldwide [39]. The quantities of sulfur measured in our samples were above the EN 590 and EN 14214 limits (max. 10 mg/kg). Thus these fuels could not be used in European countries. It is safe to presume that the quantities of sulfur measured in the produced biodiesels are a consequence of unsophisticated cleaning of the samples after production. However, the sulfur contents reported in the literature are often much higher than the limit value of the European standard. Nicolau *et al.* [113] reported sulfur contents in used diesels between 10 and 130 mg/kg. The production of our biodiesels was not made on an industrial scale and the fuels are not used in the fuel market. Thus in these cases, the significance of the sulfur content is minimal.

#### *3.5.3.5 Phosphorus content*

The significance of the phosphorus content is due to its effect on the catalytic conversion of the fuel in the vehicle's exhaust system. The presence of phosphorus depends on the type of raw material, since it is related to the phospholipids content of the oil. The quantity of phosphorus decreases if refined oils are used [114]. According to the results obtained in this thesis, the quantity in all the fuels produced is lower than the EN 14214 limit of 10 mg/kg [39]. Mendow *et al.* [93] reported that 97 % of phosphorus was found in the glycerin phase. The separation of biodiesel and glycerol was conducted overnight. This explains the low values found for the phosphorus content. A differentiation between refined and non-refined oils was not observed.

#### *3.5.3.6 Iodine number*

The iodine number is related to the number of fatty acid double bonds. Analyses of this parameter can give an insight into the sample composition. Encinar [115] reported that the higher iodine numbers, the higher the number of double bonds in

biodiesel. The limit for the iodine number is 120, according to the EN 14214 standard [39]. All our biodiesels gave levels between 139.6 and 202.9, which means the iodine numbers are too high. This could be the consequence of biodiesel ageing at the time of measurement, since as I will show further in the text, the degradation of fatty acids increases the number of double bonds. Encinar [115] also reported variations in the iodine numbers between 71.3 and 99.4 in biodiesel prepared from the same vegetable oil.

#### *3.5.3.7 Total ester content and content of linolenic acid ester*

The total ester content is a parameter that determines the quality of biodiesel, since it is related to the conversion products. Biodiesel is a biodegradable material, thus the total ester content is reduced during storage [4, 101]. This can also be observed from the results presented in Table 4, where only biodiesel from Slovenian sunflower oil maintained a relatively high ester content. This is not surprising, since according to measurements of oxidative stability (see Table 3 on page 29), sunflower biodiesel had the highest observed number. In the case of sunflower biodiesel from Spain, the low ester content could not be explained. The observed ester contents were expected due to the low oxidative stabilities of other biodiesels. According to the EN 14214 standard limit for ester content, these fuels could no longer be used as fuels [39].

The degradation of biodiesel increases the number of unsaturated fatty acids, while the quantity of linolenic acid is also increased [4, 101]. Since the EN 14214 standard limit is 12 $\%_m$, both camelina biodiesels exceed the prescribed limit. The rest of the biodiesels obtained a lower content of linolenic acid ester. According to the reports of Ramos *et al.* [105], the observed linolenic contents from 0.1 to 7.9 $\%_m$ were not significantly higher; furthermore, in the case of soya and rapeseed biodiesels our levels were significantly lower.

#### *3.5.3.8 Glycerol content*

The glycerol content is a measure of the biodiesel's separation efficiency and the age of the biodiesel. Glycerol from biodiesel separation was conducted by decantating in a column overnight. Thus, low quantities of glycerol were expected. However, glycerol is produced again during biodiesel degradation, since it is one of the decay products [4, 46, 47, 105, 116]. The results of measurements are presented

in Table 5. According to the EN 14214 standard, the total glycerol quantity exceeded the limit value only in corn biodiesel, while the free-glycerol quantities were over the limit in camelina Slovenia, jatropha, waste cooking oil, corn and soya. In the literature, Ramos *et al.* [105] reported similar total glycerol contents in corn, rapeseed and sunflower biodiesels, while the free-glycerol contents were always lower than those observed in our biodiesels. However, Mittlebach [116] reported higher free and total glycerol contents in rapeseed biodiesel (0.02 and 0.24, respectively).

**Table 5: Glycerides and glycerol measurements**

| | Non-refined [$\%_m$] | | | | | Refined [$\%_m$] | | | |
|---|---|---|---|---|---|---|---|---|---|
| **Parameter [$\%_m$]** | Cam. SI | Cam. SP | SF SI | Jat. | WCO | Rape | SF SP | Corn | Soya |
| **mono-glycerides** | 0.637 | 0.562 | 0.259 | 0.104 | 0.251 | 0.316 | 0.250 | 0.397 | 0.305 |
| **di-glycerides** | 0.104 | 0.094 | 0.171 | 0.070 | 0.142 | 0.125 | 0.095 | 0.088 | 0.040 |
| **tri-glycerides** | 0.003 | 0.031 | 0.067 | 0.016 | 0.007 | 0.105 | 0.032 | 0.051 | 0.003 |
| **Total glycerol** | 0.212 | 0.168 | 0.106 | 0.062 | 0.113 | 0.126 | 0.083 | 0.344 | 0.251 |
| **Free glycerol** | 0.034 | 0.008 | 0.008 | 0.023 | 0.028 | 0.016 | 0.002 | 0.225 | 0.167 |

Quantities of mono-, di- and tri-glycerides are oil conditioned, thus the quantities in the same oils (in our case camelina and sunflower) should have been similar. The obtained results are in agreement with this statement, since the difference between both oils (Slovenian and Spanish) does not exceed 20 %. The only exception is the case of tri-glycerides in camelinas, where biodiesel from Spanish camelina has a 10 times higher value than in the Slovenian one. In the literature, different levels were also observed. Ramos *et al.* [105] reported sunflower biodiesel levels (0.06, 0.05 and 0.31 for mono-, di- and tri-glycerides) similar to ours, while the quantities of di- and tri-glycerides in corn (0.06 and 0.01) and rapeseed (0.08 and 0.03) biodiesel were

significantly lower. In the case of soya biodiesel, Ramos *et al.* [105] obtained a biodiesel with a lower mono-glyceride content (0.21), but significantly higher di- and tri-glycerol contents (0.1 and 0.07). Mittlebach [116] reported up to 20 times higher tri-glycerol contents of rapeseed-based biodiesel. All our biodiesels would meet the criteria for the prescribed limit in the EN 14214 standard [39].

### *3.5.4 Decomposition of fatty acids*

**Table 6: Fatty acid composition a year after the preparation of biodiesels.** The levels are calculated as a percentage of the total TA present. Compared to the first analysis, a larger amount of poly-unsaturated fatty acids were observed.

| | FA | C16:0 | C16:1 | C18:0 | C18:1 | C18:2 | C18:3 |
|---|---|---|---|---|---|---|---|
| Non-refined [%m] | Camelina SI | < 0.2 | 10.6 | < 0.2 | 3.5 | 29.5 | 52.4 |
| | Camelina SP | < 0.2 | 10.2 | < 0.2 | 3.9 | 32.9 | 49 |
| | Sunflower SI | < 0.2 | 3.7 | < 0.2 | 3.3 | 91.3 | 0.3 |
| | Jatropha | < 0.2 | 25.3 | < 0.2 | 9.9 | 63.2 | 0.5 |
| | Waste cooking oil | 0.3 | 28.5 | < 0.2 | 7 | 60 | 0.7 |
| Refined oils [%m] | Rapeseed | < 0.2 | 9 | < 0.2 | 3 | 75.9 | 10.2 |
| | Sunflower SP | < 0.2 | 15.7 | < 0.2 | 9.6 | 71 | 0.6 |
| | Corn | < 0.2 | 27.5 | < 0.2 | 3.8 | 64.4 | 2.7 |
| | Soya | < 0.2 | 24.8 | < 0.2 | 9.4 | 48.7 | 14.3 |

The decomposition of biodiesel is clearly shown in some of the measured parameters from the EN 14214 standard. The fatty acid composition of biodiesels was measured immediately after their production and repeated a year after. The results of the second measurement are presented in Table 6. A change of fatty acids arrangement was observed in comparison to the data of the first measurements (see Table 2 on page 27). An increase in the unsaturated fatty acids percentage was generally observed, thus almost no palmitic (C16:0) and stearic (C18:0) acids were detected. The quantity of oleic (C18:1) acids also decreased, while the percentage of linoleic (C18:2) acid increased. A large increase was also observed in the level of

linolenic acid (C18:3), which in the first measurements was only detected in biodiesels from camelinas (37.36 and 5.8 %), rapeseed (1.24 %) and soya (1.62 %), while in the second analyses it is present in all the biodiesels. The levels are calculated as a percentage of the total TA quantity, unlike in the data from Table 4, where the quantity of linolenic acid is calculated for the total amount of sample.

#### *3.5.4.1 Cetane number*

The decomposition of the samples was also evaluated through calculation of the cetane number, as suggested by Bamgboye and Hansen [102]. The authors introduced the theory of cetane number calculations, based on biodiesel fatty acid composition. In our case, the sample's composition was measured twice, and the comparison via cetane number was conducted. The results are presented in Table 7. The average cetane number of the non-refined feedstock biodiesel was 47.9 ± 6.7, calculated from data obtained directly after production. At the same time, the refined feedstock obtained a comparable cetane number, 46.8 ± 1.3. The cetane numbers calculated from the data obtained a year after production are completely different. The average cetane number obtained in non-refined biodiesels was 36.5 ± 5.0, while the refined ones gave values of 40.4 ± 1.9. That complies with the general prescription of using refined oils for the production of biodiesels found in the technical literature [4, 101]. Multiple-times-reheated waste cooking oil showed a higher cetane number, both after production and a year after that.

The overall ageing of the biodiesel was shown in both the parameters measured in accordance with the standard EN 14214 and the fatty acid composition. In the last case, a great increase in unsaturated fatty acid showed the partial decomposition of biodiesels. This fact in theory limits the use of such fuels in experiments. However, as will be shown further in the text (see Section 7.7.5 on page 85), the decomposition of biodiesels occurring during this investigation did not affect the LSC measurements. With a changed protocol and improvements in the calculations, eventual changes in the biodiesel were taken into consideration, therefore not affecting the accuracy of the calculated activity.

**Table 7: Degradation of biodiesel via evaluation of cetane number.** Biodiesel from both non-refined and refined oils degraded. Cetane number showed that degradation of biodiesels from the refined oils degraded in a smaller extend.

| | Feedstock | Measurement after production [cetane number] | Measurement after 1 year [cetane number] |
|---|---|---|---|
| Non-refined [%m] | Camelina SI | 39 | 32.1 |
| | Camelina SP | 48.6 | 32.6 |
| | Sunflower SI | 55.3 | 38.4 |
| | Jatropha | 48.6 | 42.7 |
| | Waste cooking oil | 49.2 | 43.2 |
| Refined oils [%m] | Rapeseed | 47.4 | 37.7 |
| | Sunflower SP | 46.7 | 41.7 |
| | Corn | 45 | 41.5 |
| | Soya | 47.9 | 40.8 |

# 4 General experimental parameters in biofuel analysis

The procedures and equations that were applied several times during the thesis are explained in detail in the following subchapters.

## 4.1 LSC sample preparation

Samples measured in LSC often need radiochemical pre-treatment. Section 1.2.2 (see page 8) mentions two methods for measuring $^{14}C$ that need such a treatment. In the case of the direct method, which is the focus of this thesis, a radiochemical pre-treatment is not necessary. They are simply prepared by the addition of the original sample (in this case fuel) and a scintillation cocktail to the measuring vial.


**Figure 9: Prepared samples and used material**

In the preparation of the LSC samples, a Metler Toledo XS205 balance and semi-automatic pipettes of 0.1, 1 and 5 mL were used. The balance and pipettes were regularly checked, maintained and calibrated. Samples of bio-components and fossil fuels were stored in dark glass flasks at room temperature in a closed locker. The scintillation cocktail was stored in the original container in the same locker. The material used was out of the locker only for the duration of the LSC sample preparation.

All the LSC samples for the experiments described in the following text were prepared in 20 mL high-performance glass vials with low $^{40}K$ purchased from PerkinElmer. The vials were chosen based on the volatility of the fuels and the background counting rate. Some samples were measured in plastic vials purchased from the same producer. These vials were not used in further experiments due to the evaluation of the counting efficiency, background count rate and stability of the sample (evaporation). Ten mL of commercially available scintillation cocktail Ultima Gold™ F (PerkinElmer) was used in the mixture with 10 mL of fuel. The scintillation cocktail was chosen due to the large sample uptake and good mixing with biological samples. A few experiments with ethanol and HiSafe 3 scintillator (PerkinElmer) were conducted. The use of this scintillation cocktail was reduced for the same reason as the plastic vials.

Therefore, for the preparation of the LSC samples the following material was used:

- 20 mL high-performance glass vials,
- 10 mL of scintillation cocktail Ultima Gold™ F,
- 10 mL of sample in the desired percentage of bio-component.

In the preparation of the sample, each component added is weighed. Thus we obtain the masses of the vial, scintillation cocktail and sample (fuel). The calibration samples were prepared with a known amount of bio and fossil component. The mass percentage of biofuel was calculated using equation 4. Such a preparation was used because it was recognized as being more precise than the volumetric percentage of added components.

$$\%_m\ of\ biofuel = \frac{m_{bio}}{m_{bio} + m_{fos}} \qquad [4]$$

where: $m_{bio}$ is mass of bio-component [g]

$m_{fos}$ is mass of fossil fuel [g].

## *4.2 LSC measurement*

The LSC sample was left in the counter for at least 4 h before it was measured. This delay decreases the chance of photo-luminescence and allows the sample to

equilibrate with the counter temperature. The counter temperature was 18 °C, while the preparation temperature was between 20 and 22 °C. Unless otherwise noted, the pre-designed measurement protocol described in Section 2.2.1 was used. An unquenched standard set of $^{14}C$, $^{3}H$ and a blank sample (PerkinElmer) was used for the verification of the counter stability in the experiments.

### *4.2.1 Activity calculation*

Two types of calculations and therefore calibrations have been adopted. In the first so-called one-step calculation, the sample's count rate was adjusted for the background counts and the mass of the sample (cpm/g of sample). These data are then used in the calculation of the mass percent of biofuel in the sample ($\%_m$) in accordance with the calibration curve of the specific mixture. In the second type of calculation two steps are applied; therefore, this procedure will be addressed as the two-step calculation. The first step is the same as in the procedure just described, that is the adjustment of the count rate for the background and the mass of fuel in the LSC sample. The second step is the adjustment of the data for the counting efficiency of the specific sample. Data in the form of dpm/g of sample were then used in the calculation of the mass percentage based on the calibration curves for the specific fuel mixture.

### *4.2.2 Counting efficiency*

The counting efficiency has an important role in the second step of the activity calculation. Two possibilities for obtaining the counting efficiency were used in this thesis. The measured SQP(E) value was used in all the measurements conducted on the LSC counter. For obtaining the counting efficiency this value has to be correlated via the quench calibration curve. A $^{14}C$ labeled Ultima Gold low-level quench standard set was purchased from PerkinElmer and measured in the counter. It consists of eight LSC samples in sealed glass vials with 41000 dpm/g and various concentrations of chemical quencher. Thus the count rates of such LSC samples are different due to the differences in the observed quench. An average count rate of 3 cycles was used for the calculation of the efficiency. The quench calibration curve was fitted using correlations between the SQP(E) values and the efficiencies of the measured samples (see Figure 10).

The application of the sample spectra quench parameters (SQP(I) and SIS) was also tested. The accuracy of both parameters is related to the sample count rate, which is low in the environmental samples. Therefore the addition of radioactive material would be necessary for all biofuel samples what could cause environmental problems due to the radioactivity of the measurements waste. It was decided to use only SQP(E) in the routine measurements.

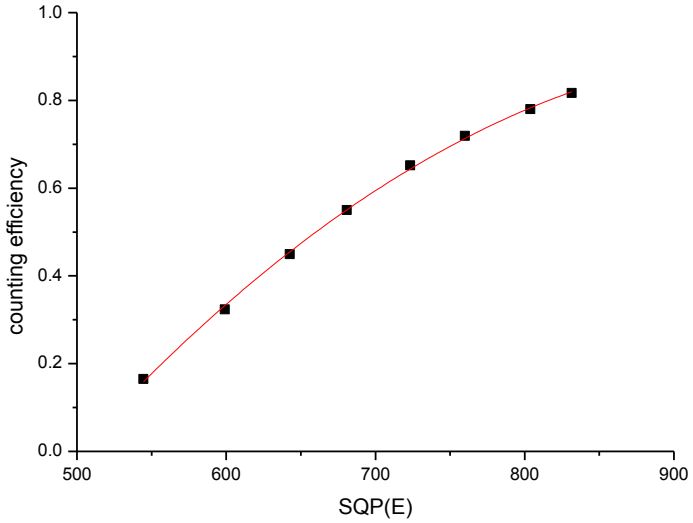


**Figure 10: Quench curve conducted from purchased samples.** Figure presents changes in the counting efficiency correlated to changes in the observed SQP(E) value of the measured LSC samples.

**Table 8: Quench curve fitting parameters.**

| Intercept | | Slope [x] | | Slope [$x^2$] | | Statistics |
|---|---|---|---|---|---|---|
| **Value** | **Error** | **Value** | **Error** | **Value** | **Error** | **$R^2$** |
| -2.814 | 0.155 | 0.008 | 4.5E-4 | -3.8E-6 | 3.3E-7 | 0.999 |

Internal standardization was the second approach used to obtain the counting efficiency. Such an approach demanded large amounts of added activity and destroyed the sample, so it was not used for all the samples. Nevertheless, the efficiencies of all the calibration samples were obtained by internal standardization. $^{14}C$ labeled toluene with a certified activity of 517000 ± 6721 dpm/g was purchased from PerkinElmer and used as an internal standard. A gravimetrically determined standard solution was prepared from standard and fossil fuel. Two solutions were

prepared: 13477 ± 144 dpm/g in fossil diesel and 11317 ± 121 dpm/g in fossil ethanol. A standard solution in fossil ethanol was used for the ethanol as well as the gasoline calibration curve. Typically, 0.1 mL of the standard solution was added to the LSC samples. The quantity was chosen based on an ability to conduct rapid measurements with sufficient counting statistics, an ability to add and weigh the amount of solution, and without changing LSC sample matrix. The SQP(E) values before and after the standard addition were within the parameter's uncertainty.

## *4.3 Optimization and validation calculations*

A maximized figure of merit (FM) was adopted as a measure for the optimization process of the setups. This was calculated via equation 5. Such an approach was chosen based on general use in LSC measurements [9, 70, 78, 79, 85, 117].

$$FM = \frac{\varepsilon^2}{B} \quad [5]$$

where: $\varepsilon$ is the counting efficiency (%),

$B$ is the background count rate (cpm).

The method was validated according to the recommendations of ISO/IEC 17025 standard, where Section 5.4.5.3 of the standard suggests an evaluation of the detection limit, linearity, repeatability and sensitivity [118]. Uncertainty and trueness were also evaluated. All the listed parameters were understood as the general terms used in metrology [119]. For the method to be applicable to the fuel market, it had to comply with the following parameters: detection limit below 1 $\%_m$, repeatability and trueness within uncertainty limits and linearity of the calibration curves.

### *4.3.1 Uncertainty*

The uncertainty of the method was calculated according to the law of propagation of uncertainties using $k = 2$ for a level of confidence of 95 %. The contribution of the variable uncertainties to the total uncertainty was evaluated using GUM guidelines [120]. The results are directly affected by the uncertainty of the balance, sample and background counting, counting efficiency and uncertainty of calibration (see equation 6). The pipetting, temperature variation and luminescence of the samples make indirect contributions to the uncertainty and are manifested in the above-

mentioned uncertainties. The uncertainty of the balance was calculated as a standard deviation of the multiple weighing measurements of the same sample. Compared to the uncertainty calculated based on the balance calibration certificate the obtained uncertainty was conservative. The uncertainty of the sample was obtained in accordance with equation 7. The background uncertainty was evaluated as a standard deviation of several measured backgrounds (more than 100 spectra). All samples with quantity of biofuel below detection limit were taken in evaluation of background variation. The uncertainties of the sample and the background were evaluated as a combined uncertainty based on equation 8. The declared uncertainty of the certified standard solution applied for the quench curve was taken for a determination of the uncertainty of the counting efficiency. The uncertainties of the calibration fitting parameters were taken as an uncertainty of the calibration. In the fitting procedure with OriginPro 8.0 software [121] all the measurement uncertainties were considered.

$$u(\%_{mass}) = \%_{mass} \cdot \sqrt{\frac{u^2(m)}{m^2} + \frac{u^2(\varepsilon)}{\varepsilon^2} + u^2(C_S - C_B) + \frac{u^2(cal)}{cal^2}} \qquad [6]$$

where: $u(m)$ is uncertainty of balance,

$u(\varepsilon)$ is uncertainty of counting efficiency,

$u(Cs\text{-}C_B)$ is uncertainty of sample and background counting,

$u(cal)$ is uncertainty of calibration

$$\mathrm{u(C_S)} = \sqrt{\mathrm{N}} \qquad [7]$$

where: $u(C_S)$ is uncertainty of sample counts in time period,

$N$ is total number of counts.

$$u(C_S - C_B) = \sqrt{\frac{u^2(C_S) + u^2(C_B)}{(C_S - C_B)^2}} \qquad [8]$$

where: $u(C_B)$ is uncertainty of background counts in time period.

### *4.3.2 Detection limit*

The limits of detection were calculated according to the, in radiochemistry, well-known Currie [122] and a new approach described in standard ISO 11929 [123]. In the latter a null measurement uncertainty is applied, and thus the probability definition in Currie and ISO 11929 differs. In classical statistics, the real quantity value is not known and its determination is the main task. On the other hand, ISO 11929 allows true value probability calculations from the observed value and its uncertainty. The detection limits were compared and used for the characterization of the level at which the measurement precision is satisfactory for a quantitative determination of the bio-component content in the fuel blends. The background count rate obtained after 1000 min of counting time was taken for the calculations, thus obtaining at least 1000 counts and enabling a measurement uncertainty of 3 % also near the limit of detection. For comparison, the limits of detection in diesel fuel were also evaluated with a long time average. In both cases, the sample counting time was used conservatively, 500 minutes per sample.

#### *4.3.2.1 Calculation in according to Currie*

Currie [122] introduced three kinds of characteristic limits where the first two were used in biofuel analysis. First, the critical limit detection level ($L_C$, equation 9) where the signal is detected with an acceptable error of the first kind.

$$L_C = k_a \cdot \sigma_B \qquad [9]$$

where: $k_a$ is uncertainty level at acceptable error of the first kind

$\sigma_B$ is standard deviation of background signal.

The value where the signal is detected and measured with the probability *1 - b* is the limit of detection ($L_D$) and calculated in accordance with equation 10.

$$L_D = L_C + k_b \cdot \sigma_D(L_D) \qquad [10]$$

where: $k_b$ is abscissa of the normal distribution at error of the second kind

$\sigma_D$ is standard deviation of background subtracted signal.

We can assume $\sigma^2 = N$ when the signal is equal to the number of counts of radioactive decay. The activity corresponding to the limit of detection is calculated in accordance with equation 11 assuming that $a = b = 0.05$.

$$A_{L_D} = \frac{2.71 + 4.65 \cdot \sqrt{N_B}}{t_S \cdot \varepsilon \cdot m} \quad [11]$$

where: $N_B$ is the number of background counts

$t_S$ is the sample counting time

$\varepsilon$ is the counting efficiency

$m$ is the sample mass.

#### *4.3.2.2 Calculation in according to ISO 11929*

The decision threshold (DT) at which the signal from the measurement system cannot be attributed to sample property with the predefined probability is calculated with equation 12.

$$DT = k_a \cdot u(0) \quad [12]$$

$$u(0) = \sqrt{w^2 \cdot \left(u^2(C_s) + u^2(C_B)\right) + A^2 \cdot u_{rel}^2(w)} \quad [13]$$

$$w = \frac{1}{m \cdot \varepsilon} \quad [14]$$

where: A is activity of the sample

$u_{rel}^2(w)$ is the sum of the squares of the relative uncertainties of the mass and efficiency

The detection limit is calculated in accordance with equation 15. In order to get result of equation 15, the equation 13 had to be rearranged and written in the form of equation 16. The result of equations 15 and 16 was modified into the form of equation 18 where activity at the detection limit is calculated.

$$DL = DT + k_\alpha \cdot u(DL) \quad [15]$$

$$u(A) = c_0 + \frac{w}{t_S} \cdot A + u_{rel}^2(w) \cdot A^2 \quad [16]$$

$$c_0 = w^2 \cdot C_B \cdot \left(\frac{1}{t_S} + \frac{1}{t_B}\right) \quad [17]$$

$$A_{DL} = 2 \cdot DT + \left(\frac{k_a}{3 \cdot DT}\right) \cdot \left(u^2(3 \cdot DT) - u^2(0)\right) \quad [18]$$

Where meaning of the parameters are as explained with the previous equations.

### *4.3.3 Validation parameters*

Linearity was demonstrated by the least-square method and the correlation coefficient $R^2$, which is the square of the Pearson product moment correlation coefficient. The least-square method was applied in the software package OriginPro 8.0 [121] when the calibration curves were fitted. The data of the fitting parameters errors, which determine the width of the calibration curve, were applied as the uncertainty of the calibration. This approach was chosen because the uncertainty of the individual calibration point was considered during the determination of the regression line.

Repeatability was evaluated as a standard deviation of the calculated results as the mass percentage of bio-component. Repeatability was taken to be acceptable when the result was within 2 standard deviations. The standard deviation was calculated by dividing the sum of results by *n-1* in order to obtain unbiased estimate of the results. For that purpose, one blend for each calibration curve was prepared and measured for ten consecutive counting cycles, each being 100 minutes long. The same measurement values were analyzed by one- and two-step calculation procedures when such a protocol was applicable. Repeatability is included in the uncertainty budget as a count-rate variation.

Two aspects were used for the verification of reproducibility: multiple measurements in a short period of time and a change of the measurement conditions. For the first evaluation, replicas of one blend for each calibration curve were prepared and measured twice in a period of a week. The applied method for standard-deviation calculations was the same as for the repeatability. In the second evaluation, samples were measured in a period of one month, when they were exposed to a

temperature change during the measurement. The reproducibility of the method was acceptable if the result of evaluation was within the uncertainty of the method.

Sensitivity was evaluated through the slope of the calibration curve. Slopes reported in the summary of the fitting parameters were evaluated. The steepest linear regression curve was determined as the most sensitive and vice versa.

The trueness of the method was tested by collaboration in international comparative measurements. Acceptability of the result was tested with ζ-test (see equation 19). As a limit for the acceptability and trueness of the method zeta-score of 2 was chosen.

$$\zeta - \text{test} = \frac{|x - x_t|}{\sqrt{u(x)^2 + u(x_t)^2}} \qquad [19]$$

Where: $x$ and $u(x)$ are the values and uncertainty of our results

$x_t$ and $u(x_t)$ are the true values and its standard uncertainty

In further text the result of ζ-test is referred as zeta-score.

# 5 Bio-ethanol as a bio-component in fuels

## 5.1 Literature overview

Bio-ethanol is used as a bio-component in gasoline and the addition or substitution of ethanol. Analyses of ethanol/bio-ethanol or gasoline/bio-ethanol blends by AMS and LSC techniques were already reported in the literature. Noakes *et al.* [63] reported the use of the AMS method and the LSC method with a benzene pre-treatment for ethanol, gasoline and ETBE measurements. A calibration for up to 100 % of biofuel has been made. The authors reported a significant correlation of the results and the accuracy of both methods. Oinonen and co-workers [19] reported the use of the AMS method for measurements of gasoline blends with bioethanol and ETBE. The samples were prepared by volume measurements and the results obtained were in accordance with the mixture ratios. Norton and Devlin [17] applied ASTM-6866 methods for the determination of various bio-based products including bio-ethanol/gasoline blends. Culp *et al.* [28, 64] published comparative studies of ASTM-6866 methods for use on fuel. According to the authors, the LSC-B method has an advantage because of its use of gram quantities, while in AMS samples are mg quantities. That makes the AMS method more susceptible to contamination. Both standardized LSC and AMS methods require complete combustion of the sample and a closely monitored transformation to measured form ($CO_2$, benzene or graphite). I would like to emphasize that in this thesis the applied direct method does not need sample pre-treatment, and thus any sample loss. It provides accurate and repeatable results, as will be demonstrated in this dissertation and was reported by Edler [9, 10] and Dijs *et al.* [8]. Edler [9, 10] reported measurements of bio-ethanol blends, while Dijs *et al.* [8] reported measurements of bio-ethanol/ethanol/gasoline blends. Yunoki and Saito [29] reported the use of direct LSC with the application of two-step ethanol extraction. The authors applied ethanol extraction by the addition of water and a determination of $^{14}C$ in a water/ethanol mixture [29]. A similar approach has been used in measurements of international comparative tests (see 8.2.1 on page 97).

## 5.2 Experimental setup

LSC samples were prepared as bio-ethanol blends in mixtures with fossil ethanol or gasoline. Fossil ethanol was obtained from Fisher Scientific, while the bio-ethanol

was from Carbo Elba; both chemicals were analytical grade. Fossil gasoline samples were kindly provided by the Customs Administration of Slovenia. Both combinations of bio-ethanol blends were determined with measurements of 10 calibration samples. Mixtures of fossil and bio-component were prepared in such a way that six samples had bio-ethanol in levels below 10 $\%_m$ and the rest in per-cent between 10 and 100. The decision for such sample preparation was made according to the market demands, the problem of low-level activities measurements and the coverage of the whole analysis range. Preparation of the sample was conducted in accordance with the procedure described in Chapter 4.1 (see page 38). Each component was weighed, and the mass percentage ($\%_m$) of biofuels could be calculated according to equation 4. The pre-designed producer protocol was used in all the bio-ethanol measurements. The counting channels used in further evaluation were determined after measurements.

## *5.3 Results*

A combination of bio-ethanol and ethanol does not present any chemical change of the matrix; therefore, a linear response was expected in the count rate when bio-ethanol was added. No quench interferences were expected, also due to colorless fuel. Slight composition changes occur in combinations of gasoline and bio-ethanol, thus some chemical quench was expected. The spectra obtained can be seen in Figure 11 and were observed between channels 140 and 450. Counts between channels 150 and 400 were considered in the calibration calculations. These were chosen based on: average released energy of $^{14}C$ decay, quenching level of samples and maximized FM.

The SQP(E) values of the ethanol/bio-ethanol blends were between 758 and 766. In relation to the counting efficiency, this means a difference of 1 %, which is within the uncertainty of the quench curve (see Chapter 4.3.1). Therefore, the counting efficiency can be excluded from further calculations of bio-ethanol/ethanol blends. One- and two-step calculations were made using the obtained data. As expected, ethanol/bio-ethanol blends have a linear response and are therefore suitable for making linear one-step and two-step calibration curves.

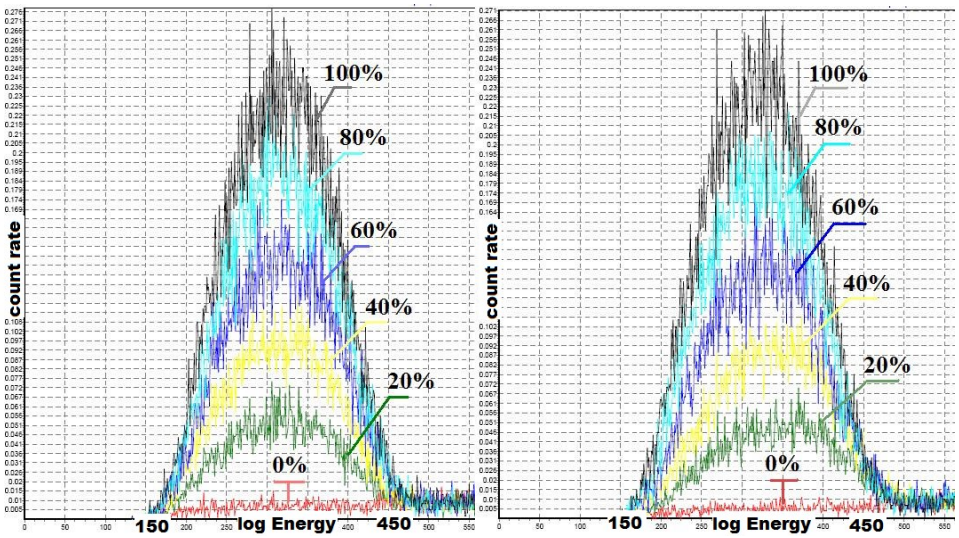


**Figure 11: Ethanol/gasoline calibration samples spectra.** Left are calibration samples for ethanol/bio-ethanol blends; gasoline/bio-ethanol calibration samples are on the right side. Mass per-cents of bio-ethanol are indicated.

The samples of gasoline/bio-ethanol blends had a SQP(E) value between 765 and 825. As can be seen in Figure 11 the position of the peak moved to lower channels/energies. The calculated counting efficiency was between 82 and 72 %. A significant change in the efficiency occurred, thus the counting efficiency needed to be taken into account. A non-linear, one-step curve was obtained, which proved the demand for a counting-efficiency consideration. In this case the quencher was bio-ethanol. Analysis of blends up to 10 $\%_m$ show a significant difference in the calculated result ($\zeta$-test > 2). Because the evaluated blends were in the target measurement range, a one-step calibration curve was discarded.

**Table 9: Bio-ethanol fitting parameters**

| Intercept | | Slope | | Statistics |
|---|---|---|---|---|
| **Value** | **Error** | **Value** | **Error** | **$R^2$** |
| 0 | - | 17.504 | 0.295 | 0.997 |

The bio-component and its activity in both types of blends were the same. The data that were obtained after individual two-step calculation were combined and one two-step calibration curve was made (see Figure 12). A summary of the parameters for the obtained linear calibration curve is presented in Table 9. The combined

calibration curve had an excellent correlation coefficient (0.997) with a low relative error of the calibration parameters.

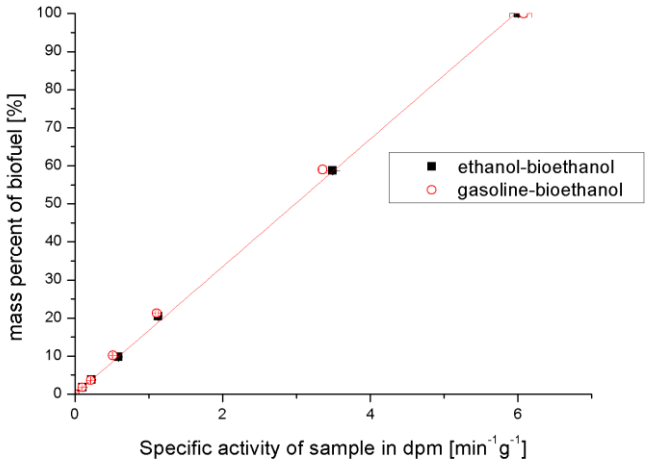


**Figure 12: Two-step calibration curve for bio-ethanol.** One linear calibration curve was obtained.

## *5.4 Validation parameters*

The validation parameters presented and discussed in this sub-chapter were calculated based on the procedure described Chapter 4.3. They are summarized in Table 10.

**Table 10: Bio-ethanol protocol validation parameters**

| Parameter | Value | |
|---|---|---|
| **Detection limit (Currie** [122]) | 1.08 $\%_m$ | |
| **Detection limit (ISO 11929** [123]) | 0.63 $\%_m$ | |
| **Linearity** | 0.997 | |
| **Repeatability** | 0.54 $\%_m$ | |
| **Reproducibility** | 2 cpm | < 1 $\%_m$ |
| **Sensitivity** | 17.5 | |
| **Trueness** | See chapter 8 | |

### *5.4.1 Uncertainty*

The uncertainties for measurements near the detection limit (Lq), at 10 % and at 100 % of biofuel were calculated and evaluated. The individual uncertainty and its contribution were calculated in accordance with the procedure described in Chapter 4.3.1. As expected, the background stability and sample counting present the largest contribution to the total uncertainty when evaluated near the DL. But its importance decreases with an increase in the bio-component quantity. Just the opposite was found in the case of the efficiency, where the contribution increased with an increasing percentage of bio-ethanol. The calibration uncertainty contribution had the greatest affect at around 10 $\%_m$ bio-ethanol. The balance uncertainty represents a negligible portion of the budget.

**Table 11:Bio-ethanol analysis uncertainty budget**

| | near DL | | at 10 $\%_m$ | | at 100 $\%_m$ | |
|---|---|---|---|---|---|---|
| | **% of total** | **absolute** | **% of total** | **absolute** | **% of total** | **absolute** |
| **Balance** | 0.001 | 0.0001 g | 0.02 | 0.0001 g | 0.02 | 0.0001 g |
| **Background cpm** | 78.9 | 1.38 ± 0.08 | 7.82 | 1.38 ± 0.08 | 0.25 | 1.38 ± 0.08 |
| **Sample cpm** | | 1.91 ± 0.11 | | 3.99 ± 0.05 | | 37.0 ± 0.19 |
| **efficiency** | 14.73 | 1.3 % | 81.59 | 1.3 % | 98.45 | 1.3 % |
| **calibration** | 6.37 | 0.5 | 10.58 | 0.5 | 1.28 | 0.5 |
| **total** | 0.21 $\%_m$ | | 0.13 $\%_m$ | | 1.3 $\%_m$ | |

### *5.4.2 Detection limit*

The detection limits were calculated in accordance with Currie [122] and ISO 11929 [123] with data for the two-step calibration curve. The background count rate obtained in 1000 min was 1.034 ± 0.046 in the same counting window as the LSC samples. As can be observed, the limits calculated with both methods are different.

The limit of the detection obtained in accordance with Currie's calculations was higher than the limit calculated with ISO 11929 for 0.45 $\%_m$ (see Table 10).

### *5.4.3 Linearity*

The linearity was demonstrated with the correlation coefficient obtained for the fitted calibration curve. As expected for the case of the one-step calibration curve, linearity was only achieved in bio-ethanol/ethanol blends where the correlation coefficient was 0.999. The one-step calibration curve for the bio-ethanol/gasoline blends was not-linear, but its quadratic fitting curve obtained a correlation coefficient of 0.999. The two-step calibration curve fitted through both fuel matrices (ethanol/gasoline) obtained a high correlation coefficient of 0.997, as can be observed in Table 9. The relative error of the fitting parameters for the two-step calibration curve is 0.44 %. The one-step calibration curve for bio-ethanol/ethanol had an error of 1 %, while the bio-ethanol/gasoline curve had an error of 0.77 %. The reason for the relatively high error for the bio-ethanol/ethanol one-step calibration curve is probably due to ethanol's hygroscopic property. The characteristics of the scintillation cocktail limit the use in measurements of aquatic LSC samples.

### *5.4.4 Repeatability*

The repeatability was evaluated with the standard deviation of the results calculated by one- or two-step calibration curves. Five LSC samples in the range from 10 to 100 $\%_m$ were measured and calculated 10 times. The evaluation of the bio-ethanol/ethanol one-step calculation shows repeatability within one standard deviation. The results of the one-step calculation in the bio-ethanol/gasoline blends exceeded two standard deviations. With extensive changes in the counting efficiency (10 %) such a result was expected and justified dismissing this calculation procedure. The standard deviation obtained from the two-step calculations was within one standard deviation, and furthermore it never exceeded 0.54 $\%_m$.

### *5.4.5 Reproducibility*

When the samples were measured ten times over a period of one week the sample count rate and the SQP(E) values were within the uncertainty of each parameter. In the second experiment the samples were measured during the changed temperature of the measurement chamber from 20 to 8 °C. The count rate between the highest and

the lowest temperature differed up to 2 cpm, which is within the uncertainty with a level of confidence 2*k*, while the SQP(E) changes were within 1*k*. According to the ζ-test, this makes both one- and two-step calculations reproducible. Nevertheless, two-step calculation is suggested because possible changes in the efficiency are taken into account.

### *5.4.6 Sensitivity*

The sensitivity of the method was evaluated through the slope of the calibration curve. Both one-step calibration curves were equally sensible. This is not surprising, since the background count rates were comparable and the bio-component used was the same, thus making several points in the proximity. The two-step calibration curve was, with a slope of 17.5, the least sensible bio-ethanol curve.

## *5.5 Discussion*

Several analysis procedures for the determination of bio-ethanol quantity can be found in the literature [8–10, 28, 29, 63]. Analyses of bio-ethanol/ethanol or gasoline blends were conducted for the purposes of this thesis in order to test the same preparation of the LSC samples and the measurement protocol on several biofuel types. The LSC samples were prepared and measured as described in the Chapter 4.1 (see page 38).

A determination of bio-ethanol in ethanol or gasoline is possible, as can be seen from the presented results. The requirements of the method were complied in all requirements. Detection limit calculated in accordance to ISO 11929 was 0.63 $\%_m$ while calculations in accordance to Currie give DL of 1.08 $\%_m$. The repeatability was 0.54 $\%_m$ thus within uncertainty budget, as well as linearity of 0.997, what proves usability of the method. The chosen sample-preparation and measurement protocol of the simple direct LSC method are applicable for analyses of fuel market samples. Both one-step calibration curves could be used for the current European fuel market. The analyses are reliable for up to 20 % of bio-ethanol, which is above the EN 228 limit for oxygenates (15 %) [38]. The drawback of the one-step calculation is its sensitivity to outside effects, such as the measurement chamber temperature changes and the quantity of water in the sample. The two-step calculation does not have such drawbacks, but requires more calculations. The calibration procedure could also be

used on fuels from non-European countries, where fuels often contain up to 100 % of biofuel, because the results for up to 100 % of bio-ethanol in the sample are reliable.

Our results could be compared to Edler [9, 10] who reported the use of a one-step calibration curve. The calculations give statistically the same results for the whole fossil/bio-component range for ethanol/bio-ethanol blends. Edler [9] reported limited use (up to 10 %) of the one-step calibration for gasoline/bioethanol blends. The one-step calibration for the bio-ethanol/gasoline blends could also be made with our results. The linearity obtained is approximately the same as Edler reported [9]. Nevertheless, the use of two-step calculations is suggested because it minimizes any external effect of the LSC sample preparation or measurement.

For the two-step calibration curve the specific activity of the sample was calculated, and thus the comparison with the results obtained by other authors was also possible. The calculated total activity of the bio-component was comparable to those reported by Edler [9, 10]. The efficiency obtained in his research was lower than observed on our LSC. The difference could be explained by the differences in the LSC counters or vials, since the same scintillation cocktail and sample/cocktail ratio were used. The author reported that the measurements were conducted in Teflon-coated plastic vials, while our measurements were performed in high-performance glass vials [9, 10]. Dijs and co-workers [8] also reported the use of sample activity for the calculation of the bio-carbon content. They use a different calculation procedure, which uses the bio-carbon fractionation (% atom/atom) obtained by measurements on the AMS and the concentration of $^{14}C$ atoms, which cannot be determined using the direct method, thus our results are not directly comparable [8].

# 6 Hydrotreated vegetable oils (HVO) as a bio-component in fuels

## 6.1 Literature overview

HVO is a rather recently developed fuel and its production is still in the pilot phase [36, 56, 58, 124, 125]. However, the literature already reported its analyses. Recently, Alves and Poppi [57] reported successful simultaneous analyses of hydrocarbon renewable diesel, biodiesel and petroleum diesel. The authors obtained accurate results using near-infrared (NIR) spectroscopy and a partial least-squares (PLS) model [57]. Oinonen and co-workers [19] reported AMS measurements that included several HVO blends. Two sample treatments were tested. The authors reported an improved sample treatment, which took around 1 h, but at higher combustion temperatures (720 °C) and using quartz tubes. A comparison with a previously used preparation method involving glass tubes and an oven temperature of 520 °C was made [19]. We would like to emphasize that the simple direct method applied on LSC does not need resource-intensive sample treatment and expensive equipment to obtain accurate and precise measurements. Norton and Woodruff [12] reported direct LSC method measurements with samples and an in-house scintillator. They reported measurements of up to 20 volumetric % of renewable diesel and a comparison of the AMS and LSC-B methods. The results of both methods were in agreement, as well as accurate, compared to the true renewable diesel concentrations [12]. Recently, Idoeta and co-workers [27] reported experiments with simultaneous measurements of HVO and biodiesel. However, analyses of the individual bio-component's quantity were not reported [27].

## 6.2 Experimental setup

The LSC samples were prepared in mixtures of HVO and gasoline or diesel. The same fossil gasoline as in the experiments with bio-ethanol was used. The fossil diesels were also kindly provided by the Customs Administration of Slovenia. The bio-components were obtained from the partner research laboratory of the University of the Basque Country, Bilbao, Spain and organizers of the international comparison tests (more data in Chapter 8.2). For calibration purposes, only the sample used in the

intercomparison tests was tested. The HVO can be made from different sources, which affects the composition and we were able to obtain four unknown feedstock samples, and thus a comparison of the results obtained from different samples of bio-component was made.

The samples for calibration purposes were prepared in the range from fossil diesel/gasoline to HVO; each combination was determined with measurements of 10 calibration samples. The HVO mixtures were prepared in the same manner as bio-ethanol, thus six samples had HVO in levels below 10 $\%_m$ and the rest in percentages between 10 and 100. The LSC sample preparation and used material is described in detail in the Chapter 4.1 (see page 38). Each component was weighed and the mass percentage ($\%_m$) of biofuels was calculated according to equation 4. Measurements were conducted in accordance with the procedure described in Chapter 4.2 (see page 39).

## *6.3 Results*

Mixtures of HVO and gasoline or diesel change the sample composition; therefore, some chemical quench was expected. The measured spectra can be seen in Figure 13. The level of quench is smaller than in the bio-ethanol, so the spectra are observed between channels 140 and 600. The parameters for the counting window determination were the same as for the bio-ethanol analysis. Those were the FM calculations, the average energy released by $^{14}C$ decay and the quench level of the samples. Keeping these parameters in mind, counts between channels 150 and 550 were used in the calibration calculations.

The SQP(E) value for the gasoline/HVO blends was between 777 and 838. A shift of the spectra to a higher channel/energy occurred for larger amounts of bio-component (see Figure 13). The fossil matrices are therefore a quencher in these types of blends. The SQP(E) values of the gasoline/HVO blends results in a counting efficiency of between 74 % and 83 %. The counting efficiency had to be considered in the calculations of the HVO's quantity in the sample. The change in the SQP(E) value was also observed in the measurements of the diesel/HVO blends. The value was between 801 and 838 and according to our quench curve resulted in counting efficiencies of between 78 % and 83 %. The differences in the counting efficiency are smaller than in the case of the HVO/gasoline blends. Nevertheless, the counting

efficiencies exceed the uncertainty and had to be taken into account when the HVO quantity in the sample was calculated. A shift of the spectra was also noticed in the diesel/HVO blends, where the fossil diesel was determined as a light quencher.

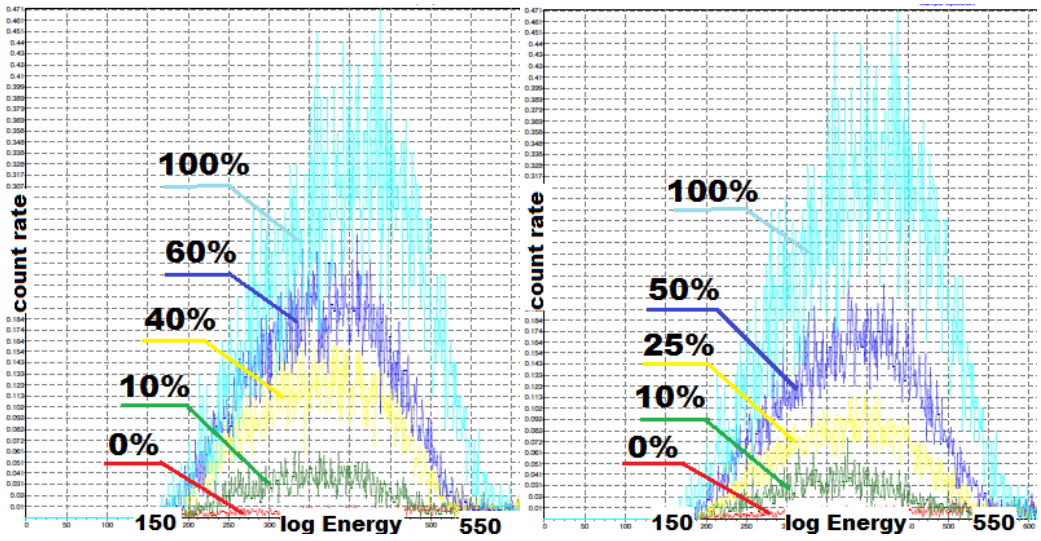


**Figure 13: Gasoline/diesel calibration samples spectra.** Left are calibration samples for gasoline/HVO blends; diesel/HVO calibration samples are on the right side. Mass per-cents of HVO are written.

The differences of the SQP(E) values indicate changes in the counting efficiency; therefore, only a two-step calibration curve was prepared. The activity of the bio-component used was the same in both matrices and the background count rate was consistent with its uncertainty. Therefore, a single calibration curve was fitted. Data obtained after two-step calculations of the HVO/gasoline and HVO/diesel measurements were used (see Figure 14). Table 12 presents a summary of the obtained fitting parameters. A linear calibration curve was obtained with a correlation coefficient $R^2$ greater than 0.99.

**Table 12: HVO fitting parameters**

| Intercept | | Slope | | Statistics |
|---|---|---|---|---|
| **Value** | **Error** | **Value** | **Error** | **$R^2$** |
| 0.712 | 0.050 | 9.156 | 0.123 | 0.998 |

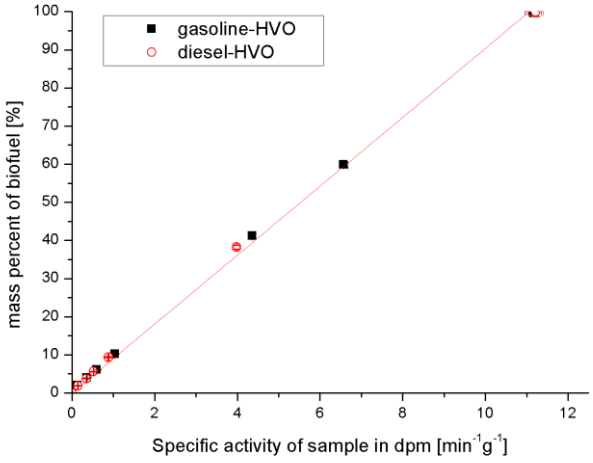


**Figure 14: Two-step calibration curve for HVO samples.** One linear calibration curve was fitted, $R^2$ coefficient is larger than 0.99.

Four HVO samples were obtained during the research, but only one was used for calibration purposes. The rest of the bio-components were used for conducting the comparison of count rates, SQP(E) values and counting efficiencies. In total, 40 measurements were conducted over a period of one month. The counting efficiencies deviated between 87.5 and 88 %, which is within the uncertainty of the parameter. The measurements of the SQP(E) values show a span from 880 to 885, while the count rates deviated from 73.1 to 75.7 cpm. All the parameters were within the uncertainty of each parameter, thus no effects on the total activity of the bio-components were observed.

## *6.4 Validation parameters*

Validation parameters presented and discussed in this sub-chapter were calculated based on the procedure described Chapter 4.3 (see page 42). They are summarized in Table 14.

### *6.4.1 Uncertainty*

The uncertainties were evaluated for measurements near the detection limit (Lq), at 10 % and at 100 % of biofuel. The individual uncertainty and its contribution were calculated in accordance with the procedure described in Chapter 4.3.1 (see page 42). The greatest contribution to the uncertainty near the detection limit was the calibration (see Table 13). Its contribution decreased with increasing bio-component

quantity. The same can be observed for the uncertainty of the count rate. The contribution of the efficiency uncertainty is increasing when higher HVO quantities are measured. The importance of the individual contributions is similar to that found for the bio-ethanol analysis, with the exception of the calibration. The contribution of the calibration uncertainty of the bio-ethanol analysis was the greatest near 10 $\%_m$, while in the HVO analysis it is the greatest near DL.

**Table 13: HVO analyses uncertainty budget**

| | near DL | | at 10 $\%_m$ | | at 100 $\%_m$ | |
|---|---|---|---|---|---|---|
| | % of total | absolute | % of total | absolute | % of total | absolute |
| Balance | 0.001 | 0.0001 g | 0.01 | 0.0001 g | 0.02 | 0.0001 g |
| Background cpm | 21.11 | 2.15 ± 0.07 | 3.98 | 2.15 ± 0.07 | 1.06 | 2.15 ± 0.07 |
| Sample cpm | | 3.05 ± 0.08 | | 8.47 ± 0.17 | | 74.52 ± 0.87 |
| efficiency | 21.04 | 1.3 % | 61.94 | 1.3 % | 93.76 | 1.3 % |
| calibration | 57.85 | 3.57 | 34.07 | 3.57 | 5.16 | 3.57 |
| total | 0.08 $\%_m$ | | 0.15 $\%_m$ | | 1.3 $\%_m$ | |

### *6.4.2 Detection limit*

The detection limits were calculated in accordance with the Currie [122] and ISO 11929 [123] procedures (see Table 14). Similar to bioethanol measurements, also in the case of HVO, detection limits calculated in accordance with Currie were higher than those calculated with ISO 11929 procedures. The limit of detection obtained in accordance with Currie's calculations was 1.41 $\%_m$, while the detection limit calculated in accordance with ISO 11929 was 1.13 $\%_m$.

### *6.4.3 Linearity*

Linearity was demonstrated with the correlation coefficient (see Table 12) obtained through fitting of the calibration curve. A high correlation coefficient of 0.998 was obtained with a two-step calculation of the HVO presence in fuel, with a

total of 20 results of HVO/gasoline and HVO/diesel blends. The obtained uncertainty for the HVO curve was 0.07 %. The curve was fitted through measurements points with small deviations, what results in a great linearity of the calibration curve. Compared to bio-ethanol curves (0.44 %, see Chapter 5.4.3), the two-step curve for HVO varied the least.

### *6.4.4 Repeatability*

Repeatability was evaluated as a dispersion of the calculated results (see Table 14). The standard deviation obtained after the two-step calculations was 0.40 $\%_m$. The result proves the repeatability of the method and it is lower than the standard deviation of the bio-ethanol measurements. The results of the gasoline/HVO mixtures showed lower standard deviations than the diesel/HVO blends, due to a yet unknown reason.

**Table 14: HVO protocol validation parameters.**

| Parameter | Value | |
|---|---|---|
| **Detection limit (Currie [122])** | 1.41 $\%_m$ | |
| **Detection limit (ISO 11929)** | 1.13 $\%_m$ | |
| **Linearity** | 0.998 | |
| **Repeatability** | 0.40 $\%_m$ | |
| **Reproducibility** | 3.5 cpm | 0.50 $\%_m$ |
| **Sensitivity** | 9.156 | |
| **Trueness** | See chapter 8 | |

### *6.4.5 Reproducibility*

The sample count rate and SQP(E) values were evaluated from the measurements obtained in a period of one week. The results obtained were within the uncertainty of each parameter. The count rate and SQP(E) values differed in a similar way as in the bio-ethanol analyses when the temperature of the measurement chamber was changed. The count rate changed by 3.5 cpm when pure HVO was measured at 20 and 8 °C. This was within the uncertainty cover of $k=2$, while at the same time the

SQP(E) variation was within *k=1* coverage. Only the two-step calculation procedure is used in the calculations of the HVO blends, and thus the changes of count rate and SQP(E) value are taken into account. The calculated results were within the uncertainty of the method (see Table 14).

### *6.4.6 Sensitivity*

The slope of the calibration curve was checked for an evaluation of the method's sensitivity. As can be seen in Table 12, the obtained slope of the calibration curve was 9.156. Compared to the bio-ethanol's two-step calibration curve, which obtained the slope of 17.629, the HVO curve was less sensitive by about 50 %.

## *6.5 Discussion*

From the results obtained, we can conclude that a simple direct LSC method could be applied for measurements of HVO in both fuels, i.e., gasoline and diesel. The requirements of the method, with the exception of detection limit, were satisfied. With 0.998, the linearity is comparable to bio-ethanol analysis, while with 0.4 $\%_m$ the repeatability is better. However, the two-step calibration curve for HVO is not the same as the two-step calibration curve for the ethanol, since the total specific activity of the sample is different. Namely, HVO has more C atoms than bio-ethanol, while the ratio $^{12}C/^{14}C$ is relatively constant. The detection limits calculated in accordance to ISO 11929 was 1.13 $\%_m$, which is close to requirements and achievable with longer background counting time. But calculation in accordance to Currie criteria (1.41 $\%_m$) gives higher DL; target detection limit wouldn't be achievable with simple prolongation of background counting time. The method is based on a two-step calculation; therefore, it is not sensitive to eventual changes in the count rate or the counting efficiencies. With reliable results for up to 100 %, such a calibration procedure could be used even if such fuel would be a substitute for fossil diesel.

The HVO analyses with the direct LSC method were reported in literature. Norton and Woodruff [12] reported the use of such a bio-component in LSC measurements. Compared to our laboratory where the calibration was done for up to 100 % of biofuel, they report only measurements for up to 20 % of renewable diesel. The authors did not report any difficulties applying a different spectrometer and scintillation cocktail. Such fuel could therefore be measured with a simple direct

method on different apparatus and with different sample preparation. Recently, Idoeta and co-workers [27] reported measurements using HVO and biodiesel in diesel. However, a precise determination of the bio-component quantity was not investigated [27]. Successful analyses of HVO in diesel applying NIR were reported in the literature [57]. However, the observed differences in the chemical composition of the fossil diesel and the HVO are small. On the other hand, LSC analyses are based on radiocarbon content, and thus its bio-origin and not the chemical composition.

# 7 Biodiesel as a bio-component in fuel

## 7.1 Literature overview

Fatty acid methyl/ethyl esters (FAME/FAEE) are the most important part of a diesel's bio-components and therefore referred to as the biodiesel. Its characteristics, chemical form and color differ according to the feedstock oils. Not just a chemical, but also a color quench, influences the calibration for biodiesel analyses. Several methods were applied for biodiesel analyses where the fatty acid ester's fingerprint is measured. Those methods were described in Chapter 1.2 (see page 7). The sensitivity of the biodiesel fingerprint can also be used in studies of differences between feedstock. One such method was used in this thesis for monitoring the biodiesel trans-esterification yield and later the decomposition of fatty acids in biodiesel samples. The latter was found to be a drawback of biodiesel fingerprinting because of sample ageing. Biodiesel ageing is shown with the decomposition of fatty acids esters, which changes the fingerprint while the radiocarbon, important for LSC analyses, is still present in the sample.

The direct LSC method was already applied for the analyses of biodiesel. Takahashi *et al.* [26] reported the use of a direct LSC method for the measurement of biodiesel and/or pure vegetable oil. The authors tested 1, 3 and 4 g of biodiesel with a commercially available scintillator. The best results were obtained with 1 g of bio-component, while 3 and 4 g showed the same response [26]. However, Norton and co-workers [16] reported accurate measurements from 2 to 20 $\%_v$ biodiesel blends with direct LSC measurements. The experiments were conducted with four known feedstock biodiesels and an in-house scintillation cocktail. The accuracy of the determined biodiesel percentages were within 0.6 $\%_v$ of biodiesel, while three measured blends misclassified the percentage by more than 1 $\%_v$ [16]. Idoeta *et al.* [27] recently reported the application of the direct LSC method on biodiesel and HVO analyses. The authors tested three commercially available scintillation cocktails in the search for an optimal scintillator : sample ratio. Among the scintillators tested, Ultima Gold F was determined as the best. In the analyses of the scintillator : sample ratio no large differences were observed, but the authors reported that the ratio of 12:8 is the best [27]. In this thesis the sample preparation was kept

uniform for all the bio-components, and thus a 10:10 ratio was also applied for the biodiesel samples.

All authors reported quench difficulties in biodiesel analyses, although the approaches were different. The bleaching and dilution of samples are the most common approaches to a reduction of color quench. $AlO_2$ and silica were unsuccessful for the bleaching of biodiesels, since the color of the sample was not stable [126]. On the other hand, Fang *et al.* [35] reported the successful bleaching of deep color biodiesel made from waste cooking oils. The authors applied 15 %(w/w) of $H_2O_2$ and 90 °C to limit the color and increase the measuring range of the biodiesel [35]. A form of dilution was already applied by Takahashi *et al.* [26], where the color of biodiesel was reduced by increasing the scintillator : sample ratio. Such an approach increases the detection limits because the number of radiocarbon atoms are decreased. In this thesis, the quench problem was addressed through a measurement perspective. Changes were made to the counting protocol, calibration and the interpretation.

## *7.2 Experimental setup*

The biodiesel experiments were conducted in two parts. In the first part of the experiments the calibration samples, as mixtures of biodiesel and diesel, were prepared. Eight biodiesel samples of unknown feedstock were kindly provided by the Customs Administration of Slovenia. The date on which the samples were obtained was used for naming them. The same fossil diesel was used as in the experiments with HVO. The LSC samples were prepared in the same manner as for bio-ethanol and HVO blends where the majority of samples contained less than 10 $\%_m$ of biodiesel and the rest between 10 and 100 $\%_m$. At least two LSC aliquots were made from each biodiesel sample set. Each component in the LSC sample was weighed and the mass % of biofuels was calculated according to equation 4. The biodiesel was measured in accordance with the procedure described in Chapter 4.2 (see page 39), which is the same as the bio-ethanol and HVO analyses.

The second part of the experiments was conducted with changes in the counting protocol and an interpretation of the results of the proposed LSC method. The biodiesel samples described in Chapter 3 (see page 20) were used for that purpose. The samples were named in accordance with the feedstock oil. The LSC samples

were made in various blends in the range up to 100 % biodiesel and were prepared in accordance with the procedure in Chapter 4.1 (see page 38). The measurement was conducted at 18 °C and changed counting protocol, which was based on the pre-designed protocol described in Chapter 2.2.1 (see page 16). The counting efficiency was determined both by a quench curve and the standard addition method, as described in Chapter 4.2.2 (see page 40). The gravimetrically determined dilution of the standard in fossil diesel with its specific activity of 26.6 ± 0.39 Bq/g of the sample was used for the preparation of an active sample. The data obtained with standard addition method was used for fitting the new color/chemical quench curve.

## *7.3 Initial biodiesel measurements*

The spectra obtained from the measurements with a pre-designed protocol can be seen in Figure 15. A greater quench compared to bio-ethanol and HVO measurements is observed, thus shifting the $^{14}C$ peak to channels between 140 and 400. According to our quench curve, a measurement of biodiesel observed up to 70 % higher quench. All the counts in the $^{14}C$ peak area were therefore considered in order to obtain good counting statistics, also with the quenched samples. From the observation of the spectra a concern has been raised that the whole $^{14}C$ peak was not recorded, and thus some of the events were misinterpreted due to the measurement setup.

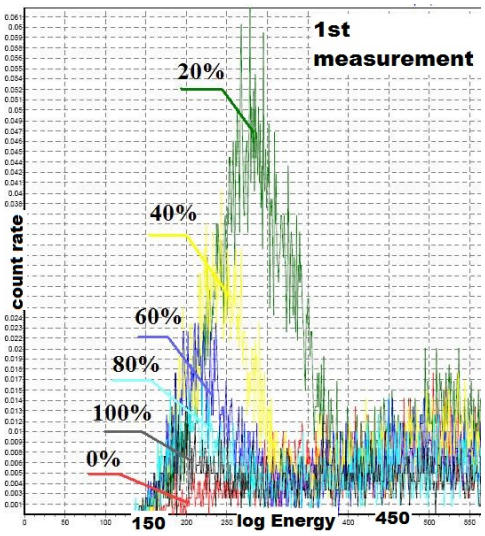


**Figure 15: Biodiesel calibration samples spectra.** Mass percent of biodiesel is indicated. Shift and decrease of $^{14}C$ peak is observed.

The values of the measured quench parameter SQP(E) indicated a large variety and an increase of the quench level. The SQP(E) value varied from 817 for fossil diesels to 552 in samples of pure biodiesel, which is reflected in counting efficiencies of between 80 and 18 %. As can be observed from Figure 15, the measured $^{14}C$ peak did not only shift to lower channels/energies but also its height decreased. This was especially noticeable in measurements of biodiesel blends above 20 $\%_{m,}$ as can be observed in Figure 16. The samples with blends below that level had an SQP(E) level between 817 and 732, thus determining the counting efficiency between 80 and 67 %. Only a two-step procedure was applied, as in the case of the HVO mixtures.

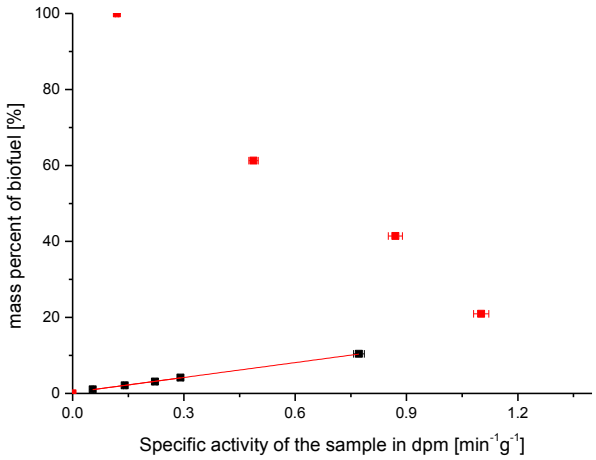


**Figure 16: Two-step calibration for biodiesel.** Linear calibration for up to 10 $\%_m$ was made. The obvious misclassification of blends with more than 20 $\%_m$ of biodiesel, where the activity is inversely proportional to the mass percentage of bio-component in the sample, led to further research described in chapter 7.4.

The two-step calibration curve was only applied for samples containing biodiesel blends up to 10 $\%_m$ (see Figure 16). For this blends a linear regression line with the parameters summarized in Table 15 was obtained. The correlation coefficient $R^2$ was 0.999. Such an approach was chosen because the obtained range was sufficient for measurable market fuel samples, which according to the standard EN 590 [37] for diesel fuels could intake a maximal 5 % of biodiesel. Amounts measureable with this method are consistent with Takahashi *et al.* [26] and Norton *et al.* [16]. Furthermore, the most used FTNIR method described in standard EN 14078 has a limit of 20 $\%_v$ biodiesel blends, which were also analyzed by the direct method, but with an unsatisfactory precision [60]. In the literature Norton *et al.* [16] reported a comparison of the direct LSC method with FTNIR and an alternative IR method. The

majority of the measured sample blends were analyzed more accurately with the direct LSC method than with the IR [16].

**Table 15: Biodiesel blends up to 10 $\%_m$ fitting parameters**

| Intercept | | Slope | | Statistics |
|---|---|---|---|---|
| **Value** | **Error** | **Value** | **Error** | **$R^2$** |
| 0.315 | 0.019 | 12.55 | 0.130 | 0.999 |

A comparison study among eight biodiesel samples used in the Slovenian market was made. We were not able to obtain any data such as production date or feedstock due to the companies' data-protection measures. The samples were prepared in 10 $\%_m$ biodiesel blends and marked according to the date of acquisition. The count rates normalized for grams of sample (cpm/g) differ significantly, as can be observed from Figure 17. The measured SQP(E) values were between 784 and 684; the highest values belonged to the oldest biodiesel (FAME090513), while the lowest belonged to FAME100401. The calculated counting efficiency differed from 76 to 56 %. A similar variability in the biodiesel count rate was also observed on four feedstock biodiesels measured by Norton *et al.* [16].

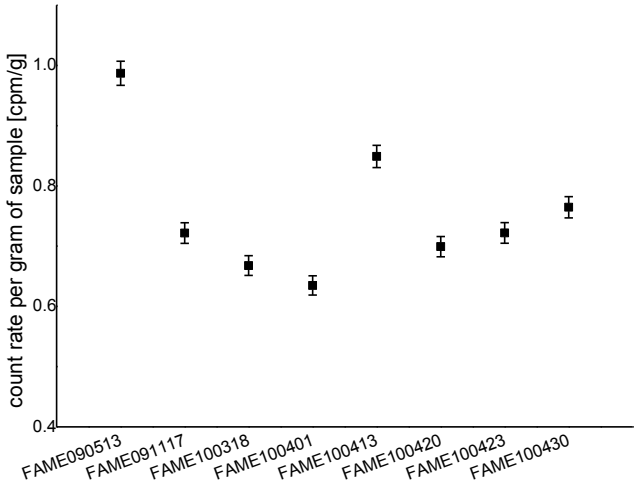


**Figure 17: Different biodiesels from the Slovenian market.** The count rates of 10 $\%_m$ blends are presented. The samples are named according to the acquisition date.

The results of FAME090513 reflect the biodiesel characteristics and the importance of oxidative stability. The feedstock of the obtained biodiesels was not known and some of the samples were already in a laboratory longer than the EN 14214 standard limit of stability (6 months), a decision was made to produce fresh biofuels on a laboratory scale from known feedstock oils [39]. A re-evaluation of the measurement protocol and correlation between biodiesel characteristics and impact on the LSC measurement was made with the newly produced biofuels.

## *7.4 LSC measurement protocol*

The LSC protocol for measurements of bio-ethanol and HVO has limited usability for biodiesel analyses. As already reported, only calibration for up to 10 $\%_m$ of biodiesel was successfully made. The rest of the results were found to be misleading, where results show that with an increase of the bio-component's quantity the activity of the sample decreases. This led to a reconsideration of the usability of the existing counting protocol and the creation of new one. As explained in Chapter 2.2.1 (see page 16) the producer of the spectrometer offers an option for changes in the protocol setup. From the description of the Quantulus electronic circuit (see Figure 4 on page 16) it was established that the coincidence circuit settings are the first possibility to obtain whole spectra with 1024 channels [86]. Namely, the pre-designed $^{14}C$ protocol is set up on a high coincidence bias, which reduces the signals below the 300$^{th}$ channel due to the elimination of the Cherenkov and fluorescence events, which are often observed in measurements of high-energy β decay. In measurements of highly quenched samples, like biodiesel, such a setup could eliminate the signals from isotope decay. This approach was also taken by Bagán *et al.* [127] in high salt matrices. Researchers applied a high-energy multi-channel analyzer configuration and a low coincident bias while measuring the LSC samples with a plastic and liquid scintillator. The salts in the samples represent the chemical quencher, which can severely decrease the count rate. Researchers reported SQP(E) values from 780 to 740, which are much higher values than observed in our measurements of biodiesel [127].

A set of nine samples containing 100 % of biodiesel produced from different oils and samples of fossil diesel was prepared and measured with the original producer's and with a changed protocol. All 1024 channels of the spectra were obtained with the

change of coincidence bias setup, as can be seen in Figure 18. In comparison with the spectra obtained with a high coincidence bias (see Figure 15 on page 66), where all the events below 140$^{th}$ channel were diminished, in a low coincidence setup also low energy events are seen. In the sample of background (in Figure 18, shown in yellow) an additional peak between 50$^{th}$ and 250$^{th}$ channel is observed, which belongs to events occurring due to the use of glass vials. As already explained (see Chapter 4.1), in the LSC sample preparation high-performance glass vials were used, and thus containing some of $^{40}$K isotope, which is a natural radioactive isotope, found in trace amounts in the glass. During decay it releases enough energy, which can produce Cherenkov events in the vial wall. Measurements of such events are discarded in the high coincidence bias due to the Quantulus electronic circuit setup. The trigger for discarding the counts is based on the released energy [86]. The recalculated released energy is lower than in the un-quenched samples due to the heavy quench of the biodiesel samples. Biodiesel released electrons are therefore misclassified and discarded if a high coincidence bias is used. It has been concluded that a low coincidence bias has to be used in measurements of biodiesel blends.

In Figure 18 it can also be seen that some $^{14}$C peaks of biodiesel are shifted to higher channels/energies, thus their counting efficiencies are higher than the average measured biodiesel. This can also be easily observed from the measurements of the SQP(E) value. These sets of biodiesel samples had SQP(E) values between 360 and 850, where the lowest value and the highest quench were observed in the samples of biodiesel produced from waste cooking oil. This also explains the shape of the spectra, which was completely different than the others. It was decided to withdrawn waste cooking oil biodiesel from thesis, since its color was black and also other characteristic such as oxidative stability were unsatisfactory. A special research on waste cooking oil biodiesel will be conducted in the future. The highest observed SQP(E) value of 850 was determined in biodiesel produced from Slovenian sunflower oil. Measurements of these biodiesel blends would also be possible with a high coincidence bias setup. The rest of the measured 100 % biodiesels obtained the following SQP(E) values: 675 in camelina from the Slovenian market, while camelina from Spanish market had 580, corn 697, jatropha 681, rapeseed 612, soya 572 and sunflower from Spanish market 680. The differences in the sunflower's SQP(E) values could be explained in the oil pre-treatment (refining). However, the

camelina's difference was not explained, since chemical composition does not suggest a major deviation from the other oils.

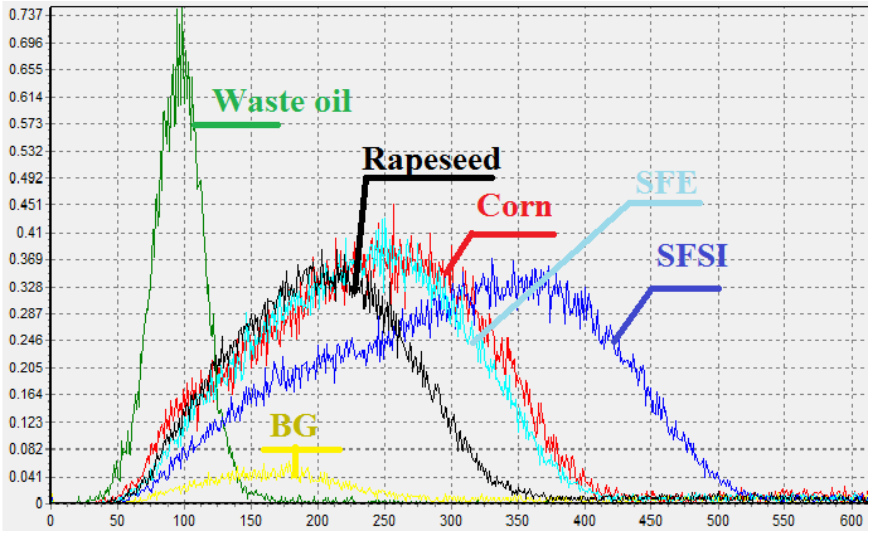


**Figure 18: Spectra obtained at low coincidence bias.** Green spectra is biodiesel from waste oil, black is biodiesel from rapeseed oil, red is biodiesel from corn oil, light blue is biodiesel from Spanish sunflower oil (SFE) and dark blue is biodiesel from Slovenian sunflower oil (SFSI). In yellow the background is presented (BG).

The counting efficiencies had to be re-evaluated to allow a proper sample activity determination due to the change in the measurements protocol. The counting efficiencies of the bio-ethanol and HVO blends were determined with a quench curve fitted through measurements of a $^{14}C$ Low level Quench set, purchased from PerkinElmer (see Figure 10 on page 41). Such a set is prepared with a chemical quencher, which in the measurements of bio-ethanol and HVO sufficiently describes the quenching level. In the measurement of biodiesel blends, differences in the observed quench occur due to the color of the sample. Thus a set of samples with 7 to 10 blends from each produced biodiesel was prepared. In total, 65 LSC samples with blends consisting of levels from 1 to 100 % of the bio-component were used. Some samples were also made with biodiesel from waste cooking oil for an expansion of the SQP(E) coverage. The samples did not contain any artificial quencher, since a variety of quench levels were already observed. After the initial measurement a standard solution was added and samples were counted again (see Chapter 4.2.2). The SQP(E) values before and after the standard addition were within the uncertainty of the parameter. The count rates in a wider window (50-550) were

used for further analyses because of the greater FM. The counting efficiency obtained and the SQP(E) value were used for the quench curve.

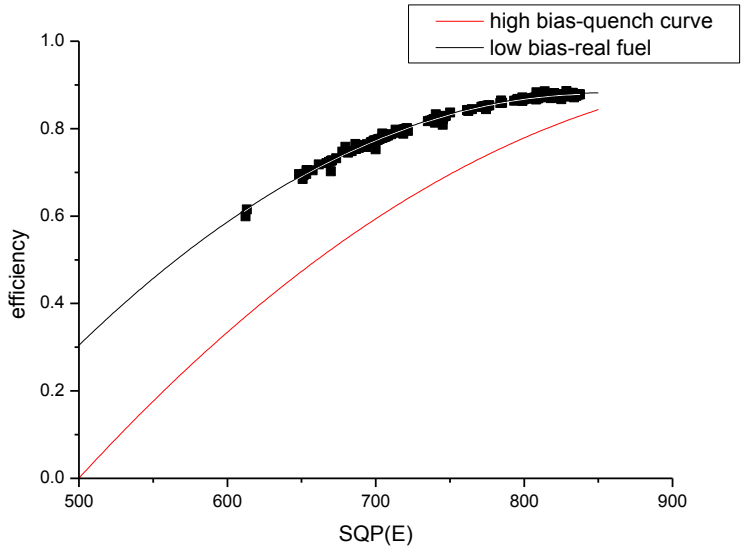


**Figure 19: Both quench curves.** In black the quench curve prepared from biodiesel samples with standard solution is presented. In red the chemical quenched curve (PerkinElmer) is presented.

**Table 16: Low-bias quench curve fitting parameters**

| Slope [$x^2$] | | Slope [x] | | Intercept | | Statistics |
|---|---|---|---|---|---|---|
| **Value** | **Error** | **Value** | **Error** | **Value** | **Error** | **$R^2$** |
| -4.69E-6 | 7.03E-8 | 0.008 | 1.06E-4 | -2.51 | 0.04 | 0.996 |

The fitted quench curves and the differences can be seen in Figure 19. The biodiesel blends were measured with the new protocol at a low coincidence bias setup due to the color quench, while the chemical quench curve was measured at a high coincidence bias. The differences can be observed across the whole range of the quench curve. A difference in the counting efficiency of colorless samples with a SQP(E) value between 750 and 850 is observed due to the change in the counting protocol and the width of counting window. This was also proven with measurements of bio-ethanol and HVO blends conducted with a standard addition, where the efficiencies obtained by both setups were in agreement. In heavily quenched samples, the difference in the counting efficiency can be explained by a combination of the counting protocol and the color of the biodiesel blends. The

quench curve obtained from a measurement of the biodiesels was used for obtaining a counting efficiency in the calibration and in later measurements.

## *7.5 Calibration*

Seven sets of samples, each containing 10 LSC samples from biodiesel with known feedstock oil, were prepared in accordance with the procedure described in Chapter 4.1 (see page 38) and measured with the new counting protocol. The blend preparation was the same as for the other bio-components. The $^{14}C$ peak was observed between channels 50 and 550 (see Figure 18) due to the wide variety of quench levels in the different biodiesel blends. On the logarithmic scale of the spectrometer the shape of the β spectra resembles a Gaussian distribution, and thus the peak's area could be described with a standard distribution of the counts around the channel of the peak. The majority of the measured samples had the centroid of the $^{14}C$ peak around the 200$^{th}$ channel, with a peak width of 200 channels. Taking into account the majority of the biodiesel samples, all of the counts in the counting window from 50 to 400 were considered in the calculation of activity. The sample's activity was plotted against the mass percent of biodiesel in the measured sample after the efficiency determination with a low bias quench curve from Figure 19.

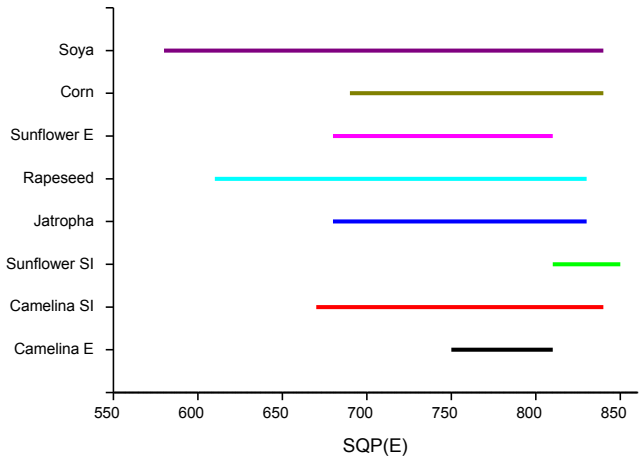


**Figure 20: Measured biodiesels SQP(E) range.** Variation of SQP(E) values of biodiesel blends from 1 $\%_m$ to pure biodiesel are presented.

The differences in the biodiesel blends could also be observed from the SQP(E) value (see Figure 20). SQP(E) values between 570 and 850 were observed, thus

according to the new biodiesel quench curve its efficiencies were between 51 and 88 %. The lowest levels were measured in blends of camelina biodiesel from the Spanish market and soya biodiesel, while the highest SQP(E) belongs to the sunflower FAEE from the Slovenian market. The rest of the biodiesel blends had SQP(E) values between those values and their span was different. As can be seen from the numbers in Figure 20 the biggest SQP(E) variation was observed in the measurements of soya biodiesel blends, while the smallest was observed in biodiesel from sunflower Slovenia. The characteristics of the biodiesel samples described in Chapter 3.5 (see page 26) were evaluated in comparison to the SQP(E) value. The measured parameters did not correlate with the differences in the observed quench parameter.

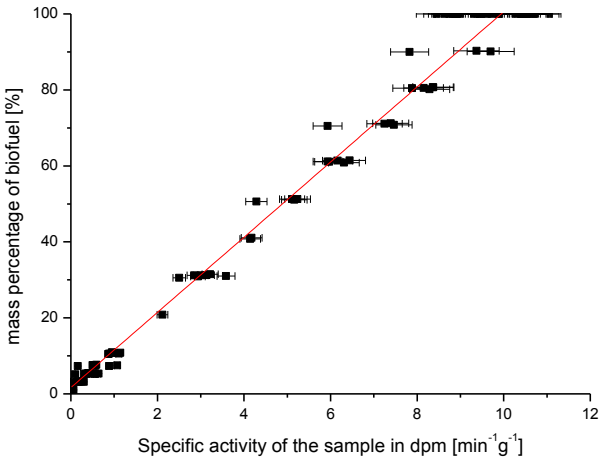


**Figure 21: Biodiesel at a low coincidence bias calibration.** Linear curve with correlation coefficient $R^2$ of 0.98 observed.

The calibration curve obtained can be seen in Figure 21. A linear regression line was obtained when the specific activities of the sample were plotted. The summary of the fitting parameters together with the correlation coefficient is presented in Table 17. The result of the fitting through dispersed sample activities was larger error of the fitting parameters. Those are taken into account in total uncertainty as the calibration uncertainty. A part of measurements with higher specific activity could be classified as outliers, because the counting window was too narrow. Those measurements belong to blends of sunflower biodiesel from the Slovenian market, which also had the highest SQP(E) value, and thus a higher counting efficiency (> 80 %) and a wider peak at different channels/energies than the rest of the biodiesel

measured. Furthermore, from the shape of the spectra, the SQP(E) values and the comparison with the fossil diesel's color, it was concluded that such samples could also be efficiently determined with the pre-designed producer's protocol used in the bio-ethanol and HVO measurements. SQP(E) value between 700 and 750 was determined experimentally as a trigger for using low or high bias protocol. Although a variety of quench levels was observed, counting with the new setup showed no limitations in the measurements of the highly quenched samples. The determination of the counting window was further evaluated in the optimization of the method in order to limit the possibility of outliers caused by the evaluation.

**Table 17: Summary of FAEE fitting parameters**

| Intercept | | Slope | | Statistics |
|---|---|---|---|---|
| **Value** | **Error** | **Value** | **Error** | **$R^2$** |
| 1.660 | 0.831 | 9.891 | 0.127 | 0.985 |

## *7.6 Background stability*

Background stability has an important role in the accuracy and the detection limit of the method. Thus the comparison of the background count rate when the measurements were conducted with a low or high coincidence bias setup was conducted. The stability of the background was expected because the spectrometer is equipped with low noise PMTs, a stable power supply, efficient active and passive shielding of detectors and samples and was used at a constant temperature obtained with a Peltier cooling unit [86]. The stability was evaluated through multiple measurements of fossil diesels and the average count rate with its deviation was calculated.

Measurements of 62 samples of diesel with approximately 440 measurements, each lasting 200 minutes, were conducted on a high coincidence bias setup. The average calculated background count rate was $0.894 \pm 0.089$ cpm (counts per minute). The count rate was taken in the counting window from 150 to 400. The dispersion of the data could be observed in Figure 22. The SQP(E) values of the measured samples varied between 709 and 880, and thus some differences could be present in the chemistry of the fossil diesel. One of explanations for the background

scattering could be in the sample origin. Measurements of the LSC samples detected as being below the detection limit were included in the experiment. As can be seen in Figure 23, only 20 measurements exceeded 2σ, and thus the stability of the counter was shown.

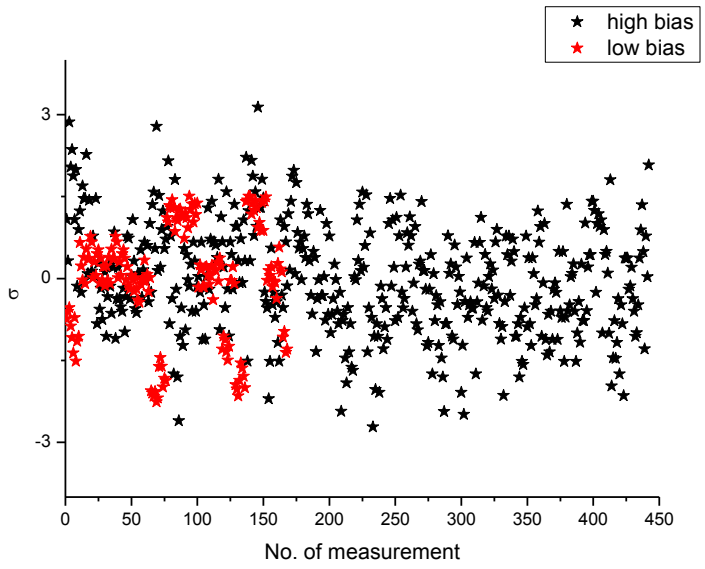


**Figure 22: Background measurements at high and low coincidence bias setups.** In black the measurements at high bias are presented, while in red are the measurements at low coincidence bias.

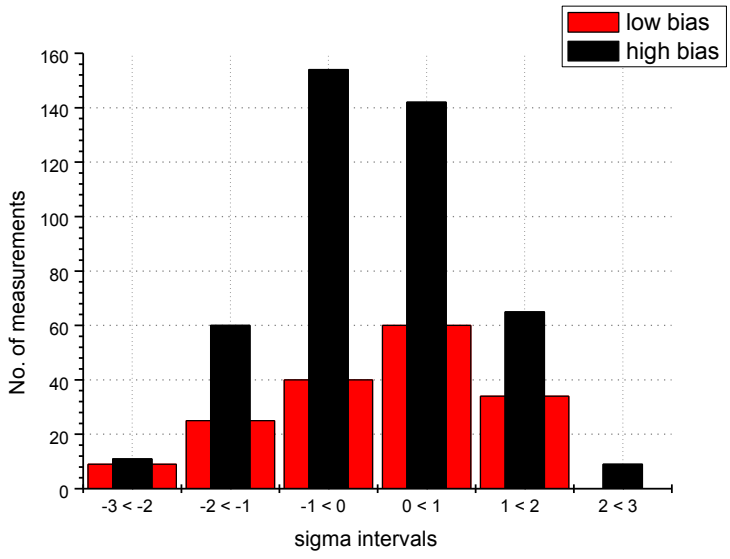


**Figure 23: Number of measurements in each interval.** On the high bias setup 440 measurements were taken, while on low bias setup there were "only" 170.

Because Cherenkov and fluorescence events are not rejected in the low coincidence bias, this means that the background count rate is much higher. The average background count rate for the low coincidence bias setup was 7.73 ± 1.09 cpm for a counting window from 50 to 400. "Only" 170 measurements from 11 samples were conducted and none of them exceeded 3σ from the average count rate (see Figure 23). The SQP(E) values of these samples also varied between 709 and 880 since they were the same samples as in the study for the high coincidence bias protocol. Further optimization of the counting protocol and the spectrometers environment was applied in order to improve the background stability and therefore improve the limits of detection.

## *7.7 Optimization*

Only small amounts of bio-component are often added to fuel samples from fuel stations. The correct calibration over the whole measuring range is important to use the method on real fuel-market samples. Accuracy and ability to measure the samples with a count rate close to background is therefore also necessary. The limit of detection is dependent on the background count rate, and thus it is significant to reduce it as much as is reasonably achievable. Passive and active shielding, coincidental circuits, etc., have already been applied to limit the background radiation interferences in liquid scintillation counters. LSC users have the ability to use several circuits for additional reduction of the background by considering its source. A description of such circuits is provided in Chapter 2.2 (see page 15).

The biodiesel protocol has the highest background count rate and thus the optimization was conducted on these samples. Different measurement conditions were tested during the optimization of the method. The literature does not report an analysis with changes in the temperature of the measurement chamber and the Pulse Amplitude Comparator (PAC), but those were the first candidates for a reduction of the background. A Pulse Shape Analyzer, which is regularly applied for α/β separation, was also tested. The background radiation is consisted of fast radiation similar to α radiation nuclides, while $^{14}C$ is a β emitter, and thus the background counts should be reduced [128]. A balanced counting window was applied in order to also take into account the quenching effect on the spectra and optimize the counting window.

### *7.7.1 Temperature of the measurement chamber*

PMTs may have some temperature-dependent noise and the efficiency of the scintillator to transfer decay energy can vary in accordance with the temperature. The temperature dependency of the counting efficiencies was evaluated. The chemical composition of the scintillation cocktail does not allow a large variety of testing temperatures, and therefore only temperatures between 8 and 20 °C were evaluated. The cooling unit of the LSC counter with four Peltier elements was used for the temperature modification. A change of temperature by 2 °C required 4 hours due to the high volume and mass of the guarding material. Unquenched standards of $^{14}C$, $^{3}H$ and a blank sample were measured after the temperature stabilization, which enabled control over the stability of the counter. Eight samples of PerkinElmer's standard quench set (see Chapter 4.2.2 on page 40) and a sample of background were measured at each tested temperature for 10 and 300 min long cycle, respectively. The counting efficiency of the background sample was obtained from the quench curve measured at the same temperature. The samples were measured only on a high coincidence bias set up because the response of the scintillation cocktail is not related to the counting protocol.

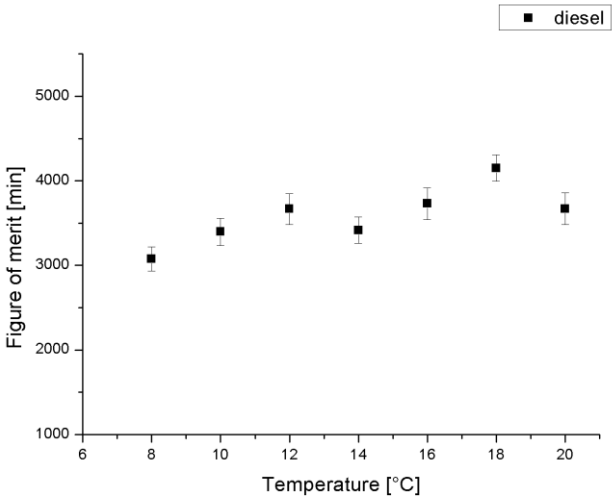


**Figure 24: FM at different temperatures.** Variation of FM at different temperatures is observed. The best FM is at 18 °C.

The results of the FM calculations at the measured temperatures are shown in Figure 24. Variations in the observed FM are not significant in the range of measured temperatures. Greater variations in the counting efficiencies and the related FM were expected. Surprisingly, the largest FM seems to be at 18 °C, while the lowest was as

expected at 8 °C, where the chemical composition of the scintillation cocktail decreases the counting efficiency. According to the ζ-test the difference between both extremes was only 3.62. The results are in contrast to the expectation of the PMT noise reduction at lower working temperatures. Based on these results, the measurement temperature was maintained at 18 °C for all the experiments.

The chemical quenched samples were also measured at different temperatures and the obtained results are presented in Figure 25. The counting efficiencies and the SQP(E) values were fitted to one quench curve. Such an evaluation was chosen because the SQP(E) values and the counting efficiencies followed the same correlation. Nevertheless, the SQP(E) values and the corresponding counting efficiency changed significantly for each tested temperature. The combined quench curve could then be used for all the temperatures since the individual and combined quench curves are statistically the same. At different temperatures the background count rate changes, and thus the calculated FM changes, as can be seen from Figure 24. Therefore it is important to measure background with each sample batch as was done in this experiment.

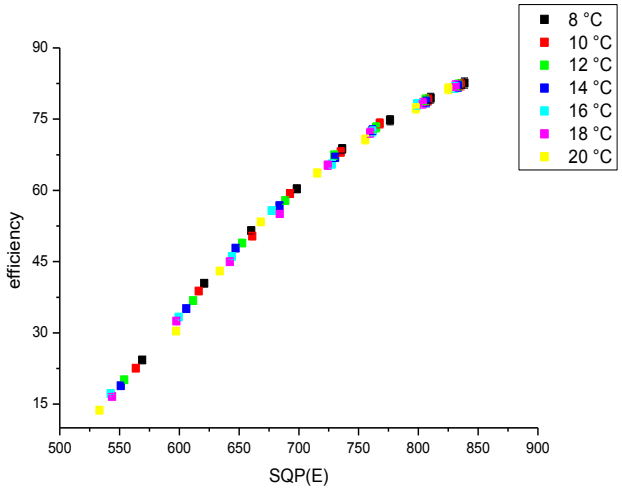


**Figure 25: Quench curve at different temperatures. All the measurements create one quench curve that is usable at all the tested temperatures.**

In the literature only Edler and Kaihola [10] reported the applied temperature of the spectrometer. Their applied temperature was the same as ours (18 °C). Other authors analyzing bio-components with the LSC technique do not report at which temperature measurements were taken [8, 9, 12, 16, 17, 27, 28, 63, 64].

### *7.7.2 Pulse Amplitude Comparator (PAC)*

Glass vials were used in the fuel measurements, thus the possibility for Cerenkov events in the vial wall or the optical crosstalk existed. Such events can be rejected or limited if the PAC threshold is set correctly. A set consisted from two samples: fossil diesel (background determination) and a sample with known activity was prepared in order to determine the influence of the PAC circuit on the fuel measurements. The LSC samples were measured at different PAC levels at a low and high coincidence bias within the software setup possibilities. The background count rate was obtained in 100 min, while for the LSC sample with known activity, the counting time was 30 min.

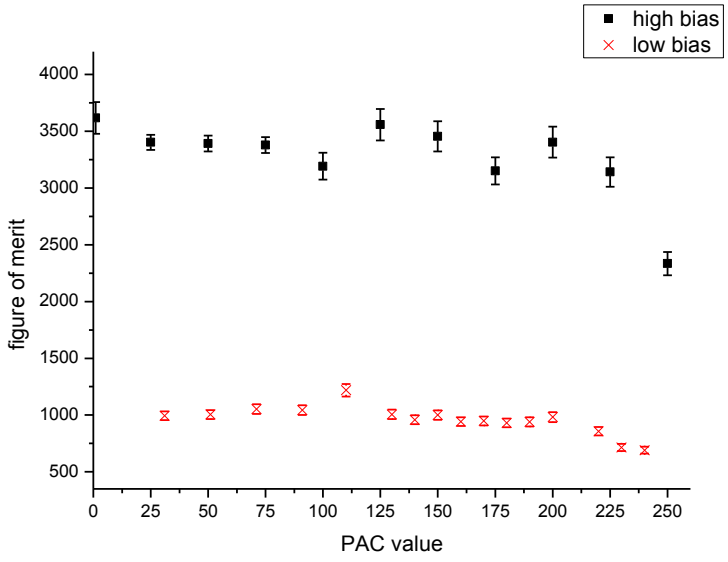


**Figure 26: PAC optimization.** Dots represent measurements at a high coincidence bias and crosses measurements at a low bias.

The FM for the high coincidence bias setup is much higher than those for measurements at a low bias, as can be seen in Figure 26. Although counting efficiencies at a low coincidence are usually higher, the background count rate is also higher due to the Cherenkov events observed below the 300$^{th}$ channel. A rather large uncertainty range was obtained for measurements at a high coincidence bias, due to the total number of background counts. Many of the results presented are not significantly different. The correct PAC setup is limited. The PAC values above the 100 have the highest potential for the best set-up. The uncertainty decreased with four repeated setups, but the calculated FM did not differ significantly.

The variations of FM are smaller in measurements at a low coincidence bias. The uncertainty of this set of results is lower due to the better counting statistics, which is a consequence of the higher background count rate. The counts of the peak below the 300$^{th}$ channel (see Figure 18 on page 71) decreased by about 20 % in the background spectra of the low coincidence bias protocol. A comparison of the pulse height on which the PAC is based could be disturbed by sample quench. Additional measurements were conducted with biodiesel samples (described in Chapter 3, page 20) for the correct set-up of this parameter (see Chapter 7.7.4).

### *7.7.3 Pulse Shape Analyzer (PSA)*

As was shown in Figure 6 (see page 19), alpha- and beta-like pulse differ in the tail of the pulse. The PSA circuit uses this pulse characteristic for differentiation between types of pulses [86]. Some of the slow florescence events can be observed in the background measurements because of the radioactivity of the vial material. A further reduction of the background count rate could be possible with the PSA because the radioactive decay and the slow florescence differ in pulse length. Normally, the PSA level is used for measurements of gross alpha and beta radionuclides in water samples [89, 90, 92, 129, 130]. The PSA is also used in radio-chemistry for the differentiation between isotopes of the same element [88, 131]. The authors already reported PSA level shifting in water samples when different pre-concentrations or quench levels were observed [90]. Furthermore, Manjon *et al.* [131] reported color quench interference with a PSA level when measurements of $^{3}$H, $^{90}$Sr, $^{99}$Tc and $^{239}$Pu were conducted. The color quench was achieved with the use of $Na_2CrO_4$ [131]. Similar details were reported by Villa *et al.* [88] when $^{210}$Pb was measured. According to Pates *et al.* [92] this occurs due to the PSA level energy dependence. It is known that the quenching shifts the spectrum to lower energies and that low energetic radionuclides have a lower optimal PSA. Furthermore, quenching agents that are electron scavengers ($O_2$, $CCl_4$) are able to interact with the solvent and reduce the delayed component [92]. This was one of the reasons why PSA was also evaluated with samples of biodiesel (see Chapter 3 on page 20).

The optimized PSA value was evaluated with a sample of fossil diesel and a sample with known activity, as in the case of the PAC. The preparation of the sample

was the same as in the PAC experiment described in Chapter 7.7.2. The standard solution was measured for 10 minutes, while the background count rate was obtained over 100 minutes. The samples were measured at every tenth level in the range from 1 to 256. The measurements were performed on high and low coincidence bias setup. According to the PSA theory, if the level is set properly the beta-like ($^{14}C$ decays) signals are directed to one spectrum and others (α like) to the second spectrum [86]. The focus of the investigation was decreasing the impact of the peak under the 300$^{th}$ channel. We can use only the count rate in the beta spectra for a calculation of the FM and the observation of the background count rate decreased because the measured samples contained only $^{14}C$, which is a pure β emitter.

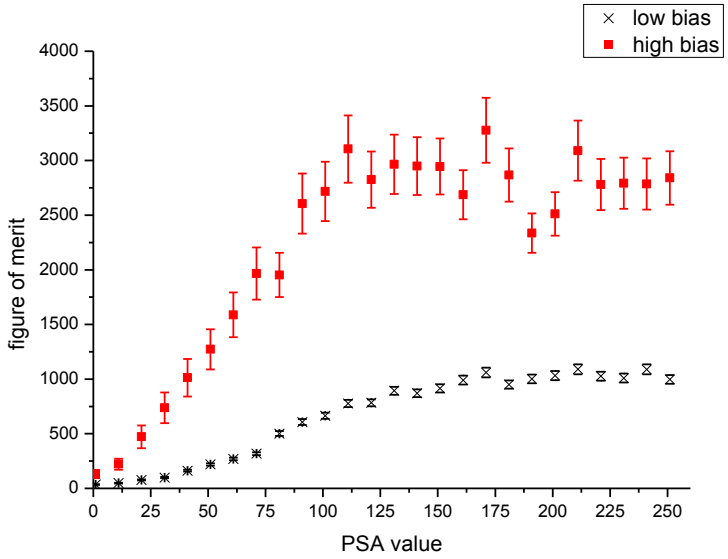


**Figure 27: PSA setting**. Dots represent measurements at a high coincidence bias and crosses the measurements at a low bias.

The FM was much higher in measurements at a high coincidence bias also in the PSA setup. The PSA circuit improved the FM to some extent, as shown by the high coincidence bias results on Figure 27. The FM reaches a plateau at a PSA between value 110 and 170, but due to the large uncertainty, the results were not significantly different ($\sigma < 1$). This set of results has poorer counting statistics with a total of background counts between 680 and 1300, and thus a higher uncertainty than in the measurements at a low coincidence bias. The same was also shown in the case of the PAC setup. This is consequence of the limited background counting time, which in these experiments was 100 min for each level tested.

A smooth curve with a stabilized FM at values above 170 was obtained for measurements with the PSA in a low coincidence bias. This was expected, since higher levels mean the signal is beta-like. The experiment did not confirm the expectation that using the PSA optimization the counting efficiency will remain at previously measured levels, while the background count rate would drop below 4 cpm. That would enable a limit of detection of around 2 $\%_m$. All of the authors evaluated reported similar findings with a smaller possible PSA level setup in other matrices and for other radionuclides. For instance, Palomo *et al.* [90] reported that the preparation procedures could affect the determination of the optimal PSA level for up to 25 %. The PSA level threshold between levels 40 and 120 in beta emitters ($^{99}$Tc and $^{90}$Sr) was reported by Manjon *et al.* [131]. An analysis of the water samples conducted on the same LS counter as biofuel in this thesis showed that the optimal PSA was around 100 [132].

### *7.7.4 Multi- Channel Analyzer setup changes (MCA)*

The Quantulus is equipped with multi-channel analyzers (MCA), as discussed in Chapter 2.2 (see page 15). Some authors have already studied the effect of MCA changes. Kaihola [133] used this approach for gamma emission monitoring. The author successfully applied the approach to measurements of two beta- and gamma-emitting isotopes $^{137}$Cs and $^{60}$Co [133]. The same author also reported the use of a cosmic particle spectrum as a quench monitor [134]. The same approach was also used by Manjon *et al.* [131] in their research.

The MCAs were used for the application of PAC and PSA in our research. Both analyzers were used simultaneously, introducing the possibility for combined affects (see Table 18). The protocol for measurements of high-energy β emitters was used as a basis. The MCA's inhibit and memory split were changed in MCA1, meanwhile MCA2 was set as for a pre-designed protocol. The usual MCA2 guard measurements were discarded. Different combinations of PAC and PSA were set on the entire range from 1 to 256. PAC and/or PSA were re-evaluated due to the possibility of a combined effect at every 50$^{th}$ PAC and PSA level. The experiments were conducted only on a low coincidence bias setup, where the highest background was observed. The LSC samples containing 100 % biodiesel and fossil diesel were prepared in accordance with Chapter 4.1 (see page 38) and measured with a new circuit setup.

The biodiesel samples produced in the laboratory were used for this experiment (see Chapter 3, page 20).

**Table 18: Special protocol circuit setup. MCA1 was changed while MCA2 was set to pre-designed $^{14}C$ measurements. The guard measurement of the pre-designed protocol was discarded.**

| | MCA1 | MCA2 |
|---|---|---|
| **ADC Input** | LRSUM | LRSUM |
| **ADC Trigger** | L*R | L*R |
| **Inhibit** | G | N |
| **Memory Split** | PAC+PSA | PAC+G |

The results in Figure 28 present the best and worst case scenarios that were chosen based on the SQP(E) values. Soya biodiesel is a representative of the lowest SQP(E) value, while biodiesel from Slovenian sunflower was of the highest SQP(E) value. A comparison of the results obtained using only the PAC or PSA circuit on low coincidence bias and those obtained with the combined circuit were conducted. The improvement in the FM was up to 50 % for samples with a lower SQP(E) than usually observed in real market samples. The experiment confirmed the dependency between the PAC level and the observed quench (SQP(E) value). For the combined experiments it was shown that the highest FM was obtained with a PAC level of 50. This was also proven in the evaluation of only this parameter (MCA2), where level 50 obtained the highest FM in the low SQP(E) samples. The Slovenian sunflower biodiesel's PAC levels of 50, 100 and 150 obtained, statistically, the same result ($\zeta$-test < 1). The optimal PAC is lower than expected based on results of previous work on diesel fuels (see Figure 26), where values of around 100 were the best. This leads to the conclusion that the PAC value is affected by the sample quench level since pure biodiesel had lower SQP(E) values than the fossil diesel used in the first experiments.

The application of PSA in the measurements of quenched samples cannot be done precisely because the applied level changes with an increasing quench, as can be observed in Figure 28. Each quench level would therefore require a different PSA setup. However, the PSA setup could be efficiently introduced if the variability of the

quench level is smaller. This is shown in measurements of the Slovenian sunflower biodiesel. Such an approach was introduced by Hiller *et al.* [91], who used PSA for the background reduction in $^{14}$C-benzene counting and reduced the limits of detection. The method proposed by Pujol and Sanchez-Cabeza [89], where a short measurement of SQP(E) would tell which value of PSA is the most efficient, was not applied due to the great variety of SQP(E) values and therefore a need for special set of measurements for each obtained sample.

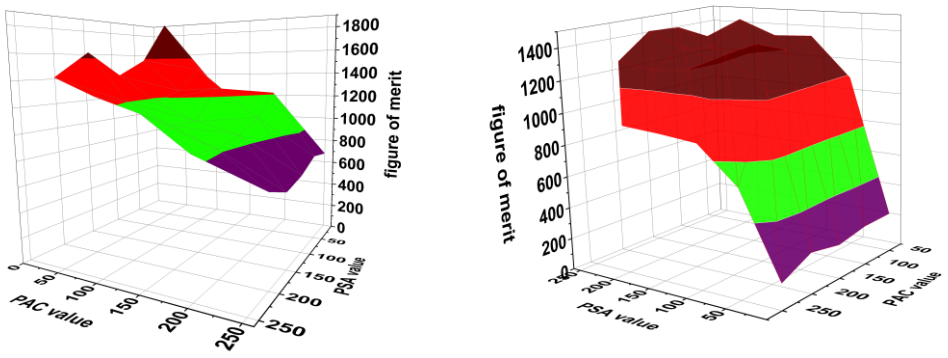


**Figure 28: Changed MCA circuit. On the left side the results of biodiesel from the soya oil with a SQP(E) value of 605 are presented. On the right are the results for the biodiesel from the Slovenian sunflower oil; its SQP(E) value was 808.**

From this experiment, it was concluded that quenching has a major role in an optimal PSA setup; therefore, when the quench may vary significantly, as observed in fuels, it is not usable. The counting-window width and position were evaluated for a reduction of the background count rate and a further optimization of the protocol.

### *7.7.5 Quench balanced counting window*

The approach was introduced by Ross [135], who changed the window voltage on early LSC systems and tested them with eight different quenchers. Recently, Theodórsson *et al.* [136] applied the balanced-window method on a laboratory-built single PMT system. After an adjustment of the high voltage of the counter to maximize the $^{14}$C counting efficiency, several channel ratios were tested and an energy calibration was conducted. The authors reported a high counting stability [136]. Tudyka *et al.* [137] used the approach of Theodórsson *et al.* [136] and adjusted it for use in commercially available LS counters such as the Quantulus 1220™. The approach was tested on a limited quench range where the system gives a linear response [137]. For some researchers who use a software programmable

window [138], a quench balanced counting window means extra labor since the determination of the quench level and the rest of calculation have to be made in advance (prior measurement). A different approach was taken in this thesis.

Different levels of quench were observed in measurements of different biodiesel blends. Furthermore, the SQP(E) value for the same blend changed with the type and age of the biodiesel. The counting window to obtain $^{14}C$ counts had to be wide in order to calibrate a variety of biodiesels. As explained before, the window was chosen based on the average width of the $^{14}C$ peak because the majority of biodiesels were covered and the counting window was kept small. This has a significant impact on the background count rate and the detection limit. Some of the blends, especially the Slovenian sunflower biodiesel, were misinterpreted because the activity was not determined correctly. An experiment with a quench balanced counting window was made in order to limit the counting window and reduce the background count rate and the detection limit. The problem was observed only in diesel samples, and thus an additional analysis of the spectra was conducted on them.

Measurements of approximately 170 LSC samples, made from all the biodiesels described in Chapter 3 (see page 20), were taken into account. The bio-components were mixed with fossil fuel in samples containing from 5 to 100 $\%_m$ of biodiesel. Measurements of the SQP(E) were conducted for each cycle in accordance with the Quantulus protocol and values between 360 and 910 were obtained. The counting efficiency was determined through the quench curve depicted in Figure 19 (see page 72). Spectra obtained from the Quantulus on a logarithmical energy scale were converted to the ACSII-gls format with home-made software [139]. The program RadWare [140] was used as a tool for the determination of the full width at half maximum (FWHM) and the centroid of the $^{14}C$ peak. RadWare is a software package for interactive graphical analysis of the gamma-ray coincidence data [140]. It can be used on a beta-emitting radionuclide because the logarithmically presented spectra follow a Gaussian distribution. RadWare was also used for resolving the counting window while measuring the $^{3}H$ in urine by a colleague from the laboratory [141]. The ACSII-gls version of the Quantulus spectra was fitted. Two-peak fitting was chosen because the low coincidence bias protocol has a $^{14}C$ peak and an additional peak below the $300^{th}$ channel. Channels up to the $700^{th}$ were used in the evaluation, thus the $^{14}C$ decay energies from $E_0$ to $E_{max}$ were used. The count rate used in the

calibration and a further analysis was obtained from the individually calculated counting window.

#### *7.7.5.1 Determination of spectra position*

The first step in the determination of the counting window is to determine the position of the $^{14}C$ peak. In addition to the sample spectra also the SQP(E) values were used for further evaluation. In this part of the experiment, the SQP(E) value was used not just as an indicator for quenching but also as a parameter for choosing the correct position of the $^{14}C$ peak. Figure 29 presents the correlation of SQP(E) value and the position of the $^{14}C$ peak obtained from RadWare for a given quench. The fitted positions of the spectra tell us where the centroid of the $^{14}C$ peak is. It should be noted that the position is related only to the $^{14}C$ peak and not to the entire spectra. The SQP(E) value was also used in a measurement efficiency determination for the activity calculation. A polynomial fit shows that the SQP(E) levels below 600 could be overestimated. Highly quenched LSC samples are presented with a lower energy/channel, which is limited by the PMT efficiency. Limitations in the SQP(E) value calculation were noted in measurements of high-energy emitting isotopes [142]. However, the correlation between the position of the $^{14}C$ spectra in various biodiesel blends and the amount of quenching in the measured sample proves the usability of the quench parameter for a determination of the peak's and the counting window's position also for colored samples.

**Table 19: Fitting parameters for SQP(E)-position correlation**

| Slope [$x^2$] | | Slope [x] | | Intercept | | Statistics |
|---|---|---|---|---|---|---|
| **Value** | **Error** | **Value** | **Error** | **Value** | **Error** | **$R^2$** |
| -3.338 | 1.467 | 0.48 | 0.09 | 24.67 | 12.61 | 0.718 |

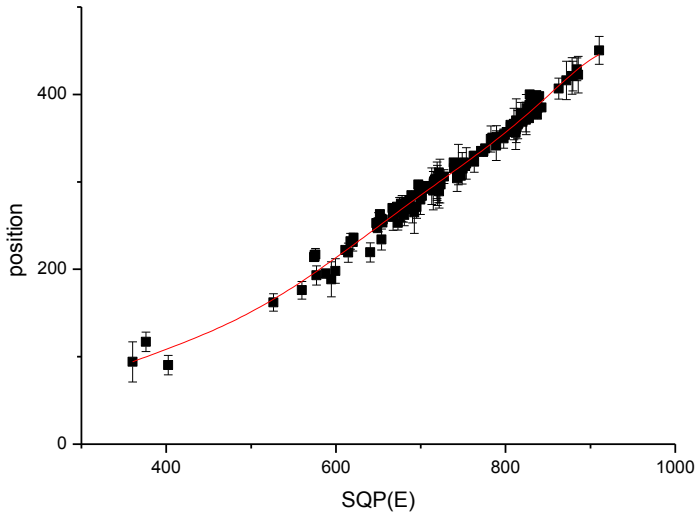


**Figure 29: SQP(E) and position of C14 spectra correlation.**

### *7.7.5.2 Determination of counting-window width*

The position of the $^{14}C$ spectra, determined as explained previously, is used as an argument in Figure 30 where the relation to the $^{14}C$ peak width is presented. The widths of the peak (FWHM) and its uncertainties were also obtained with the same RadWare fitting as the peak's position. The dispersion of the results could be observed since the fits were individually made for each spectrum. As a consequence of such a dispersion, the correlation was fitted with a cubic polynom. For an improvement of the counting statistic and a reduction of the dispersion contribution it was decided to use a width times 2 and therefore using the 2 sigma (98 %) of the $^{14}C$ peak as a counting window. Although the window is still relatively wide, it changes with quench, and thus compared to the window used in the calibration before, it is more sample specific.

**Table 20: Fitting parameters for $^{14}C$ peak width determination**

| Slope [$x^3$] | | Slope [$x^2$] | | Slope [x] | | Intercept | | Statistics |
|---|---|---|---|---|---|---|---|---|
| **Value** | **Error** | **Value** | **Error** | **Value** | **Error** | **Value** | **Error** | **$R^2$** |
| 4E-06 | 1E-06 | -3E-03 | 1E-03 | 1.28 | 0.31 | -35.61 | 25.73 | 0.728 |

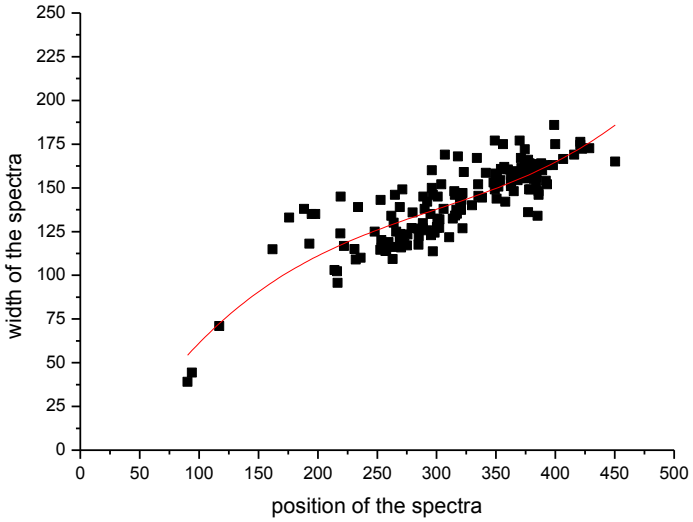


**Figure 30: $^{14}C$ peak width determination**

### *7.7.5.3 Calibration with balanced window*

A new calibration curve was made with a changed counting window. The measurement results of the calibration set of samples that was used in Chapter 7.5 were re-evaluated with the new counting windows. The counting window and the corresponding background were determined for each repetition. This decreased the background count rate for the majority of measurements. This improved detection limit will be discussed in Chapter 7.8.2. The linear calibration curve obtained in the re-evaluation is presented in Figure 31.

The correlation between the newly calculated specific activities of the samples and the mass percentages of biofuel shows improvements made with a balanced counting window in relation to a fully opened counting window. This was observed in all of the validation parameters that will be discussed later in the text. Although each data point is burdened with an additional uncertainty in the counting window determination, a decrease of the background variation count rate also decreases the total uncertainty for each point. Also, the errors of each fitting parameter decreased in comparison to those obtained before (see Table 17 at page 75) as can be seen in Table 21. The correlation coefficient is comparable to those observed in the calibration for bio-ethanol and HVO, even though the measurement protocol was changed and additional calculations had to be made. All of the characteristics of the curve were used in validation (see chapter 7.8).

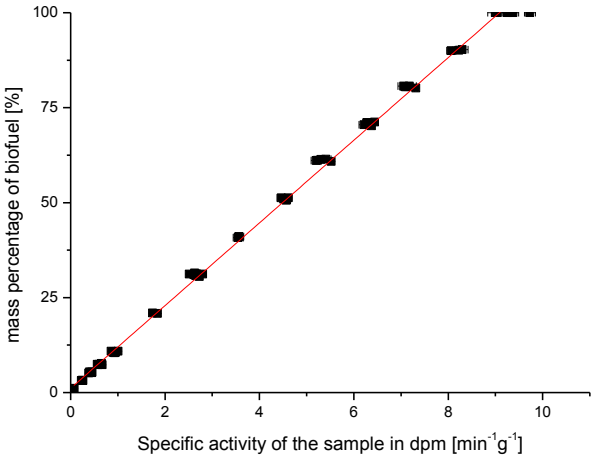


**Figure 31: Biodiesel calibration with quench balanced window.** Linear calibration curve with correlation coefficient $R^2$ larger than 0.99 was obtained. Background was calculated for each measurement and it is used as a parameter in uncertainty budget.

**Table 21: Fitting parameters for a balanced counting window protocol.**

| Intercept | | Slope | | Statistics |
|---|---|---|---|---|
| **Value** | **Error** | **Value** | **Error** | **$R^2$** |
| 1.137 | 0.280 | 10.882 | 0.059 | 0.998 |

## *7.8 Validation parameters*

The validation parameters presented and discussed in this sub-chapter were calculated based on the procedure described in Chapter 4.3 (see page 42). They are summarized in Table 23.

### *7.8.1 Uncertainty*

The uncertainties for the measurements near the detection limit, at 10 % and at 100 % of biofuel, were calculated and evaluated (see Table 22). The individual uncertainty and its contribution were calculated in accordance with the procedure described in Chapter 4.3.1 (see page 42). The background stability and the sample counting were evaluated as a combined uncertainty and represent the smallest, still significant, contribution to the total uncertainty. This is consequence of the quench balance counting window, which optimizes the window based on the sample's quench. An important uncertainty source for all biofuels is the uncertainty of the

standard solution for the determination of the quench curve and the counting efficiency. Compared to other measured biofuels, a calibration uncertainty has a 20 % larger impact. This is not surprising since changes in the protocol and a different evaluation of the counting window had to be applied. It includes a determination of the position and the width of the counting window where each parameter is burdened with an additional uncertainty.

**Table 22: Biodiesel protocol uncertainty budget**

| Source | near DL | | at 10 $\%_m$ | | at 100 $\%_m$ | |
|---|---|---|---|---|---|---|
| | % of total | absolute | % of total | absolute | % of total | absolute |
| Balance | 0.001 | 0.0001 g | 0.01 | 0.0001 g | 0.02 | 0.0001 g |
| Background cpm | 8.62 | 2.66 ± 0.04 | 5.06 | 3.00 ± 0.24 | 0.78 | 4.84 ± 1.15 |
| Sample cpm | | 3.49 ± 0.60 | | 9.76 ± 0.30 | | 53.05 ± 15.92 |
| Efficiency | 12.49 | 1.3 % | 32.79 | 1.3 % | 83.40 | 1.3 % |
| Calibration | 78.89 | 2.4 | 62.14 | 2.4 | 15.80 | 2.4 |
| Total | 0.25 $\%_m$ | | 0.28 $\%_m$ | | 1.32 $\%_m$ | |

### *7.8.2 Detection limit*

The Currie [122] and ISO 11929 [123] procedures were used in the calculation of the detection limits for each variation of the biodiesel calibration as described in Chapter 4.3.2 (see page 44). The results of the evaluation are depicted in Table 23. The limits calculated by both methods differ, where Currie's limit was higher than already observed with other measured biofuels. The lowest limit of detection calculated in accordance with Currie's calculations was obtained with a high bias (0.89 $\%_m$), while the detection limit calculated in accordance with ISO 11929 was 0.66 $\%_m$. The highest limit of detection was calculated from a low-bias protocol where a fixed window was used (2.73 $\%_m$). The ISO 11929 detection limit for the same protocol was 2.26 $\%_m$. The application of the quench balanced window decreased the detection limit by at least 0.59 $\%_m$, but did not achieve the limits

calculated for the high-bias protocol. The quench balanced window protocol has a higher limit of detection, by at least 1 $\%_m$. Therefore, for precise measurements of the fuel with a low biodiesel percentage the high-bias protocol is more suitable, while for measurements of unknown amounts of biodiesel a low-bias protocol with a quench balanced window could be used.

**Table 23: Biodiesel protocols validation parameters**

| Parameter | High bias | | Low bias | | Balanced window | |
|---|---|---|---|---|---|---|
| **Detection limit (Currie [122])** | 0.89 $\%_m$ | | 2.73 $\%_m$ | | 1.96 $\%_m$ | |
| **Detection limit (ISO 11929 [123])** | 0.66 $\%_m$ | | 2.26 $\%_m$ | | 1.67 $\%_m$ | |
| **Linearity** | 0.999 | | 0.985 | | 0.998 | |
| **Repeatability** | 0.5 $\%_m$ | | 0.58 $\%_m$ | | 0.44 $\%_m$ | |
| **Reproducibility** | 0.27 cpm | 0.1 $\%_m$ | 0.35 cpm | 0.2 $\%_m$ | 0.19 cpm | 0.2 $\%_m$ |
| **Sensitivity** | 12.546 | | 9.891 | | 10.882 | |
| **Trueness** | See chapter 8 | | | | | |

### *7.8.3 Linearity*

Linearity was demonstrated with the correlation coefficient obtained during the calibration curve fitting. The correlation coefficients for all biodiesel protocols are depicted in Table 15 (see page 68), Table 17 (see page 75) and Table 21 (see page 90). The highest correlation coefficient was obtained with a high-bias protocol, while the lowest was in a low-bias protocol, 0.999 and 0.985, respectively. If we compare both protocols conducted on a low-bias setup we can conclude that the application of the quench balanced window improved the correlation coefficient. With the application of a quenched balanced window a correlation coefficient of 0.998 was obtained, which is comparable to the high-bias biodiesel protocol as well as the protocols of the other biofuels presented before. The high bias protocol's calibration curve obtained an error of 0.06 %, what is more linear than any other biofuel measurements with a high bias protocol. The linearity of the points decreased with

the introduction of the low bias protocol, as expected. The uncertainty of the curve was 0.5 %, but with the introduction of the quench balanced window the uncertainty reduced to 0.25 %.

### *7.8.4 Repeatability*

Repeatability was evaluated as the standard deviation of the results obtained from 10 consecutive counting cycles. In high-bias measurements, the standard deviation obtained after two-step calculations was 0.50 $\%_m$. When samples were measured with a low coincidence bias protocol, the dispersion of the results was 0.58 $\%_m$. The results were also evaluated using a protocol with a quench balanced window. With such an evaluation, the repeatability improved to 0.44 $\%_m$ for the same 10 $\%_m$ sample. This improves the accuracy of the quench balanced window protocol and further improves the achievements of the high-bias protocol.

### *7.8.5 Reproducibility*

The high coincidence bias protocol was used in measurements at different temperatures. The samples count rate and SQP(E) values changed at each temperature beyond the parameter's uncertainty, but the results are calculated with a specific activity where such changes are taken into account. The sample count rate and the SQP(E) values were also evaluated from the measurements with the same protocol obtained over a period of one week. The calculated results were within the uncertainty of each measuring protocol.

### *7.8.6 Sensitivity*

To evaluate the method's sensitivity, the slope of the calibration curve was checked. The high coincidence bias setup had a slope of 12.546 (see Table 15 on page 68). The low coincidence bias protocol is, with 9.891, less sensitive than the high bias protocol, but has a larger measurement range (see Table 17 on page 75). The sensitivity of the protocol of the low coincidence bias with a quench balanced window is 10.882, which is an improvement compared to the low coincidence bias protocol, but less sensitive compared to the high coincidence bias protocol (see Table 21 on page 90). The large measurement range in the low bias protocol, which covers the whole range from 0 to 100 $\%_m$ of biodiesel, is an advantage compared to the high-bias protocol. The latter has a measurement range only up to 10 $\%_m$.

# 8 Comparison with other methods

For the inauguration of the direct method, some samples were also measured using the LSC method with $CO_2$ capture, which is a long-established method. The evaluation of the method's acceptability was conducted by participation in international comparative tests. The results obtained are presented further in the text.

## 8.1 $CO_2$ measurements with LSC

The direct method was compared to the LSC method, which uses $CO_2$ in a preparation of the sample [68]. A cooperating laboratory at the National Institute for Cryogenic and Isotope Technologies, Râmnicu Valcea, Romania performed the measurements with the $CO_2$ absorption method. The LSC sample preparation is made in three stages. First, a scintillation cocktail mixture is prepared. The laboratory uses their own LS cocktail made from 2-Methoxyethylamine. Commercially available Carbosorb E and Permaflour $E^+$ (PerkinElmer) were not used because saturation of the $CO_2$ solution could not be achieved. A sample (approx. 1.5 g) was placed in a Parr bomb, filled with oxygen and burned in the second stage of the sample preparation. In the third stage, the sealed bomb was fitted to the bubbling line. The $CO_2$ is circulated through a bubbler containing the LS cocktail until the cocktail is fully saturated. The bubbling line is equipped with two additional traps to recover any vapor from the LS cocktail. The LSC samples prepared in accordance with this procedure were measured in the LS counter Quantulus (Wallac Oy, PekinElmer). Blends from 5 to 30 $\%_m$ and pure biodiesels (a total of 30 samples) were analyzed by $CO_2$ and the direct method. The LSC samples analyzed with the direct method were prepared in accordance with the procedure described in Chapter 4.1 (see page 38).

The results of the $CO_2$ method are reported in Bq/g of C, while the direct method operates with specific activities (dpm/g of sample). The comparison of the results was conducted both in Bq/g of C and Bq/g of sample. The carbon content in the specific sample was obtained by the cooperating laboratory. The average content of carbon in the measured samples was in agreement with the reported values in the literature [17, 28, 63]. The recalculation was made by dividing a specific activity in Bq/g of sample with the content of carbon in biodiesel and vice versa. The

uncertainty of the direct method was calculated in accordance with the procedure described in Chapter 4.3.1 (see page 42). The analyses conducted with the $CO_2$ method are reported with only the counting uncertainty, since the full uncertainty budget was not yet evaluated.

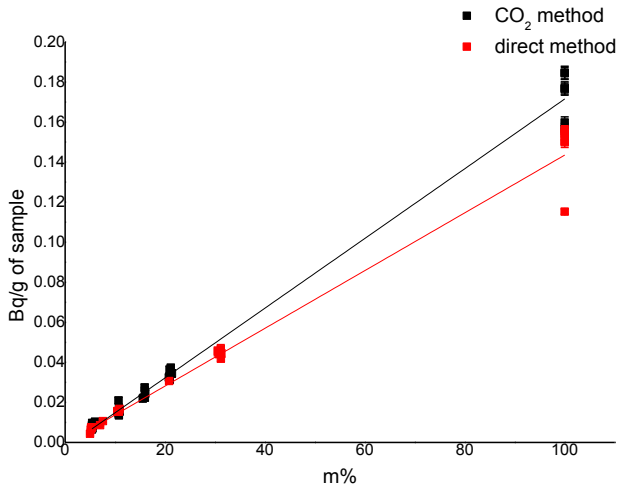


**Figure 32: $CO_2$ and direct method comparison in Bq/g of sample.** Results of biodiesel blends up to 30 $\%_m$ are comparable, within the uncertainty. The greatest difference in activities is obtained when pure biodiesel is measured.

The specific activities (see Figure 32) obtained after analyses with both methods are in agreement for blends up to 30 $\%_m$. All the results of 100 % biodiesel samples for the direct method show lower calculated activities than in the case of the method with $CO_2$ preparation. The same was also observed when specific activities were recalculated to activities per gram of carbon (Bq/g of C). The trueness of these results is presented in Figure 33. The largest error was obtained in the analysis of soya biodiesel. One of the reasons for such a result could be a misinterpretation of the quench. The observed SQP(E) value was around 550, and thus at the bottom limit of our quench curve. A new evaluation with a quench balanced window could also present a misinterpretation in the background count rate. In this case, the background count rate would be lower than the calculated one. Although the measured samples were used for calibration purposes, the errors observed in this evaluation do not present a concern, because they are part of the sample count rate variation, which is included in the conservatively calculated uncertainty budget. In addition the result

reported to the customer is in the form of mass percent where variations in composition and activities are taken into uncertainty budget.

Given the current fuel market and its prediction the most interesting analyses are those of blends up to 20 $\%_m$. Therefore we decided to evaluate trueness of data obtained with direct and $CO_2$ method for blends up to 20 $\%_m$ by applying ζ-test (see equation 19). As a limit for the acceptability zeta-score of 2 was chosen. As in the case of the pure biodiesel samples, the activities of blends of up to 20 $\%_m$ were lower than those obtained from the $CO_2$ method. However, the results presented in Figure 33 show that the trueness of our results is acceptable, even if a recalculation to Bq/g of C needs to be conducted. As was explained before, the recalculation was done with data obtained from the collaborating laboratory, since the direct method does not give such data.

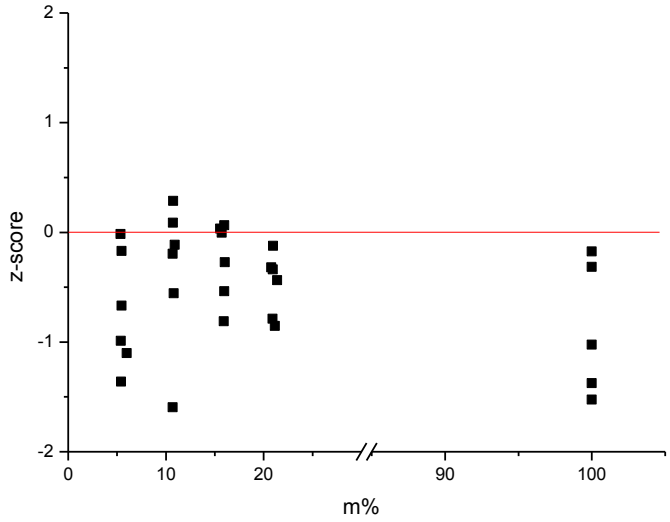


**Figure 33: Trueness of direct method measurements.** Results in Bq/g of C are compared. Equation 19 was used for calculation, where both measurements uncertainties were taken into account.

In order to apply the method on the fuel market where the bio-component quantity is often lower than the 5 % comparison of background count rate and the resulting detection limit was also conducted. The background count rate of the $CO_2$ method was much lower (2.22 cpm) than those obtained with the direct method, which varied from 2.52 cpm to 6.1 cpm. In the direct method the background count rate is determined individually, given the sample quench. On the other hand, the $CO_2$

method gives more uniform background count rates, which vary only within the parameter's uncertainty. However, the limits of detection calculated for both methods with a background of 5 $\%_m$ of biodiesel were comparable. This biodiesel blend was the sample with the lowest bio-component quantity measured in the scope of this comparison. The comparison presented shows the limitations of the direct methods when pure biodiesel analyses have to be performed. However, quantities of bio-components below 20 $\%_m$ and especially near the detection limit can be equally accurately determined by both the $CO_2$ and direct method.

## *8.2 International comparative tests*

The method was evaluated by three international comparative tests organized by the European Union Group of Customs Laboratories [143–145]. One was organized in the winter 2010/2011 and two in winter 2012/2013. Summarized results are presented in Figure 34. Acceptability was evaluated with a ζ-test, while the limit was set to two. All of the evaluated results were acceptable. Involvement in the tests in 2010/2011 was a great honor, since this was the first organized comparative test for biofuels.

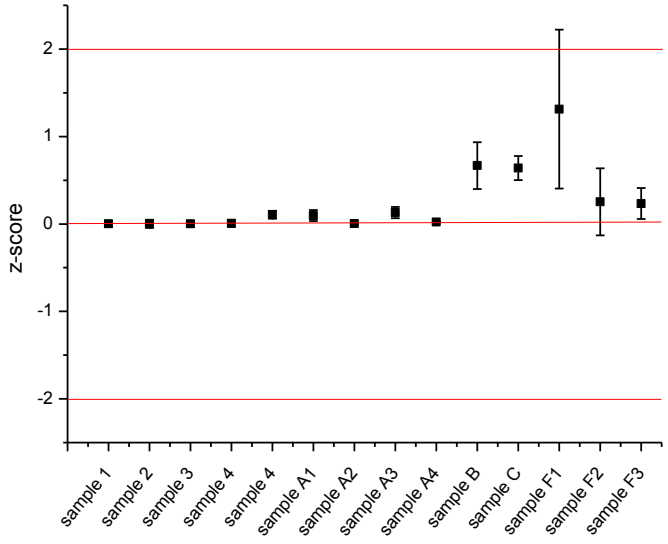


**Figure 34: Comparative tests.** Red lines are acceptability limits.

### *8.2.1 GCL bio-components in fuels 2010/2011*

Measurements were made on four samples of different compositions. HVO and/or bio-ethanol were used as a bio-component and gasoline and diesel as fossil

fuels. The results were reported with expanded uncertainty with a coverage of 95 %. The calculated values were a robust mean and the standard deviation of the reported values of all the labs. The ζ-test was calculated for each set of results by the organizer of the inter-laboratory test. Organizer reported also gravimetrically determined real values. For the parameter of bioethanol quantity in sample 4 the organizers did not conduct ζ-test due to the lack of reported results. The preparation of the samples for the comparison was described in official report, and thus we used this data for the evaluation of our method.

**Table 24: GCL bio-components in fuels 2010/2011 comparison.** BioEtOH stands for bioethanol. Result marked with * was compared to real value reported in official report, and thus does not contain the standard deviation of the reported results.

| Sample No. | Sample constitution | Measured quantity | Reported values | Calculated values | Real values |
|---|---|---|---|---|---|
| 1 | BioEtOH & EtOH | BioEtOH | 79.84 ± 2.74 | 79.77 ± 1.02 | 79.98 |
| 2 | BioEtOH, EtOH, gasoline | BioEtOH | 5.82 ± 0.28 | 5.82 ± 0.84 | 6.19 |
| 3 | HVO & diesel | HVO | 18.71 ± 0.59 | 18.67 ± 0.43 | 18.88 |
| 4 | HVO, BioEtOH & gasoline | BioEtOH | 10.2 ± 0.4 | * | 10.13 |
| | | HVO | 12.1 ± 0.5 | 10.94 ± 1.78 | 10.34 |

All of reported results were declared as successful, which can also be seen in Figure 34, where a summary of the results obtained is presented (see the first 5 points) and in Table 24 where the reported results are depicted. The relative difference between the reported and calculated values is the biggest in the sample with HVO and ethanol in gasoline (sample 4), where the result of the HVO quantity in gasoline had to be reported. The measurement was conducted after separation of the ethanol from the original sample, and thus the separation was not completed. The separation was made with the addition of water, as proposed by Yunoki and Saito [29]. All the other samples were prepared and measured in accordance with the procedure described in Chapter 4.1 (see page 38). Samples with different bio-components can be therefore be successfully analyzed with additional

preparation steps. The results obtained were satisfactory. Furthermore, compared to the other laboratories that performed the LSC techniques, we were one of the laboratories with the most consistent and accurate results [143].

### *8.2.2 GCL bio-components in fuels 2013*

Six samples of different compositions were measured for this international comparative test (see Table 25). Samples A1, A2, A3 and A4 consisted of diesel and HVO; sample B was a mixture of diesel, FAME and HVO, while in sample C gasoline, fossil ethanol, bio-ethanol and ETBE were used. The evaluation of the results was conducted in the same manner as in a previous comparative test. All the reported values presented in Figure 34 satisfied the acceptability level of two. The points from sample A1 to sample C represent this cooperative test.

**Table 25: GCL bio-component in fuels 2013 test.** BioHC stands for bio-based hydrocarbons, while BioEtOH stand for bio-based ethanol.

| Sample No. | Sample constitution | Measured quantity | Reported values | Calculated values | Real values |
|---|---|---|---|---|---|
| A1 | Diesel & HVO | BioHC | 9.86 ± 0.57 | 9.0 ± 1.0 | 10 |
| A2 | Diesel & HVO | BioHC | 93.52 ± 0.73 | 93.0 ± 2.0 | 90 |
| A3 | Diesel & HVO | BioHC | 10.16 ± 0.58 | 9.0 ± 1.0 | 10 |
| A4 | Diesel & HVO | BioHC | 93.02 ± 0.68 | 91.0 ± 2.0 | 90 |
| B | Diesel, FAME, HVO | BioHC | 16.68 ± 2.68 | 10.0 ± 6.0 | 9.3 FAME 6.7 HVO |
| C | Gasoline, EtOH, BioEtOH, ETBE | BioEtOH | 13.12 ± 1.10 | 8.0 ± 4.0 | 6 BioEtOH 10 ETBE |

All our reported values were higher than the true value. For samples A1, A2, A3 and A4 this can be explained by an over-estimation of the calculated activity. One of the reasons could be the different concentration of carbon atoms in the measured samples compared to the calibration ones. Samples B and C were made from unusual mixtures of samples, which could be the reason for such an error and overestimated activity. Namely, the samples were evaluated by the calibration curve for HVO or bio-ethanol, while they also contained unknown amounts of other bio-components

(FAME and ETBE) with different total activities. A new limitation of the method was shown with the participation in this comparative test when samples with various bio-components had to be measured. One of organizer's conclusions was that the sample mixtures were unrealistic (sample C) and should be abandoned in future [144]. Nevertheless, we were satisfied with the obtained results, which proved the ability to analyze even samples with mixtures of different types of bio-components with an acceptable trueness. But in the future the variety of laboratory reference samples should be widened, which would improve the calibrations and indicate problems. The organizers also pointed out the problem of differences in the sample calculations. They suggest a uniform calculation and an analytical procedure for future comparative tests [144].

### *8.2.3 GCL FAME in gasoil 2013*

Only three samples were obtained in this international cooperative test (see Table 26). We only obtained samples for measurements of near-background values since the test was designed for a near-detection-threshold evaluation of the standardized method EN 14078. The samples were prepared and measured according to the optimized method for a determination of the biodiesel in diesel. Samples were also measured on a high coincidence bias setup where the limit of detection is lower because the levels of biodiesel in the test samples were below our threshold. The values reported by the method EN 14078 are in v/v%, and thus our results were recalculated with the use of the average density of the biodiesel described in [146].

**Table 26: GCL FAME in the gasoil 2013 test**

| Sample No. | Sample constitution | Measured quantity | Reported values | Calculated values | Real values |
|---|---|---|---|---|---|
| F1 | Diesel & FAME | FAME | 0.53 ± 0.21 | 0.23 ± 0.04 | 0.2 |
| F2 | Diesel & FAME | FAME | 0.64 ± 0.19 | 0.51 ± 0.03 | 0.5 |
| F3 | Diesel & FAME | FAME | 1.26 ± 0.18 | 1.02 ± 0.04 | 1.0 |

The ζ-test was calculated for a comparison with true values and it is presented in Figure 34 (see points F1, F2 and F3). For all the measured samples good acceptability of the results was obtained. However, in the case of sample F1 it was

shown that the result was between the critical and detection limit calculated by Currie [122]. The quantity of biodiesel in this sample would be classified as below detection limit in routine measurements. The other obtained values were between DL and 1 $\%_v$. The misclassification of the bio-component content led to concern about the over-estimated detection limits; therefore, additional work and measurements need to be applied. The introduction of the ISO 11929 calculation of the detection limit [123] and the use of Bayesian statistics is shown as a good approach.

# 9 Measurements of real fuel samples

Slovenia is a transit country and as such has a specific fuel market: diesel represents 2/3 of the fuel sold and only 1/3 of consumed fuel is gasoline. Ethanol is not used as a fuel but only as an additive to gasoline. Therefore, it has been decided to focus the testing of the method on diesel samples.

## 9.1 Sampling

The sampling campaign was performed on regular gas stations across the country. Sample points were distributed through the whole country, as can be seen in Figure 35. One-third of samples were taken on highways and two-thirds on regional roads, which is in accordance with the ratios of sold fuels on different types of roads. Namely, the most significant distributor of fuels in Slovenia, which covers 85 % of the market, has sold 36 % of their diesel fuel on highways [108]. Some 35 % of the highway's gasoline stations of different providers were included in the sampling plan, while other gasoline stations on regional and local roads were sampled to a much smaller extent (9 %). A total of 75 samples at 75 different places were collected during the sampling campaign, which lasted from March to November 2011.

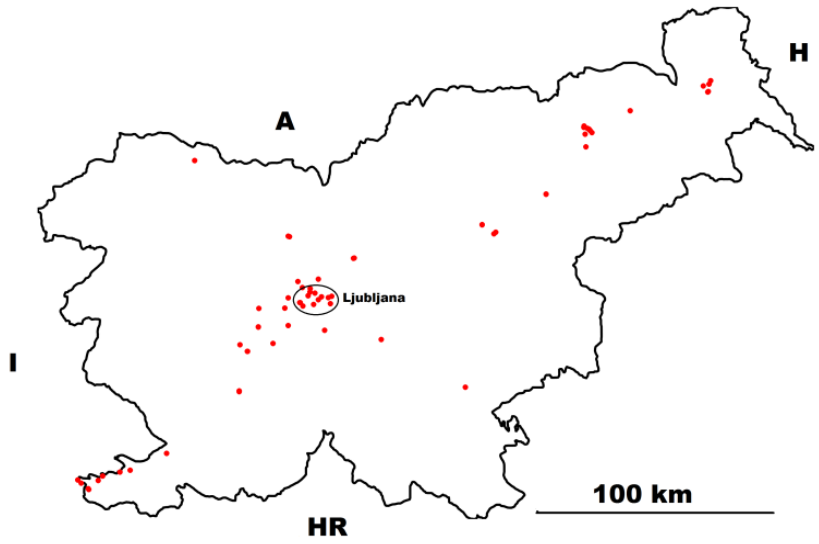


**Figure 35: Sampling points on map of Slovenia**

## *9.2 Experimental*

The LSC samples were prepared in accordance with the procedure described in 4.1 (see page 38). Small amounts of biodiesel were expected, and thus the measurements and evaluation were conducted in accordance with the high-bias protocol (see Chapter 7.3 on page 66). A counting window from 150 to 400 was used. Five counting cycles were performed, with each one lasting 100 min. The average count rate obtained in measurements of 20 different fossil fuels was taken as a background. Every background sample was measured for 1000 min in 5 cycles. The background count rate was 0.93 cpm with a standard deviation of 0.09. The SQP(E) value of the background samples varied between 800 and 850. Although the method's protocol uses the SQP(E) value for the determination of the counting efficiency, 15 samples were also subject to a standard addition method (see Chapter 4.2.2 on page 40).

## *9.3 Results and discussion*

The samples had the same color, but the SQP(E) value varied from 681 to 815, with a standard dispersion of 46. Such a variation of the SQP(E) values corresponds to the counting efficiency in the range from 55.1 % to 79.8 %, in accordance with the quench curve. These measurements pointed out that in measurements of real market samples the color of the sample is not likely the only reason for quenching. The main source of quenching is therefore the chemistry of the sample. Several additives for improving individual characteristics are added to market fuels. The range of the quench and counting efficiency was therefore larger than for the samples of the calibration curve (0 - 10 $\%_m$) and the background. This occurred because the samples measured for the calibration curve did not contain any additives. Samples with a higher range of quench were checked by the standard addition method. The SQP(E) of the samples before and after the standard addition were the same, so we assumed that the counting efficiency did not change. The differences between the counting efficiencies calculated via the standard addition, on the one hand, and the quench curve, on the other hand, were around 0.5 %. This is within the uncertainty of the standard solutions, as was already shown in the uncertainty budget (see Chapter 7.8.1 on page 90).

Measurable amounts of bio-component were found in 44 samples, what means 58.7 % of the collected samples (see Figure 36). The quantity of the bio-component's span in the samples was from the limit of detection up to $5.84 \pm 0.55$ $\%_m$. The average quantity of biodiesel in measurable samples was 3.65 $\%_m$ , with a spread of 1.56 $\%_m$. The samples with results below the detection limit were considered as having a zero value, and thus the average quantity in all the samples was lower, 2.14 $\%_m$ , with the dispersion of results equal to 2.17 $\%_m$.

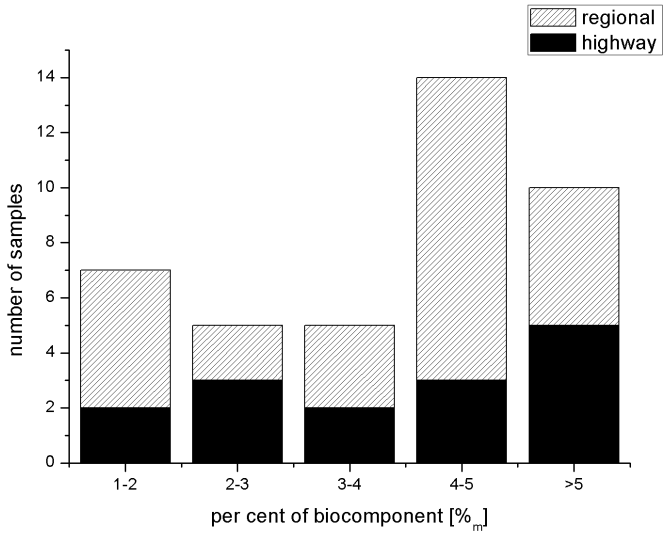


**Figure 36: Distribution of samples in accordance with the biodiesel quantity.**

The relative percentage distribution of biodiesel in gasoline stations located on regional roads and highways is shown in Figure 36. The bio-component was not detected in 41 % of the samples. A total of 32 % of the samples contained more than 4 $\%_m$, while samples from classes below 4 $\%_m$ represented a share of 27 %. Such behavior can be explained by the fact that an extensive pretreatment of the gasoline station's fuel tanks is needed in order to be able to accept a fuel with biodiesel. Distributors are therefore interested to introduce bio-components only at gasoline stations that have a higher sales frequency. This was also confirmed by a correlation between the location of the gasoline station and the vicinity of a major transit road or proximity to major towns, as can be seen in the first four rows of Table 27. The sampling locations in major towns or on highways contain comparable mass percentage of bio-component (rows 1, 3). The situation outside the towns differs significantly (rows 3, 4).

The second half of Table 27 (rows from 5 to 8) shows the comparisons with respect to the geographical position of the sampling point. Slovenia is divided into four regions: Ljubljana and its surroundings are the most densely populated part of Slovenia. A high amount of bio-components was therefore expected in this region. Our results show just the opposite. Detailed inspection of sampling points indicates that gasoline stations that cover a larger population area had a higher percentage of bio-component. However, the highest mass ratio of biodiesel was found on the Slovenian coast. The traffic there is relatively dense because of tourists and transit passengers in the vicinity of the Italian and Croatian borders. The average temperature along the Adriatic is higher than in other parts of Slovenia, which is favorable circumstance for the temperature-sensitive biodiesel. Eastern Slovenia demonstrates higher values of bio-components than the western part. The reasons might be the climate (high mountains on the west) and the easier availability of the bio-components in the agricultural eastern part of the country.

**Table 27: Averages and ranges of the results obtained in the survey.**

| Row No. | Location | All sampling points | | | | Sampling points with results above DL | | | | highways |
|---|---|---|---|---|---|---|---|---|---|---|
| | | No. of stations | Average [%m] | Dispersion [%m] | Max. [%m] | No. of stations | Averaged [%m] | Dispersion [%m] | Min. [%m] | No. of stations |
| 1 | city | 44 | 2.29 | 2.18 | 5.30 | 27 | 3.73 | 1.52 | 0.71 | 2 |
| 2 | countryside | 31 | 1.94 | 2.16 | 5.84 | 17 | 3.53 | 1.67 | 0.70 | 21 |
| 3 | Highways out of the cities | 21 | 2.25 | 2.39 | 5.84 | 12 | 3.93 | 1.78 | 0.70 | 21 |
| 4 | Regional roads in countryside | 10 | 1.29 | 1.48 | 3.44 | 5 | 2.57 | 0.90 | 1.63 | 0 |
| 5 | Ljubljana and surroundings | 19 | 1.58 | 1.71 | 4.65 | 10 | 2.99 | 1.08 | 0.71 | 1 |
| 6 | Eastern Slovenia | 30 | 2.23 | 2.42 | 5.84 | 17 | 3.93 | 1.86 | 0.70 | 11 |
| 7 | Western Slovenia | 16 | 1.59 | 1.93 | 5.22 | 8 | 3.19 | 1.49 | 1.63 | 8 |
| 8 | Slovenian coast | 10 | 3.85 | 1.80 | 5.07 | 9 | 4.28 | 1.26 | 1.12 | 3 |

## *9.4 Comparison with EUROSTAT reports*

A slightly lower quantity of biodiesel in diesel, compared with the measured results of this work has been found in official reports [147], where 1.85 $\%_m$ is declared as the mass percentage of bio-component in the fuel (see Table 28). Nevertheless, the agreement between the reported official value, which is obtained from the total amount of consumed bio and fossil components in the country and the result of our single sampling campaign, is surprisingly good. The discrepancy is 0.3 $\%_m$ or 15.6 %. In other words: in accordance with ζ-test, both numbers do not differ significantly if we assume nearly 18 % of the relative uncertainty of the average 2.14 $\%_m$ from this study. This is a reasonable estimation if we take into account the measurement uncertainties, the properties of the distribution of the obtained results, the representativeness and the scale of the sampling net. The difference can be explained by the fact that the campaign was performed mainly in the spring and fall when the contents of bio-components are typically higher than in cold part of the year.

**Table 28: Official report and EU directive comparison**

| | Quantity of biodiesel [$\%_m$] | Quantity of biodiesel [$\%_E$] |
|---|---|---|
| **Result of this study** | 2.14 | 1.85 |
| **Official report** | 1.85 | 1.6 |
| **EU directive** | 6.35 | 5.5 |

The results of this study were also compared with the recommendations of the European directive 2009/28/EC [5]. The first step was the recalculation of mass percentages ($\%_m$) into energy per cents ($\%_E$) because the recommendations in European directive 2009/28/EC are set out in this unit. The ratio between the average energies released from biodiesel and diesel from the EU directive 2009/28/EC was taken into account for this recalculation [5]. The energy percentage ($\%_E$) of our results and the officially reported data are compared in Table 28. Comparable official data and the values from our study are below the prescribed values in the EU directive 2009/28/EC.

# *10 Conclusions*

Environmental changes, mainly caused by the automotive industry, have been observed in recent years. Biofuels are added to fuel in attempts to reduce transport's carbon footprint. Several biofuels can be found on the fuel market. Namely, bio-ethanol, ETBE and FAME/FAEE, which are regularly added to gasoline or diesel fuel in the whole European Union. In recent years the sustainability of their production was questioned. In established production they are produced from food grade oils, and thus fuel competes with food production. New types of biofuels have been developed in recent years. Some of them just changed the type of feedstock to non-edible oil, while some others changed the whole production process (HVO). Such fuels are the so-called new generation of fuels produced from algae, wood wastes, etc. which are still in the research phase. The variety of biofuels also means differences in fuel characteristics. Many analytical methods were developed to cover every fuel characteristic, including the quantity of biofuels. The applicability of one simple method for a determination of the various biofuels' quantity was tested in this thesis. A variety of biofuels from different feedstock oils had to be analyzed to imitate the developing fuel market. Some biodiesel samples were also produced because of the limited information regarding the effect of the type of feedstock and production differences on the fuels' characteristics.

The production of biodiesel was conducted using eight oils of first- and second-generation feedstock materials. Oils of camelina (2x), corn, jatropha, rapeseed, soya and sunflower (2x) were selected from the most used feedstock oils. The first tests of the production conditions were conducted on cheap waste cooking oil, while the scale up production was made on all oils. Sulfuric acid and ethanol were used for both stages of the production tests. Optimal conditions determined with waste cooking oil experiments were magnetic agitation, 5 % w/w $H_2SO_4$, 80 °C and 6:1 EtOH:oil ratio. All the oils obtained between 90 and 100 % of FAEE yield within 7 h of the reaction. Some EN 14214 parameters were analyzed after cleaning the biodiesel products with active charcoal. All the produced biodiesels had some parameters that suited the demands of the EN 14214 standard and some which did not. Three parameters which could have an effect on the LSC measurement (water and sulfur content, acidity value) were above the prescriptions of the EN standard.

The water content could affect the mixing of the sample to the scintillation cocktail, while the sulfur content could add to the radiocarbon count rate, due to $^{40}S$. However, no difficulties in the sample preparation or an additional $^{40}S$ peak were found during the biodiesel analysis. The hypothesis of using the acidity value as an indicator of the chemical quench was disregarded because no correlations were observed. Furthermore, the highest acidity value was observed in sunflower biodiesels, which had the lowest observed quench. The densities of the biodiesels were comparable, while the oxidative stabilities showed differences in the life span of the produced biofuels. Two sets of biodiesel composition measurements were conducted immediately after their production and a year later. Their comparative analyses showed a decrease in the ester content with ageing. Although after some period of time the biofuels started to decompose, a direct LSC method could still be applied. On the other hand, other methods for biodiesel analysis are based on distinct characteristics, such as the content of esters, which changed over time. Furthermore, it was found that the decomposition of biodiesel makes LSC analysis even easier with increasing counting efficiencies and a decreasing observed chemical quench.

Methods like FTNIR, GC, HPLC, NMR and recently TL spectroscopy were used for a determination of the new biodiesel quantity with good precision and accuracy. However, all those methods rely on methyl ester measurements, while for bio-ethanol, ETBE or new biofuels (HVO) such measurements are not possible. Although the quantity of bio-ethanol and ETBE could be determined with a GC analysis, their bio-origin is assumed. The bio-origin of these fuels could only be determined by a measurement of the radiocarbon content. Two techniques, AMS and LSC, are well known in the precise measurement of radiocarbon content since they are already used for an age determination of different samples. AMS is more precise and accurate than the LSC technique when trace amounts of radiocarbon are determined. In measurements of biofuel such a difference is not seen since the environmentally present levels of $^{14}C$ are determined. In addition the LSC technique is cheaper, and even though it requires larger sample quantities this is not a concern with bio-components measurements.

Three LSC methods are in use for the $^{14}C$ measurements, namely $CO_2$ capture, benzene production and the direct method. The direct LSC method was adapted as an analytical technique in this thesis. Compared with other LSC or AMS methods its

main advantage is the lack of sample preparation, a source of several human errors. Easy sample preparation also enables many processed samples in a short period of time. Its drawback tackled in this thesis was the disturbance caused by persistent quench, originating with the chemical mixtures and color of the sample. Direct LSC method applications for a determination of the bio-ethanol, ETBE and biodiesel quantity were already reported in limited extent in the literature [8–10, 12, 16, 17, 26, 28, 29, 63]. Colorless liquids, such as bio-ethanol and ETBE, should not present any difficulties regarding the quenching direct LSC method application. Problems with a heavy quench were reported in an analysis of the biodiesel, which limits the utilization of such a method [16, 26, 27]. Similar problems were already reported in measurements of many biological samples, like urine or blood cells [141, 148]. At first glance the biological samples and biofuels do not have anything in common, but in LSC measurement problems like persistent color, which causes a shift of spectra, and thus a signal and count rate decrease, were the same underline. Biodiesel analysis is prone to different types of quench due to the chemistry of the sample. The approaches used for biological samples were tested on biodiesel measurements and further studies of the protocol changes were done.

Analyses of bio-ethanol and renewable diesel (HVO) already reported in the literature were repeated in order to test the uniformity in the preparation of the samples. Namely, all the LSC samples were prepared as a mixture of 10 ml of scintillation cocktail and 10 ml of sample. Both bio-ethanol and HVO were analyzed successfully, but the counting-efficiency changes had to be considered. A quench set with a chemical quencher was purchased and measured for that purpose and the chemical quench curve was fitted. The measurement range in the bio-ethanol analysis is comparable to the literature. On the other hand, the HVO analysis could be conducted over a broader range, from the detection limit to 100 $\%_m$, while in the literature a measurement range from 0 to 20 % was reported. Linear calibration curves with correlation coefficients larger than 0.99 were obtained in the analysis of both biofuels. The limit of detection calculated in accordance to Currie [122] was 76 % lower in the bio-ethanol analysis compared to the HVO analysis. In the bio-ethanol analysis the ISO 11929 [123] detection limit was also lower, by 55 % compared to the HVO. The precision was better (for 0.37 %) in the HVO analysis,

but the sensitivity of the calibration curves was higher (17.504) in the bio-ethanol analysis, compared to the 9.156 obtained in the HVO.

Initial measurements of the biodiesel with the same protocol as for the bio-ethanol and HVO were not successful. The spectra and the SQP(E) value showed severe quenching and, as a consequence, only a calibration in the range up to 10 $\%_m$ was made. Based on the sample appearance a color quench was determined as a major culprit of the observed quench. The commonly used approach of reducing the color quench is bleaching and dilution. The latter was tested with biodiesel samples where the sample:scintillator ratio was changed. The procedure was not adopted for further measurements because the highest counting efficiency was achieved at a sample:scintillator ratio of 1:19. This would increase the detection limit, as was also observed by Idoeta *et al.* [27]. The authors reported the application of a 6:14 sample:scintillator ratio, but noted an increase in the detection limits from 1 Bq/l to close to 10 Bq/l for strongly colored biodiesels [27]. The second, often used approach to bleaching introduces more chemical quench. Colleagues in PerkinElmer's lab [149] experimented with $AlO_2$ and silica cleaning with limited success. Although the color was eliminated at the beginning, the color of the sample was not stable. The forced oxidation of different biodiesels with a UV lamp and oxide was tested in our laboratory. This approach was diminished because consistent results were not achieved. The measurement angle for solving this problem was chosen in this thesis. First, a simple coincidence circuit setup changes were applied. The change from a high to a low coincidence bias setup was made. The LSC samples became measurable with simple coincidence circuit changes, despite the observation of the heavy color quench in them. The approach with a sample-based quench curve was chosen for the determination of the counting efficiency. Biodiesels were used as samples for the preparation of a new quench curve because of the observed variety of quenching. A chemical/color quench curve measured in a low coincidence bias was obtained since in biodiesel analyses both color and chemical quench are present. This is not a common approach but a chemical quench alone did not describe all of the observed quenching in a biodiesel analysis. The changed measurement protocol allowed an analysis of amounts up to 100 % of biodiesel, which is more than reported in the literature. So far the most successful analyses were conducted by Norton *et al.* [16]. But their calibration allows measurements of up to 20 % of

biodiesel. Although the linearity of the calibration curve was obtained, the detection limit was too high (DL 2.73 $\%_m$) for measurements of real market fuels.

Several approaches were taken for the reduction of the limits of detection, namely, a change in the counting chamber temperature, PAC, PSA and changed counting window. However, only one of them improved the method significantly. This was the application of a quench balanced counting window, where the count rate is taken from the window determined by the sample quench. The procedure is based on the relation of the LSC sample quench and a change of the observed decay energy. A determination of the $^{14}C$ peak position and the width, therefore the corresponding counting window is determined for each measurement individually according to observed quench level (SQP(E) value). Although such an approach needs additional computational work after the measurement thus can be programed and obtained automatically. Researchers who use a pre-programed counting window cannot apply such an approach or they firstly have to perform measurements of the quench value and then re-program the counting windows individually. The sensitivity of the calculated radiocarbon activities improved by 10 %, while the precision improved by 50 % when the data was evaluated with the quench balanced window. Compared to the low bias protocol, the limit of detection reduced by 0.77 $\%_m$ using the balanced window. The detection limit calculated in accordance with ISO 11929 lowered by 0.59 $\%_m$ compared to the low bias protocol. In addition to the detection limits, also the correlation coefficient improved to 0.998 when the quench balanced window procedure was used, which is comparable to the high bias protocol.

Two different procedures were applied in the analysis of biofuels. A pre-designed protocol with a high coincidence bias setup was used for the measurements of bio-ethanol and HVO. Biodiesel was measured with a pre-designed protocol and a newly designed low coincidence bias setup coupled with quench balanced counting window evaluation. Although the best validation parameters were obtained with the pre-designed protocol its measurement range is only up to 10 $\%_m$. Based on current biodiesel applications this calibration is sufficient for measurements of real fuel samples. This was also proven with a survey of the Slovenian diesel market, where 75 different samples were analyzed. The results were in agreement with the official report of biofuel usage. The survey also helped in testing the method for sensitivity

to fuel additives, which are present in real market fuel but were not present in the calibration samples. The observed SQP(E) values in the survey samples were of larger variety (from 681 to 815) than in the calibration LSC samples (from 732 to 817). Nevertheless, difficulties in the analysis with a pre-designed protocol were not detected. The protocol was also tested in international cooperative tests where near detection limit quantities of biodiesel were analyzed. The tests proved the ability to measure such samples, but indicated over-estimated limits of detection. Introducing the ISO 11929 standard, which uses Bayesian statistics, was shown as a good approach to further decrease the detection limits. Applied changes in the biodiesel counting and evaluation protocol extended the measurement range to 100 $\%_m$ but increased the detection limit to 1.67 $\%_m$ when calculated based on the ISO 11929 standard. Nevertheless, this protocol could be primarily used for an analysis of a pure or high quantity of biodiesel. According to the EU directive, the predictions of biodiesel use in fuel are up to 10 %, but the standard EN 590 limits the use of biodiesel to 5 volumetric %. Regardless of which direction the fuel market will be driven, accurate analyses are possible with both protocols. Furthermore, the improved method is applicable for analysis of the fuel for heavy-duty vehicles where a larger percentage of biodiesel is added.

The same approach with a low coincidence bias setup and a quench balanced counting window evaluation could also be applied in measurements of bio-ethanol and HVO. But such an approach was not taken, since the observed quench did not affect the bio-component's quantity determination with a pre-designed protocol. Predictions for the HVO analyses are similar to those for biodiesel. According to the European Customs Laboratories predictions the application of HVO will be in addition to biodiesel in fuel in order to the achieve demands of the EU directive [144]. On other hand, ethanol analysis is mainly in the determination of the bio-origin, and thus the analysis of 100 % bio-ethanol. Concluding from results of international comparative tests the applied method is accurate enough to enable such an analysis. The analyses of near 100 and below 10 % of bio-ethanol were proven to be successful when measured in the first comparative tests in 2010/2011. HVO was successfully measured in levels around 10, 20 and 90 % in different matrixes in two cooperation tests (2010/2011 and 2013). The method proved to be applicable for analyses of impurities in gasoline since accurate analyses of the HVO in gasoline

were achieved. HVO is shown as an impurity since its characteristics and chemical formula places it as diesel fuel.

In combined analysis of HVO and biodiesel we should not expect greater quench difficulties since HVO and biodiesel quench levels work conversely with each other. The greatest difficulties would be in an analysis of biofuel quantity, if such measurements would be needed. In that case calculations would have to change, since now the specific activity of the sample (in dpm/g of sample) is used in the determination of the bio-component percentage. As can be observed in the total activity of the calibration samples the specific activities are different because the carbon densities differ. The quantity of carbon atoms cannot be measured with the direct LSC method, and thus additional measurements of the sample composition would be needed. These measurements would allow a recalculation of the sample activity per gram of carbon, similar to those made in a comparison of the $CO_2$ absorption method. The results of this comparison show that the procedure has its limitations, mainly in the dependency of the external measurements. Biofuels are mainly produced from limited quantities of feedstock; therefore, the database of the carbon contents could be established. The database would improve the uncertainties in the recalculation. A simple calibration curve relating the sample activities and the bio-component would have to be repeated. Calculations based on the carbon content could also improve the comparison between different laboratories using the LSC technique. A similar idea was also expressed by the organizers of the international comparative test, who expressed their desire for a uniform calculation procedure to obtain an easier data evaluation.

# 11 References


1. KLASS, Donald L. *Biomass for Renewable Energy, Fuels and Chemicals*. Academic Press, 1998.

2. LANGEVELD, Hans, SANDERS, Johan and MEEUSEN, Marieke. *The Biobased Economy: Biofuels, Materials and Chemicals in the Post-oil Era*. Firts edit. Earthscan, 2010.

3. DEMIRBAS, M.F. and BALAT, Mustafa. Recent advances on the production and utilization trends of bio-fuels: A global perspective. *Energy Conversion and Management*. September 2006. Vol. 47, no. 15-16, p. 2371–2381.

4. SOETAERT, Wim and VANDAMME, Erick J. *Biofuels*. John Wiley & Sons Ltd., 2009.

5. *DIRECTIVE 2009/28/EC OF THE EUROPEAN PARLIAMENT AND OF THE COUNCIL of 23 April 2009 on the promotion of the use of energy from renewable sources and amending and subsequently repealing Directives 2001/77/EC and 2003/30/EC*. 2009. Official Gazette of European Union.

6. MORIARTY, Partick and HONNERY, Damon. Low-mobility: The future of transport. *Futures*. 2008. P. 865–872.

7. RAJAGOPAL, D., SEXTON, S.E., ROLAND-HOLST, D. and ZILBERMAN, D. Challenge of Biofuel: filling the tank without emptying the stomach? *Environmental Research Letters*. 2007. P. 9.

8. DIJS, Ivo J, VAN DER WINDT, Eric, KAIHOLA, Lauri and VAN DER BORG, Klaas. Quantitative determination by component in fuels 14 c analysis of the biological component in fuels. *Radiocarbon*. 2006. Vol. 48, no. 3, p. 315–323.

9. EDLER, Ronald. The use of liquid scintillation counting technology for the determination of biogenic materials. *LSC 2008, Advances in Liquid Scintillation Spectrometry*. 2009. P. 261–267.

10. EDLER, Ronald and KAIHOLA, Lauri. Differentiation between fossil and biofuels by liquid scintillation beta spectrometry – direct method. *Nukleonika*. 2010. Vol. 55, no. September 2009, p. 127–131.

11. KRIŠTOF, Romana and KOŽAR LOGAR, Jasmina. Direct LSC method for measurements of biofuels in fuel. *Talanta*. 15 July 2013. Vol. 111, p. 183–188.

12. NORTON, Glenn a. and WOODRUFF, Mary X. Simplified Radiocarbon Analysis Procedure for Measuring the Renewable Diesel Concentration in

Diesel Fuel Blends. *Journal of the American Oil Chemists' Society*. 22 November 2011. Vol. 89, no. 5, p. 797–803.

13. ASTM. ASTM D6866 - 12 Standard Test Methods for Determining the Biobased Content of Solid, Liquid, and Gaseous Samples Using Radiocarbon Analysis. 2012.

14. DONAHUE, Douglas J. Radiocarbon analysis by accelerator mass spectrometry. *International Journal of Mass Spectrometry and Ion Processes*. 25 May 1995. Vol. 143, p. 235–245.

15. KNOTHE, Gerhard. Determining the blend level of mixtures of biodiesel with conventional diesel fuel by fiber-optic near-infrared spectroscopy and 1H nuclear magnetic resonance spectroscopy. *Journal of the American Oil Chemists' Society*. October 2001. Vol. 78, no. 10, p. 1025–1028.

16. NORTON, Glenn a., CLINE, Anna M. and THOMPSON, Greg C. Use of radiocarbon analyses for determining levels of biodiesel in fuel blends -- Comparison with ASTM Method D7371 for FAME. *Fuel*. June 2012. Vol. 96, p. 284–290.

17. NORTON, Glenn a. and DEVLIN, Steven L. Determining the modern carbon content of biobased products using radiocarbon analysis. *Bioresource Technology*. November 2006. Vol. 97, no. 16, p. 2084–2090.

18. MONTEIRO, M, AMBROZIN, A, LIAO, L and FERREIRA, A. Critical review on analytical methods for biodiesel characterization. *Talanta*. 15 December 2008. Vol. 77, no. 2, p. 593–605.

19. OINONEN, M, HAKANPÄÄ-LAITINEN, H, HÄMÄLÄINEN, K, KASKELA, A and JUNGNER, H. Biofuel proportions in fuels by AMS radiocarbon method. *Nuclear Instruments and Methods in Physics Research Section B: Beam Interactions with Materials and Atoms*. April 2010. Vol. 268, no. 7–8, p. 1117–1119.

20. OLIVEIRA, Jefferson S, MONTALVÃO, Rafael, DAHER, Leila, SUAREZ, Paulo a Z and RUBIM, Joel C. Determination of methyl ester contents in biodiesel blends by FTIR-ATR and FTNIR spectroscopies. *Talanta*. 15 July 2006. Vol. 69, no. 5, p. 1278–84.

21. PESONEN, Antto. *Characterization of chemical composition of fuel biofractions by different analytical techniques*. University of Helsinki, 2012.

22. VENTURA, M, SIMIONATTO, E, ANDRADE, L H C and LIMA, S M. Thermal lens spectroscopy for the differentiation of biodiesel-diesel blends. *Review of Scientific Instruments*. 2012. Vol. 83.

23. VENTURA, M, SIMIONATTO, E, ANDRADE, L H C, SIMIONATTO, E L, RIVA, D and LIMA, S M. The use of thermal lens spectroscopy to assess oil – biodiesel blends. *Fuel*. 2013. Vol. 103, p. 506–511.

24. VERAS, Germano, DE ARAUJO GOMES, Adriano, DA SILVA, Adenilton Camilo, BIZERRA DE BRITO, Anna Luiza, ALVES DE ALMEIDA, Pollyne Borborema and DE MEDEIROS, Everaldo Paulo. Classification of biodiesel using NIR spectrometry and multivariate techniques. *Talanta*. 2010. Vol. 83, p. 565–568.

25. YANG, Zeyu, HOLLEBONE, Bruce P, WANG, Zhendi, YANG, Chun, BROWN, Carl and LANDRIAULT, Mike. Forensic identification of spilled biodiesel and its blends with petroleum oil based on fingerprinting information. *J. Sep. Sci.* 2013. Vol. 36, p. 1788–1796.

26. TAKAHASHI, Yui, SAKURAI, Hirohisa, INUI, Emiko, NAMAI, Saori and SATO, Taiichi. Radiocarbon Measurement of Biodiesel Fuel Using the Liquid Scintillation Counter Quantulus. In : CASSETTE, Philippe (ed.), *LSC 2010, Advances in Liquid Scintillation Spectrometry*. Paris, France, 2010. p. 41–46.

27. IDOETA, R, PÉREZ, E, HERRANZ, M and LEGARDA, F. Characteristic parameters in the measurement of (14)C of biobased diesel fuels by liquid scintillation. *Applied radiation and isotopes : including data, instrumentation and methods for use in agriculture, industry and medicine*. 6 February 2014. DOI 10.1016/j.apradiso.2014.01.019.

28. CULP, Randy, CHERKINSKY, Alex and RAVI PRASAD, G V. Comparison of radiocarbon techniques for the assessment of biobase content in fuels. *Applied radiation and isotopes : including data, instrumentation and methods for use in agriculture, industry and medicine*. 30 January 2014. DOI 10.1016/j.apradiso.2014.01.007.

29. YUNOKI, Shunji and SAITO, Masaaki. A simple method to determine bioethanol content in gasoline using two-step extraction and liquid scintillation counting. *Bioresource Technology*. 2009. Vol. 100, p. 6125–6128.

30. POLACH, Henry A. Evaluation and status of liquid scintillation counting for radiocarbon dating. *Radiocarbon*. 1987. Vol. 29, no. 1, p. 1–11.

31. L'ANNUNZIATA, Michael F. *Handbook of Radioactivity Analysis*. Second Edi. Elsevier, 2003.

32. NAYAR, S., GOH, B. P L and CHOU, L. M. Interference of chlorophyll a in liquid scintillation counting of phytoplankton productivity samples by the 14C technique. *Estuarine, Coastal and Shelf Science*. 2003. Vol. 56, p. 957–960.

33. MOORE, P A. Preparation of whole blood for liquid scintillation counting. *Clinical chemistry*. 1981. Vol. 27, p. 609–611.

34. PENG, C T. Quenching of fluorescence in liquid scintillation counting of labeled organic compounds. *Analytical Chemistry*. 1960. Vol. 32, no. 10, p. 1292–1296.

35. FANG, ZHXNIEKL and LI, T A N TianWei DENG. Bleaching of deep color biodiesel made from waste cooking oils by oxidation. *Journal of Beijing University of Chemical Technology (Natural Science Edition)*. 2009. P. S1.

36. MIKKONEN, Seppo, HARTIKKA, Tuukka, KURONEN, Markku and SAIKKONEN, Pirjo. *HVO, hydrotreated vegetable oil – a premium renewable biofuel for diesel engines*. 2012.

37. *EN 590:2004 Automotive fuels- Diesel- Requirements and test metods*. 2004.

38. *EN 228:2012 Automotive fuels - Unleaded petrol - Requirements and test methods*. 2012.

39. *EN 14214:2008 Automotive fuels - Fatty acid methyl esters (FAME) for diesel engines - Requirements and test methods*. 2008.

40. AATOLA, Hannu, LARMI, Martti, SARJOVAARA, Teemu and MIKKONEN, Seppo. Hydrotreated Vegetable Oil ( HVO ) as a Renewable Diesel Fuel : Trade-off between NO x , Particulate Emission , and Fuel Consumption of a Heavy Duty Engine. *SAE International*. 2008.

41. STÖCKER, Michael. Biofuels and Biomass-To-Liquid Fuels in the Biorefinery: Catalytic Conversion of Lignocellulosic Biomass using Porous Materials. *Angewandte Chemie International Edition*. 17 November 2008. Vol. 47, no. 48, p. 9200–9211.

42. AMIN, Sarmidi. Review on biofuel oil and gas production processes from microalgae. *Energy Conversion and Management*. 2009. Vol. 50, p. 1834–1840.

43. LAM, Man Kee, LEE, Keat Teong and MOHAMED, Abdul Rahman. Homogeneous, heterogeneous and enzymatic catalysis for transesterification of high free fatty acid oil (waste cooking oil) to biodiesel: A review. *Biotechnology Advances*. 2010. Vol. 28, no. 4, p. 500–518.

44. VYAS, Amish P, VERMA, Jaswant L and SUBRAHMANYAM, N. A review on FAME production processes. *Fuel*. 2010. Vol. 89, no. 1, p. 1–9.

45. WATANABE, Yomi, SHIMADA, Yuji, SUGIHARA, Akio and TOMINAGA, Yoshio. Enzymatic conversion of waste edible oil to biodiesel fuel in a fixed-bed bioreactor. *Journal of the American Oil Chemists' Society*. July 2001. Vol. 78, no. 7, p. 703–707.

46. MIAO, Xiaoling, LI, Rongxiu and YAO, Hongyan. Effective acid-catalyzed transesterification for biodiesel production. *Energy Conversion and Management*. October 2009. Vol. 50, no. 10, p. 2680–2684.

47. MA, Fangrui and HANNA, Milford A. Biodiesel production : a review. *Bioresource technology*. 1999. Vol. 70, p. 1–15.

48. KUMARI, Annapurna, MAHAPATRA, Paramita, GARLAPATI, Vijay Kumar and BANERJEE, Rintu. Biotechnology for Biofuels Enzymatic transesterification of Jatropha oil. *Biotechnology for Biofuels*. 2009. Vol. 2, p. 1–7.

49. HERNÁNDEZ-MARTÍN, Estela and OTERO, Cristina. Different enzyme requirements for the synthesis of biodiesel: Novozym 435 and Lipozyme TL IM. *Bioresource technology*. January 2008. Vol. 99, no. 2, p. 277–86.

50. FJERBAEK, Lene, CHRISTENSEN, Knud V and NORDDAHL, Birgir. A review of the current state of biodiesel production using enzymatic transesterification. *Biotechnology and Bioengineering*. 2009. Vol. 102, no. 5, p. 1298–1315.

51. ZHANG, Y, DUBÉ, M A, MCLEAN, D D and KATES, M. Biodiesel production from waste cooking oil: 1. Process design and technological assessment. *Bioresource Technology*. August 2003. Vol. 89, no. 1, p. 1–16.

52. EFOA. *Technical Product Bulletin: ETBE*. 2006.

53. MIELENZ, Jonathan R. Ethanol production from biomass: technology and commercialization status. *Current Opinion in Microbiology*. 1 June 2001. Vol. 4, no. 3, p. 324–329.

54. DAVILA-GOMEZ, F. J., CHUCK-HERNANDEZ, C., PEREZ-CARRILLO, E., ROONEY, W. L. and SERNA-SALDIVAR, S. O. Evaluation of bioethanol production from five different varieties of sweet and forage sorghums (Sorghum bicolor (L) Moench). *Industrial Crops and Products*. 2011. Vol. 33, p. 611–616.

55. KUMAR, Sachin, SINGH, Surendra P, MISHRA, Indra M and ADHIKARI, Dilip K. Recent Advances in Production of Bioethanol from Lignocellulosic Biomass. *Chem. Eng. Technol.* 2009. Vol. 32, no. 4, p. 517–526.

56. SMAGALA, Thomas G, CHRISTENSEN, Earl, CHRISTISON, Krege M, MOHLER, Rachel E, GJERSING, Erica and MCCORMICK, Robert L. Hydrocarbon Renewable and Synthetic Diesel Fuel Blendstocks: Composition and Properties. *Energy & Fuels*. 12 November 2012. Vol. 27, no. 1, p. 237–246.

57. ALVES, Julio Cesar Laurentino and POPPI, Ronei Jesus. Simultaneous determination of hydrocarbon renewable diesel, biodiesel and petroleum diesel contents in diesel fuel blends using near infrared (NIR) spectroscopy and chemometrics. *The Analyst*. 7 November 2013. Vol. 138, no. 21, p. 6477–87.

58. NIGAM, Poonam Singh and SINGH, Anoop. *Production of liquid biofuels from renewable resources*. 2011. ISBN 0360-1285.

59. DAMARTZIS, T. and ZABANIOTOU, A. *Thermochemical conversion of biomass to second generation biofuels through integrated process design-A review*. 2011. ISBN 1364-0321.

60. *CSN EN 14078:2009 Liquid petroleum products - Determination of fatty acid methyl ester (FAME) content in middle distillates - Infrared spectrometry method*. 2009.

61. *CSN EN 1601:1997 Liquid petroleum products - Unleaded petrol - Determination of organic oxygenate compounds and total organically bound oxygen content by gas chromatography (O-FID)*. 1997.

62. *CSN EN 13132:2000 Liquid petroleum products - Unleaded petrol - Determination of organic oxygenate compounds and total organically bound oxygen content by gas chromatography using column switching*. 2000.

63. NOAKES, J. E., CHERKINSKY, A. and CULP, R. Comparative Radiocarbon Analysis for Artificial Mixes of Petroleum and Biobased Products. In : CASSETTE, Philippe (ed.), *LSC 2010, Advances in Liquid Scintillation Spectrometry*. Paris, France, 2010. p. 15–21.

64. CULP, R., NOAKES, J. E., SMITH, D. R., GREENWAY, L., SMITH, F. S. and MARKOWICZ, B. K. Biobase Product Determination by ASTM Method 6866-08 Using Liquid Scintillation Counting and Benzene Synthesis: Progress and Performance in an Expanding Market. In : CASSETTE, Philippe (ed.), *LSC 2010, Advances in Liquid Scintillation Spectrometry*. Paris, France, 2010. p. 23–34.

65. FUNABASHI, Masahiro, NIOMIYA, Fumi, KUNIOKA, Masao and OHARA, Keiichi. Biomass Carbon Ratio of Biomass Chemicals Measured by Accelerator Mass Spectrometry. *Bulletin of the Chemical Socciety of Japan*. 2009. Vol. 82, no. 12, p. 1538–1547.

66. REDDY, Christopher M., DEMELLO, Jared A., CARMICHAEL, Catherine A., PEACOCK, Emily E., XU, Li and AREY, J. Samuel. Determination of Biodiesel Blending Percentages Using Natural Abundance Radiocarbon Analysis: Testing the Accuracy of Retail Biodiesel Blends. *Environmental Science & Technology*. April 2008. Vol. 42, no. 7, p. 2476–2482.

67. STUVIER, Minze and POLACH, Henry A. Reporting of 14C Data. *Radiocarbon*. 1977. Vol. 19, p. 355–363.

68. VARLAM, Carmen, STEFANESCU, Ioan, VARLAM, Mihai, BUCUR, Cristina, POPESCU, Irina and FAURESCU, Ionut. Optimization of 14 C concentration measurement in aqueous samples using the direct absorption method and LSC. In : CHALUPNIK, Stanislaw, SCHONHOFER, Franz and NOAKES, John (eds.), *LSC 2005, Advances in Liquid Scintillation Spectrometry*. University of Arizona, 2006. p. 423–428.

69. SALONEN, Laina, KAIHOLA, Lauri, CARTER, Brian, COOK, Gordon T. and PASSO, Charles J. Environmental Liquid Scintillation Analysis. In : *Handbook of Radioactivity Analysis*. 2013. p. 625–693.

70. WOO, H. J., CHUN, S. K., CHO, S. Y., KIM, Y. S., KANG, D. W. and KIM, E. H. *Optimization of liquid scintillation counting techniques for the determination of carbon-14 in environmental samples*. 1999. ISBN 0236-5731.

71. MENDONÇA, Maria Lúcia T G, GODOY, José M., DA CRUZ, Rosana P. and PEREZ, Rhoneds A R. Radiocarbon dating of archaeological samples (sambaqui) using CO2 absorption and liquid scintillation spectrometry of low background radiation. *Journal of Environmental Radioactivity*. 2006. Vol. 88, p. 205–214.

72. KRAJCAR BRONIĆ, I, HORVATINCIĆ, N, BARESIĆ, J and OBELIĆ, B. Measurement of 14C activity by liquid scintillation counting. *Applied radiation and isotopes : including data, instrumentation and methods for use in agriculture, industry and medicine*. 2009. Vol. 67, p. 800–804.

73. BETAANALYTIC. Biofuels. [online]. [Accessed 11 March 2011]. Available from: http://www.betalabservices.com/biofuels.html

74. KRIŠTOF, Romana and KOŽAR LOGAR, Jasmina. Quenching parameter in the measurement of biodiesel by liquid scintillation counting. In : CASSETTE, Philippe (ed.), *LSC 2010, Advances in Liquid Scintillation Spectrometry*. Paris, France, 2010. p. 35–39.

75. ASTM. *ASTM D7371-12 Standard Test Method for Determination of Biodiesel (Fatty Acid Methyl Esters) Content in Diesel Fuel Oil Using Mid Infrared Spectroscopy (FTIR-ATR-PLS Method)*. 2012.

76. *CSN EN 14103:2011 Fat and oil derivatives - Fatty Acid Methyl Esters (FAME) - Determination of ester and linolenic acid methyl ester contents*. 2011.

77. KAHN, Bernd (Ed.). *Radioanalytical Chemistry*. Springer Netherlands, 2007.

78. MAKINEN, Pekka O. *Handbook of Liquid Scintillation Counting*. Turku Institute of Technology, 1995.

79. HORROCKS, Donald L. *Applications of liquid scintillation counting*. Academic Press, 1974.

80. MARTIN, James E. *Physics for Radiation Protection: A Handbook*. Second Edi. WILEY-VCH, 2006.

81. KESSLER, Michael J. *Liquid Scintillation Analysis*. Pacard Instrument Company, 1989.

82. PENG, C. T. A review of methods of quench correction in liquid scintillation counting. In : BRANSOME, Edwin D (ed.), *The Current Status of Liquid Scintillation Counting 1969 Proceedings of a Conference at the Massachusetts Institute of Technology*. 1969. p. 283–292.

83. NEARY, M. P. and BUDD, A. L. Color and Chemical quench. In : EDWIN D BRANSOME, Jr. (ed.), *The Current Status of Liquid Scintillation Counting 1969 Proceedings of a Conference at the Massachusetts Institute of Technology*. 1969. p. 273–282.

84. RUNDT, Kenneth, OIKARI, Timo and KOURU, Heikki. Quench correction of colored samples in LSC. In : *New Trends in Liquid Scintillation Counting and Organic Scintillators*. 1989. p. 677–689.

85. KNOCHE, Herman W, PARKHURST, Anne M and TAM, S William. The effect of volume and quenching on estimation of counting efficiencies in liquid scintillation counting. *The International Journal of Applied Radiation and Isotopes*. 1979. Vol. 30, no. 1, p. 45–49.

86. PERKINELMER. *Instrumental Manual: Wallac 1220 Quantulus - Ultra Low Level Liquid Scintillation Spectrometer*. 1.D. Turku, Finland, 2005.

87. PERKINELMER. *Wallac WinQ - Windows software for controling Wallac 1220 Quantulus*. Turku, Finland, 2004.

88. VILLA, M., MANJÓN, G. and GARCÍA-LEÓN, M. Study of colour quenching effects in the calibration of liquid scintillation counters: The case of 210Pb. *Nuclear Instruments and Methods in Physics Research, Section A: Accelerators, Spectrometers, Detectors and Associated Equipment*. 2003. Vol. 496, p. 413–424.

89. PUJOL, Lluis and SANCHEZ-CABEZA, Joan-Albert. Role of Quenching on Alpha / Beta Separation in Liquid Scintillation Counting for Several High Capacity Cocktails. *Analyst*. 1997. Vol. 122, p. 383–385.

90. PALOMO, M., VILLA, M., CASACUBERTA, N., PANALVER, A., BORRULL, F and AGUILAR, C. Evaluation of different parameters affecting the liquid scintillation spectrometry measurement of gross alpha and beta index in water samples. *Applied Radiation and Isotopes*. 2011. Vol. 69, p. 1274–1281.

91. HILLER, Achim, ANDERSON, Robert and COOK, G.T. T. Effects of a range of quenching agents on 14C-benzene counting efficiency when employing Pulse-Shape Analysis ( TR-LSC ® ). In : *LSC 1994, Liquid Scintillation Spectrometry*. 1994. p. 347–355.

92. M. PATES, Jacqueline, T. COOK, Gordon, B. MACKENZIE, Angus and J. PASSO JR., Charles. Implications of beta energy and quench level for alpha/beta liquid scintillation spectrometry calibration. *Analyst*. 1998. Vol. 123, no. 10, p. 2201–2207.

93. MENDOW, G, MONELLA, F C, PISARELLO, M L and QUERINI, C A. Biodiesel production from non-degummed vegetable oils: Phosphorus balance throughout the process. *Fuel Processing Technology*. May 2011. Vol. 92, no. 5, p. 864–870.

94. THANH, Le Tu, OKITSU, Kenji, SADANAGA, Yasuhiro, TAKENAKA, Norimichi, MAEDA, Yasuaki and BANDOW, Hiroshi. Ultrasound-assisted production of biodiesel fuel from vegetable oils in a small scale circulation process. *Bioresource Technology*. 2010. Vol. 101, no. 2, p. 639–645.

95. HELWANI, Z., OTHMAN, M. R., AZIZ, N., FERNANDO, W. J N and KIM, J. Technologies for production of biodiesel focusing on green catalytic techniques: A review. *Fuel Processing Technology*. 2009. Vol. 90, p. 1502–1514.

96. MEHER, L. C., DHARMAGADDA, Vidya S S and NAIK, S. N. Optimization of alkali-catalyzed transesterification of Pongamia pinnata oil for production of biodiesel. *Bioresource Technology*. 2006. Vol. 97, p. 1392–1397.

97. STAMENKOVIĆ, Olivera S., VELIČKOVIĆ, Ana V. and VELJKOVIĆ, Vlada B. *The production of biodiesel from vegetable oils by ethanolysis: Current state and perspectives*. 2011. ISBN 00162361.

98. DARNOKO, D and CHERYAN, Munir. Continuous production of palm methyl esters. *Journal of the American Oil Chemists' Society*. 2000. Vol. 77, no. 12, p. 1269–1272.

99. WANG, Yong, OU, Shiyi, LIU, Pengzhan, XUE, Feng and TANG, Shuze. Comparison of two different processes to synthesize biodiesel by waste cooking oil. *Journal of Molecular Catalysis A: Chemical*. June 2006. Vol. 252, no. 1-2, p. 107–112.

100. CANDEIA, R A, SILVA, M C D, CARVALHO FILHO, J R, BRASILINO, M G A, BICUDO, T C, SANTOS, I M G and SOUZA, A G. Influence of soybean biodiesel content on basic properties of biodiesel–diesel blends. *Fuel*. April 2009. Vol. 88, no. 4, p. 738–743.

101. TOMES, D, LAKSHMANAN, P and SONGSTAD, D. *Biofuels: global impact on renewable energy, production agriculture, and technological advancements*. Springer, 2010.

102. BAMGBOYE, AI and HANSEN, AC. Prediction of cetane number of biodiesel fuel from the fatty acid methyl ester (FAME) composition. *International Agrophysics*. 2008. No. 1996, p. 21–29.

103. *CSN EN 14112:2003 Fat and oil derivatives - Fatty Acid Methyl Esters (FAME) - Determination of oxidation stability (accelerated oxidation test)*. 2003.

104. *CSN EN 14104:2003 Fat and oil derivatives - Fatty Acid Methyl Esters (FAME) - Determination of acid value*. 2003.

105. RAMOS, María Jesús, FERNÁNDEZ, Carmen María, CASAS, Abraham, RODRÍGUEZ, Lourdes and PÉREZ, Angel. Influence of fatty acid composition of raw materials on biodiesel properties. *Bioresource technology*. January 2009. Vol. 100, no. 1, p. 261–8.

106. WAUQUIER, J P, SMITH, D H and DU PÉTROLE, Institut Français. *Petroleum Refining*. Editions Technip, 1995. Institut Fran{ç}ais du P{é}trole publications.

107. BIOFUEL SYSTEMS GROUP LTD. Biodiesel standards. [online]. [Accessed 3 April 2014]. Available from: https://www.biofuelsystems.com/biodiesel/specification.htm

108. *Personal communication with Mr. Salkič, Head of Corporate Comunications, Petrol d.d.*

109. *ISO 3675:1998 Crude petroleum and liquid petroleum products -- Laboratory determination of density -- Hydrometer method*. 1998.

110. *ISO 12185:1996 Crude petroleum and petroleum products - Determination of density - Oscillating U-tube method*. 1996.

111. SRIVASTAVA, Anjana and PRASAD, Ram. Triglycerides-based diesel fuels. *Renewable and Sustainable Energy Reviews*. June 2000. Vol. 4, no. 2, p. 111–133.

112. DEMIRBAS, Ayhan. Progress and recent trends in biodiesel fuels. *Energy Conversion and Management*. January 2009. Vol. 50, no. 1, p. 14–34.

113. NICOLAU, Aline, LUTCKMEIER, Camila V., SAMIOS, Dimitrios, GUTTERRES, Mariliz and PIATNICK, Clarisse M S. The relation between lubricity and electrical properties of low sulfur diesel and diesel/biodiesel blends. *Fuel*. 2013. Vol. 117, p. 26–32.

114. LIRA, Liliana Fátima Bezerra, DOS SANTOS, Daniele C.M.B. M B, GUIDA, Mauro a.B. B, STRAGEVITCH, Luiz, KORN, Maria das Graças a., PIMENTEL, Maria Fernanda and PAIM, Ana Paula Silveira. Determination of phosphorus in biodiesel using FIA with spectrophotometric detection. *Fuel*. November 2011. Vol. 90, no. 11, p. 3254–3258.

115. ENCINAR, José M JM, GONZÁLEZ, Juan F, RODRÍGUEZ-REINARES, Antonio and GONZALEZ. Biodiesel from Used Frying Oil. Variables Affecting the Yields and Characteristics of the Biodiesel. *Industrial & Engineering Chemistry Research*. 15 June 2005. Vol. 44, no. 15, p. 5491–5499.

116. MITTELBACH, Martin. Diesel fuel derived from vegetable oils, VI: Specifications and quality control of biodiesel. *Bioresource Technology*. 1996. Vol. 56, no. 1, p. 7–11.

117. MCCORMAC, F.G. Liquid scintillation counter characterization, optimization. *Radiocarbon*. 1992. Vol. 34, no. 1, p. 37–45.

118. ISO. *ISO 17025 General requirements for the competence of testing and calibration laboratories*. 2005. ISBN IEC 17025.

119. JOINT COMMITTEE FOR GUIDES IN METROLOGY. *International vocabulary of basic and general terms in metrology (VIM)*. 2004.

120. TAYLOR, Barry N. and KUYATT, Cris E. *Guidelines for Evaluating and Expressing the Uncertainty of NIST Measurement Results*. 1994. Gaithersburg : NIST.

121. ORIGINLAB CORPORATION. *Origin Pro 8* [online]. OriginLab Corporation. 8. Available from: http://www.originlab.com/

122. CURRIE, Lloyd a. Limits for qualitative detection and quantitative determination. Application to radiochemistry. *Analytical Chemistry*. 1 March 1968. Vol. 40, no. 3, p. 586–593.

123. ISO. *ISO 11929: Determination of the characteristic limits (decision threshold, detection limit and limits of the confidence interval) for measurements of ionizing radiation — Fundamentals and application*. 2010.

124. GARRAÍN, Daniel, HERRERA, Israel, LAGO, Carmen, LECHÓN, Yolanda and SÁEZ, Rosa. Renewable Diesel Fuel from Processing of Vegetable Oil in Hydrotreatment Units: Theoretical Compliance with European Directive 2009/28/EC and Ongoing Projects in Spain. *Smart Grid and Renewable Energy*. 2010. Vol. 01, p. 70–73.

125. MIKULEC, Jozef, CVENGROŠ, Ján, JORÍKOVÁ, Ľudmila, BANIČ, Marek and KLEINOVÁ, Andrea. Second generation diesel fuel from renewable sources. *Journal of Cleaner Production*. June 2010. Vol. 18, no. 9, p. 917–926.

126. *Personal communication with Dr. Culp, Associate Reasearch Scientist, The University of Georgia, Center for Applied Isotope Studies*.

127. BAGÁN, H., HARTVIG, S., TARANCÓN, A., RAURET, G. and GARCÍA, J. F. Plastic vs. liquid scintillation for 14C radiotracers determination in high salt matrices. *Analytica chimica acta*. 12 January 2009. Vol. 631, no. 2, p. 229–36.

128. *Personal communication with Mr. Passo, Associate Product Leader, Radiometric Detection, PerkinElmer*.

129. KLEINSCHMIDT, Ross I. Gross alpha and beta activity analysis in water — a routine laboratory method using liquid scintillation analysis. *Applied Radiation and Isotopes*. 2004. Vol. 61, p. 333–338.

130. PATES, J M, COOK, G T, MACKENZIE, A B and THOMSON, J. The development of an alpha/beta separation liquid scintillation cocktail for aqueous samples. *Journal of Radioanalytical and Nuclear Chemistry*. 1993. Vol. 172, no. 2, p. 341–348.

131. MANJON, G, ABSI, A, VILLA, M, MORENO, H P and GARCIA-TENORIO, R. Efficiency, background and interference in colored samples using an LSC Quantulus 1220. In : *LSC 2001, Advances in Liquid Scintillation Spectrometry*. 2002. p. 83–91.

132. VODOPIVEC, Tina. *Tekočinskoscintilacijska spektrometrija za določanje skupnih aktivnosti sevalcev [alfa] in [beta] v vodi*. Univerza v Ljubljani, Fakulteta za Matematiko in Fiziko, 2011.

133. KAIHOLA, Lauri. Gamma Emission Monitoring Capabilities of Quantulus. *LSC 2005, Advances in Liquid Scintillation Spectrometry*. 2005.

134. KAIHOLA, Lauri. Cosmic particle spectrum as a quench monitor in low level liquid scintillation spectrometry. *Nuclear Instruments and Methods in Physics Research Section A: Accelerators, Spectrometers, Detectors and Associated Equipment*. January 1994. Vol. 339, no. 1-2, p. 295–296.

135. ROSS, H H. Liquid scintillation counting of C< sup> 14</sup> using a balanced quenching technique. *The International journal of applied radiation and isotopes*. 1964. Vol. 15, no. 5, p. 273–277.

136. THEODÓRSSON, P, INGVARSDOTTIR, S. and GUDJONSSON, G. I. Balanced window method in 14C liquid scintillation counting. *Radiocarbon*. 2003. Vol. 45, no. 1, p. 113–112.

137. TUDYKA, Konrad, PAWLYTA, Jacek and PAZDUR, Anna. Fixed energy balance window quench correction for high precision LSC 14C dating. *Radiation Measurements*. 2011. Vol. 46, no. 10, p. 1176–1180.

138. *Personal communication with Dr. Idoeta, Research Scientist, University of Basque Country, Department for Nuclear Energy and fluid mechanics*.

139. *Personal communication with Dr. Petrovič, Associate Research Scientist, Jozef Stefan Institute*.

140. RADFORD, David (Oak Ridge National Laboratory). *RadWare* [online]. Available from: http://radware.phy.ornl.gov/main.html

141. VODOPIVEC, Tina. *Tekočinskoscintilacijka spektrometrija in tritij v urinu*. Univerza v Ljubljani, Fakulteta za Matematiko in Fiziko, 2013.

142. MINNE, Etienne, HEYNEN, Fabienne, DELPORTE, Cecile and HALLEZ, Serge. Effect on 90Sr determination resulting from a possible over-estimation of the external standard quench parameter on Quantulus 1220. In : *LSC 2008, Advances in Liquid Scintillation Spectrometry*. 2008. p. 183–192.

143. SCHOLL and CONRAD. *Proposal of Report GCL Action 2 Ring test on the bio-origin determination of bio components in fuels*. 2010.

144. SCHOLL and STENDER. *GCL Action 2: Study on biocomponents in fuels 2012-2013*. 2013.

145. *GCL Action 2 – Working group " Biocomponents in fuel " Ring test on gas oil with low FAME ( fatty acid methyl ester ) content- Draft Report*. 2013.

146. Pravilnik o vsebnosti biogoriv v gorivih za pogon motornih vozil. *Uradni list RS*. 2005. Vol. 83.

147. EUROSTAT. *Energy statistics*. 2013.

148. VILLAR, Marina, AVIVAR, Jessica, FERRER, Laura, GALME, Margalida, VEGA, Fernando and CERDA, Victor. Automatic and Simple Method for 99 Tc Determination Using a Selective Resin and Liquid Scintillation Detection Applied to Urine Samples. *Analytical Chemistry*. 2013. Vol. 85, p. 5491–5498.

149. *Personal communication with Mr. ter Wiel, Staff Scientist, PerkinElmer*.

# *12 Appendix*

1. GCL comparative test 2010 results
2. GCL comparative test 2012/2013 results
3. Diesel analysis diagram

Appendix 1: GCL comparative test 2010 results. Name of the lab: LAB1

| Laboratory Code | Sample 1 | Z-scores |
|---|---|---|
| LAB8 | **72.00** | -7.63 |
| LAB9 | **72.00** | -7.63 |
| LAB4 | **79.43** | -0.33 |
| LAB7 | **79.60** | -0.17 |
| LAB1 | **79.80** | 0.03 |
| LAB6 | **80.16** | 0.38 |
| LAB3 | **80.50** | 0.72 |
| LAB5 | **80.70** | 0.91 |
| LAB2 | **81.16** | 1.37 |

| | |
|---|---|
| Size : | 9 |
| Mean : | 78.37 |
| **Robust Mean:** | **79.77** |
| Standard Deviation : | 3.65 |
| **Robust SD:** | **1.02** |
| Min : | 72.00 |
| Max : | 81.16 |

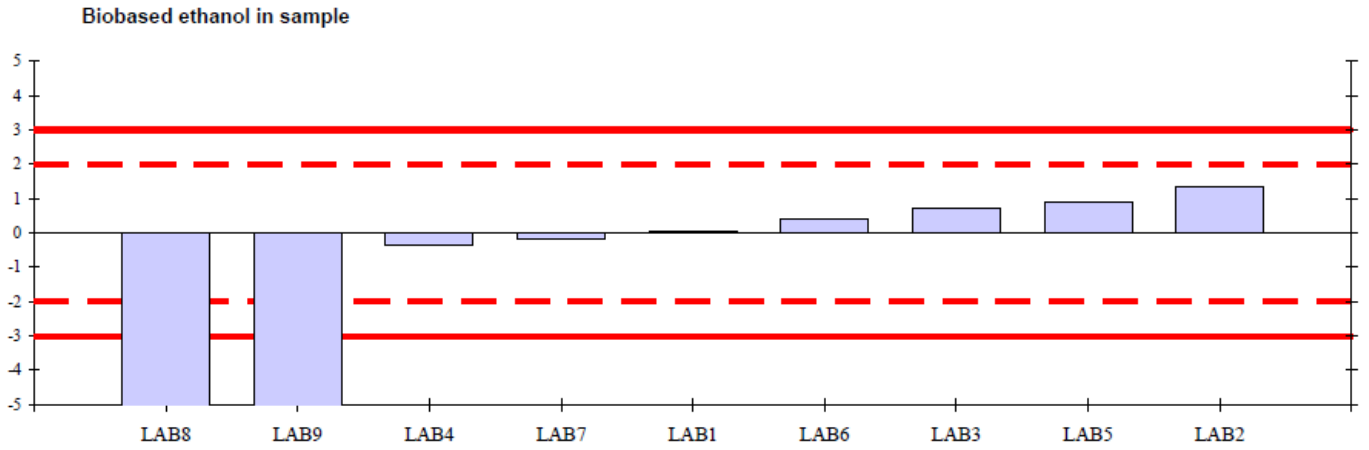

Appendix 1: GCL comparative test 2010 results. Name of the lab: LAB1

| Laboratory Code | Sample 2 | Z-scores |
|---|---|---|
| LAB9 | **0.00** | -6.90 |
| LAB4 | **4.34** | -1.76 |
| LAB7 | **4.80** | -1.21 |
| LAB1 | **5.80** | -0.03 |
| LAB5 | **6.00** | 0.21 |
| LAB2 | **6.16** | 0.40 |
| LAB3 | **6.45** | 0.74 |
| LAB6 | **6.55** | 0.86 |
| LAB8 | **7.00** | 1.40 |

| | |
|---|---|
| Size : | 9 |
| Mean : | 5.23 |
| **Robust Mean :** | **5.82** |
| Standard Deviation : | 2.14 |
| **Robust SD:** | **0.84** |
| Min : | 0.00 |
| Max : | 7.00 |

**Biobased ethanol in sample**

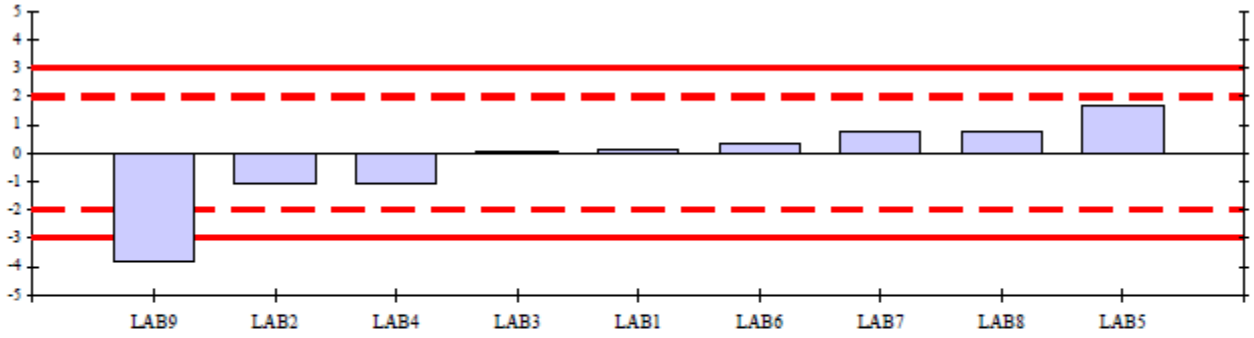

Appendix 1: GCL comparative test 2010 results. Name of the lab: LAB1

| Laboratory Code | Sample 3 | Z-scores |
|---|---|---|
| LAB9 | **17.00** | -3.86 |
| LAB2 | **18.21** | -1.06 |
| LAB4 | **18.21** | -1.06 |
| LAB3 | **18.70** | 0.08 |
| LAB1 | **18.71** | 0.10 |
| LAB6 | **18.80** | 0.31 |
| LAB7 | **19.00** | 0.77 |
| LAB8 | **19.00** | 0.77 |
| LAB5 | **19.40** | 1.69 |

| | |
|---|---|
| Size : | 9 |
| Mean : | 18.56 |
| **Robust Mean :** | **18.67** |
| Standard Deviation : | 0.70 |
| **Robust SD:** | **0.43** |
| Min : | 17.00 |
| Max : | 19.40 |

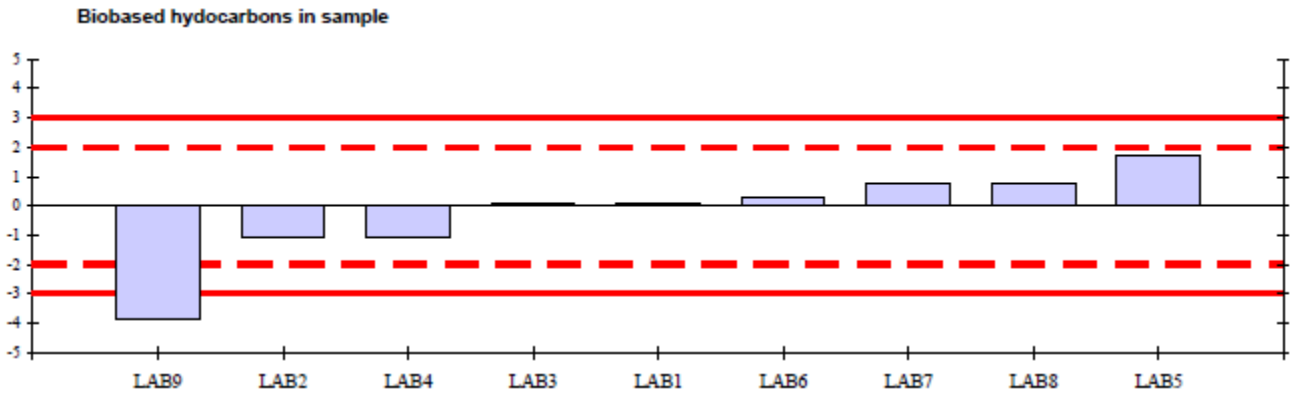

Appendix 1: GCL comparative test 2010 results. Name of the lab: LAB1

| Laboratory Code | Sample 4 | Z-scores |
|---|---|---|
| LAB7 | **8.90** | -1.14 |
| LAB8 | **9.00** | -1.09 |
| LAB2 | **10.09** | -0.48 |
| LAB6 | **10.77** | -0.09 |
| LAB4 | **12.06** | 0.63 |
| LAB1 | **12.10** | 0.65 |
| LAB3 | **20.80** | 5.53 |

| | |
|---|---|
| Size : | 7 |
| Mean : | 11.96 |
| **Robust Mean :** | **10.94** |
| Standard Deviation : | 4.11 |
| **Robust SD:** | **1.78** |
| Min : | 8.90 |
| Max : | 20.80 |

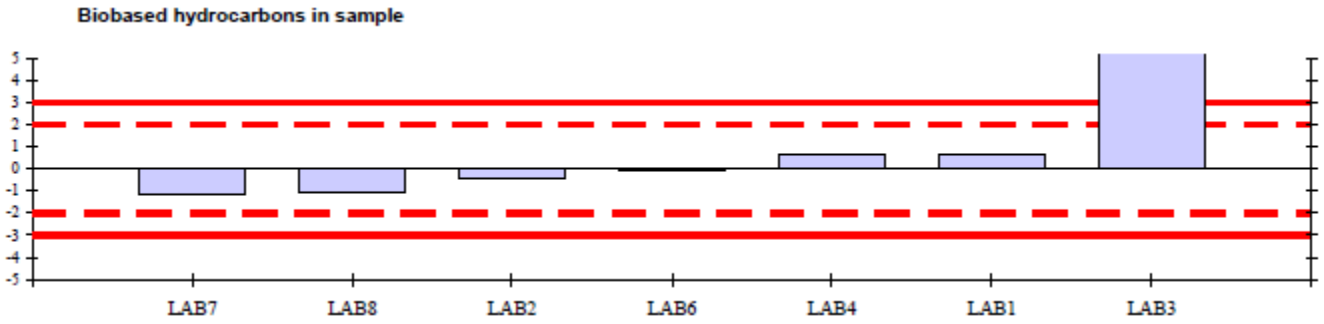

Appendix 2: GCL comparative test 2012/2013 results. Name of the lab: 2272

| Biobased hydrocarbons – w/w % | | |
|---|---|---|
| X | 10 | |
| $u_x$ | 1 | |
| $s^*_x$ | 1 | |
| $p_x$ | 7 | |
| Min | 8 | |
| Max | 11 | |
| Mean | 9 | |
| SD | 1 | |
| Lab code | Sample A1 | z-scores |
| 2272 | 10 | 0,00 |
| 2662 | 9 | -1,00 |
| 4737 | 11 | 1,00 |
| 5624 | 10 | 0,00 |
| 6364 | 9 | -1,00 |
| 6808 | 8 | -2,00 |
| 9006 | 10 | 0,00 |

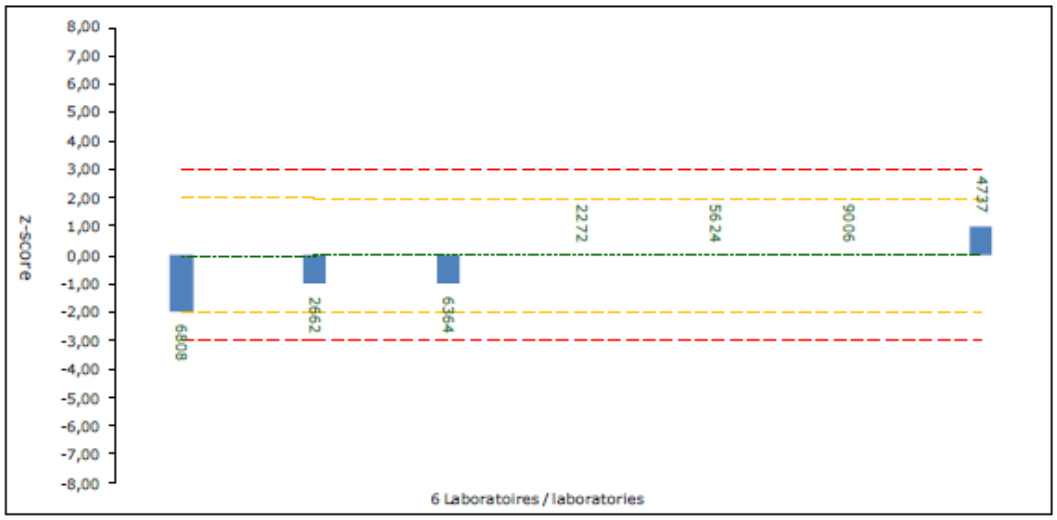

Appendix 2: GCL comparative test 2012/2013 results. Name of the lab: 2272

| Biobased hydrocarbons – w/w % | | |
|---|---|---|
| X | 93 | |
| $u_x$ | 1 | |
| $s^*_x$ | 2 | |
| $p_x$ | 7 | |
| Min | 86 | |
| Max | 98 | |
| Mean | 93 | |
| SD | 3 | |
| Lab code | Sample A2 | z-scores |
| 2272 | 94 | 0,50 |
| 2662 | 92 | -0,50 |
| 4737 | 93 | 0,00 |
| 5624 | 91 | -1,00 |
| 6364 | 94 | 0,50 |
| 6808 | 98 | 2,50 |
| 9006 | 93 | 0,00 |

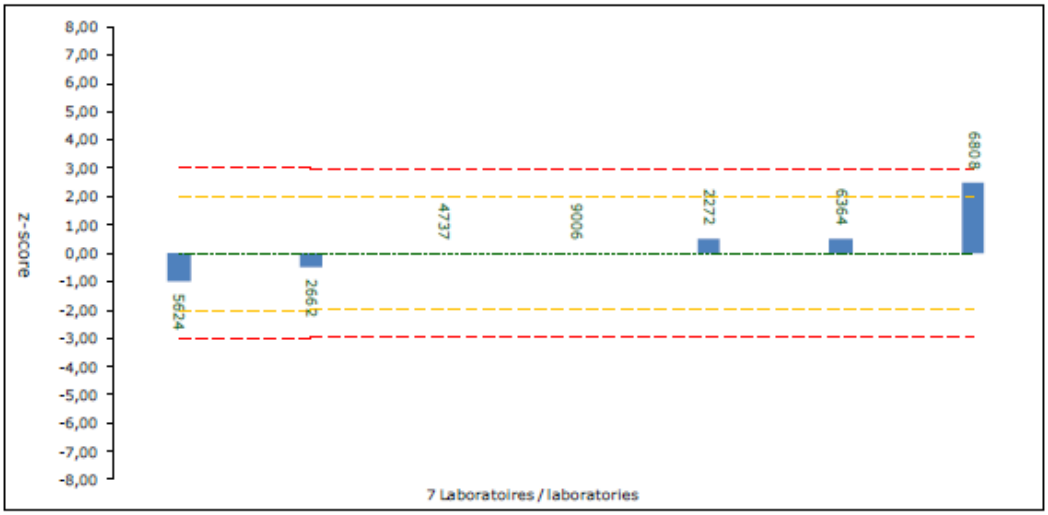

Appendix 2: GCL comparative test 2012/2013 results. Name of the lab: 2272

| Biobased hydrocarbons – w/w % | | |
|---|---|---|
| X | 10 | |
| $u_x$ | 1 | |
| $s^*_x$ | 1 | |
| $p_x$ | 7 | |
| Min | 8 | |
| Max | 11 | |
| Mean | 9 | |
| SD | 1 | |
| Lab code | Sample A3 | z-scores |
| 2272 | 10 | 0,00 |
| 2662 | 9 | -1,00 |
| 4737 | 11 | 1,00 |
| 5624 | 10 | 0,00 |
| 6364 | 10 | 0,00 |
| 6808 | 8 | -2,00 |
| 9006 | 9 | -1,00 |

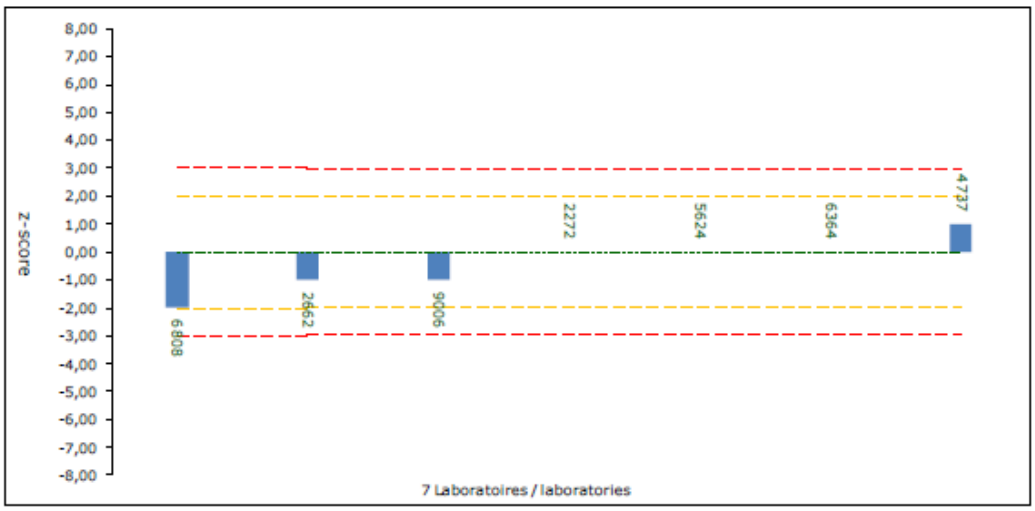

Appendix 2: GCL comparative test 2012/2013 results. Name of the lab: 2272

| Biobased hydrocarbons – w/w % | | |
|---|---|---|
| X | 92 | |
| $u_x$ | 1 | |
| $s^*_x$ | 1 | |
| $p_x$ | 7 | |
| Min | 87 | |
| Max | 93 | |
| Mean | 91 | |
| SD | 2 | |
| Lab code | Sample A4 | z-scores |
| 2272 | 93 | 1,00 |
| 2662 | 92 | 0,00 |
| 4737 | 92 | 0,00 |
| 5624 | 91 | -1,00 |
| 6364 | 93 | 1,00 |
| 6808 | 88 | -4,00 |
| 9006 | 92 | 0,00 |

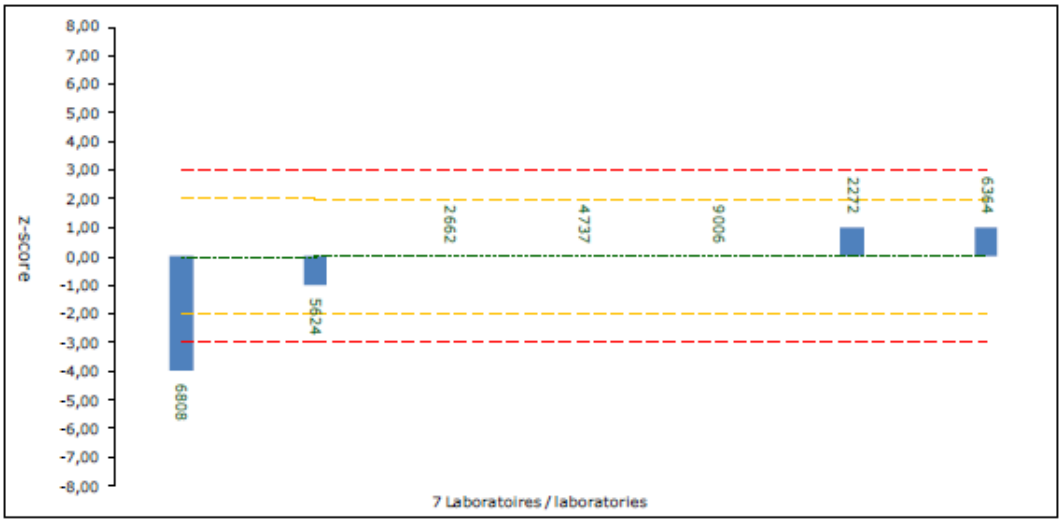

Appendix 2: GCL comparative test 2012/2013 results. Name of the lab: 2272

| Biobased hydrocarbons – w/w % Results for total Biobased hydrocarbons | |
|---|---|
| Min | 12 |
| Max | 17 |
| Mean | 15 |
| SD | 2 |
| Lab code | Sample B |
| 2272 | 17 |
| 6808 | 16 |
| 9866 | 12 |

| Biobased hydrocarbons – w/w % Results for HVO only | |
|---|---|
| Min | 5 |
| Max | 8 |
| Mean | 7 |
| SD | 1 |
| Lab code | Sample B |
| 2662 | 5 |
| 4737 | 8 |
| 5624 | 6 |
| 9006 | 7 |

| Biobased ethanol – w/w % | | |
|---|---|---|
| X | 8 | |
| $u_x$ | 2 | |
| $s_x$ | 4 | |
| $p_x$ | 5 | |
| Min | 5 | |
| Max | 13 | |
| Mean | 8 | |
| SD | 3 | |
| Lab code | Sample C | z-scores |
| 2272 | 13 | 1,25 |
| 2662 | 9 | 0,25 |
| 4737 | (*) | |
| 5624 | 5 | -0,75 |
| 6808 | 8 | 0,00 |
| 9006 | 6 | -0,50 |

Appendix 3: Diesel analysis diagram